Spring 5-7-2021

DEVICE DEVELOPMENT FOR LONG-TERM SYSTEMIC ORAL BIOLOGIC DRUG DELIVERY

Benjamin Wankum
University of Nebraska-Lincoln, bwankum2@unl.edu

DEVICE DEVELOPMENT FOR LONG-TERM SYSTEMIC ORAL BIOLOGIC DRUG DELIVERY

By

Benjamin Paul Wankum

A THESIS

Presented to the Faculty of

The Graduate College at the University of Nebraska

In Partial Fulfillment of Requirements

For the Degree of Master of Science

Major: Mechanical Engineering and Applied Mechanics

Under the Supervision of Professor Benjamin S. Terry

Lincoln, Nebraska

May, 2021

DEVICE DEVELOPMENT FOR LONG-TERM SYSTEMIC BIOLOGIC DRUG DELIVERY

Benjamin Paul Wankum, M.S.

University of Nebraska, 2021

Advisor: Benjamin Terry

A biologic drug is a drug that is produced by a living organism. Biologic drugs are used to treat various medical conditions such as arthritis, diabetes, or certain forms of cancers due to their high potency and high selectivity of action. Drawbacks of biologics include their poor stability in the gastrointestinal tract and their poor absorption. In effect, this gives the drugs very low bioavailability and short therapeutic half-lives. To combat these obstacles, current delivery methods include subcutaneous injections at home or intravenous or intramuscular injections in a medical facility.

The overall scientific goal of the research was to utilize subcutaneous needle injection methodology used for parenteral systemic biologic drug delivery to solve the problem of delivering biologics orally for treating diseases like diabetes, arthritis, or cancers. Previous prototype tissue attachment mechanism (TAM) systems have shown tissue attachment in vivo, without the delivery of a drug. The methodology of this study was to use the same successful device but integrate an osmotic pump and a hypodermic needle to deliver a drug after attachment to the intestine. The delivery of the drug was deemed successful based on the drug's concentration in blood samples.

The integrated TAM and drug delivery needle were designed, tested, and integrated on the benchtop until consistent successful drug delivery results were obtained. Once the device reliably delivered drug on excised tissue, it was tested in vivo on six

swine for systemic drug delivery. The first study had shorter than expected TAM attachment times causing minimal drug to be delivered, but the methodology of the study was learned. After improving the device and study setup, a second in vivo study was performed on another six swine. The study showed much stronger evidence of drug delivery. Both positive controls and one of the three experimental groups showed systemic drug delivery. Both studies were a methods development study, so the number of pigs in the results did not meet the power for statistical significance.

Also, in this work, a theoretical osmotic pump was designed to be integrated with the TAM and full capsule. Although not actually fabricated, the osmotic pump would be fabricated using the same material and ratio of drug to total volume as a commercial osmotic pump. The commercial osmotic pump was tested in a swine small intestine and showed proof of drug delivery.

Acknowledgments

I would like to thank the Institutional Animal Care Program (IACP) staff at UNL who helped perform the surgical procedures, obtained radiographs and blood draws in the early mornings and late nights, and provided overall husbandry to the animals used in my research. Dr. Craig Kreikemeier-Bower, Dr. Anna Fitzwater, Bayliegh Bohn, Cindy Wooledge, and Jesse Baumann-Berg deserve acknowledgment for the time required to complete our objectives.

This research could not have been done without the previous groups' research. I would like to thank all previous members who worked on this project, including those whom I was lucky enough to work with, Sayeed Mohammed, Trevor Perey, and Musharrat Mustaree Mau. Much of this work was done as Sunandita Sharker simultaneously developed the tissue attachment mechanism (TAM) for long-term attachment. Sunandita introduced me to this project, worked with me the entire time, and continued to work on the project after the drug delivery objectives were completed. She was the backbone of the project during my time, and I could not thank her enough.

In addition, I want to thank my committee members Dr. Mark Carlson and Dr. Ryan Pedrigi for contributing their time, effort, and expertise. I wish to thank my committee chairman and advisor, Dr. Benjamin Terry, for allowing me to become a research assistant in the Terry Research Lab (TRL). He gave me the chance to gain knowledge and experience in prototyping, scientific methodology, and technical writing skills. I thank him for his advice, timely guidance, and the invaluable experience I gained at the TRL.

I wish to thank our sponsor, Progenity inc., for the funds to accomplish our goals, especially Ryan Jones, Jeff Shimizu, and Gabe Chow for their precious advice and guidance. I would also like to thank Nikki Lee from Progenity and Alok Pandey from PBL Assay Science for their time and effort running and analyzing the plasma samples.

Lastly, I would like to thank my family for their support and unconditional love over my academic career. I truly would not be where I am today without their guidance and impact on my life.

Disclosure

This research was funded in part by Progenity, Inc. The views and opinions expressed herein are those of the authors and do not necessarily reflect those of Progenity, Inc.

Table of Contents

Chapter 1: Introduction 1

1.1 Biological Drugs 1

1.2 Oral Drug Delivery Devices 4

1.3 Previous Research and Approach 8

1.4 Research Objectives 12

Chapter 2: Drug Delivery System 13

2.1 Functional Requirements of Drug Delivery System 13

1. Location of Delivery 13

2. Duration of Administration 13

3. Success Rate 13

4. Animal 13

5. Component Materials and Properties 13

6. MRI Compatibility 13

7. Cost 14

8. Manufacturability 14

2.2 Initial design of the Drug Injection Needle 14

2.3 Alternative Designs for Drug Delivery 21

2.4 Down Selection Process 25

2.5 Design 28

2.6 Benchtop Experiments 30

2.7 In vivo Experiment 1 33

2.7.1 Introduction 33

2.7.2 Objectives 34

2.7.3 Hypothesis 34

2.7.4 Materials and Methods 34

2.7.5 Results 42

2.7.6 Complications/Conclusions 45

2.8 In vivo Experiment 2 46

2.8.1 Introduction 46

2.8.2 Objectives 46

2.8.3 Hypothesis 47

2.8.4 Materials and Methods 47

2.8.5 Results 50

2.8.6 Discussion/Conclusions 55

Chapter 3: Osmotic Pump 57

3.1 Introduction 57

3.2 Theory of Osmotic Pumps 58

3.3 Functional Requirements of Osmotic Pump 61

1. Component Materials and Properties 61

2. Drug Chemistry, Manufacturing, and Controls (CMC) 62

3. Drug Loading..... 62

4. Manufacturability 62

5. Drug Payload Description 62

6. Drug Payload Material and Viscosity..... 62

3.4 Design of Osmotic Pump 62

3.5 Function of Osmotic Pump in the Intestine..... 67

Chapter 4: Discussion and Conclusions..... 69

4.1 Future Work 70

References..... 73

Appendices..... 78

Appendix A: Standard Curves and Raw Data from In Vivo Experiment 2 78

Appendix B: Drug delivery TAM fabrication process..... 87

List of Figures

Figure 1. An example graph showing the area under the curve (AUC) of an oral dose and an IV dose [41]..... 3

Figure 2. GI-MAPS oral device comprising mucoadhesive patches and an enterically coated capsule [54]. 5

Figure 3. SOMA self-orienting to its stable position and delivering drug [56]. 6

Figure 4. The luminal unfolding microneedle injector (LUMI) actuation scheme [53]. 7

Figure 5. The RaniPill actuation process [59]. 8

Figure 6. Schematic showing the noninvasive implantation of attachment mechanism on the mucosal lining of the GI tract via a long-term ingestible capsule robot (ICR). 9

Figure 7. A) TAM orifice and TAM needles. B) TAM Body 11

Figure 8. Schematic of the brain infusion kit from ALZET. 16

Figure 9. CAD design of a capsule compatible with the BIN. 16

Figure 10. CAD design of a capsule compatible with the BIN (cross-section). 17

Figure 11. CAD design of a capsule compatible with the BIN (bottom-view). 17

Figure 12. CAD assembly of a capsule with the BIN. 18

Figure 13. CAD assembly of a capsule with the BIN (cross-section). 18

Figure 14. Assembly of a capsule with the BIN. 18

Figure 15. Assembly of a capsule with the BIN (bottom-view). 19

Figure 16. Aspiration system with TAM/drug delivery needle. 19

Figure 17. A representative image of BIN delivering a "drug" bolus. Colored (green) water was used in this benchtop study. 20

Figure 18. Several “drug” boluses showing successful drug delivery using the BIN prototype. 20

Figure 19. A) ALZET's blunt canula (needle) and B) a beveled hypodermic needle..... 21

Figure 20. Concept model of capsule illustrating a torus-shaped osmotic pump. 22

Figure 21. Concept model of a 1) perpendicular drug injection needle, 2) spring-loaded drug injection needle, 3) dual-purpose drug injection needle, 4) spring-loaded drug injection needle within the capsule, 5) drug pool within the capsule 24

Figure 22. A) CAD design of dual-purpose needle TAM. B) CAD design of perpendicular needle TAM. C) Cross-section CAD design of dual-purpose TAM. D) Cross-section CAD design of perpendicular TAM. E) Top view of the dual-purpose needle TAM. F) Side view of perpendicular needles TAMs. 1 mm needle on the left and 5 mm needle on the right. The heigh of the needles could be altered. G) Side view of ... 29

Figure 23. Attached dual-purpose needle. 31

Figure 24. Perpendicular needle delivering drug. 32

Figure 25. Colored water is shown in/around vessels of the small intestine after delivery from the perpendicular drug injection needle. 32

Figure 26. Several boluses of colored water were delivered into the small intestine from the perpendicular needle. 33

Figure 27. TAM/Drug delivery needle and the capsule chamber for tissue aspiration 35

Figure 28. Capsule chamber/TAM/drug delivery needles connected to a 200 ul osmotic pump via catheters. Note: The device is attached to the vacuum system. 35

Figure 29. Tissue aspirated into TAM/drug delivery needle 40

Figure 30 Tissue still aspirated after TAM/drug delivery needle has been removed from the aspiration system..... 40

Figure 31. Sutured marker beads for reference of TAM/drug delivery needle during radiographs..... 41

Figure 32. A representative x-ray of an attached TAM/Drug delivery needle. The yellow square outlines the osmotic pump and the red circle outlines the TAM/Drug delivery needle. Between the two are the marker beads. 43

Figure 33. A representative x-ray of a detached TAM. Only the marker beads are shown in the x-ray. 44

Figure 34. Adalimumab plasma concentration levels from in vivo study 1. Exp 1, Exp 2, Exp 3, and Exp 4 used the TAM/Drug delivery needle and either a 7-day osmotic pump or a 1-day osmotic pump. Pos 1 used a direct needle injection using a manual syringe pump (No TAM/Drug delivery device). Neg 1 used only an osmotic pump sutured into the intestinal lumen. 44

Figure 35. Smaller profile TAM and drug delivery needle device connected to a catheter. 47

Figure 36. Osmotic pump with a hole drilled into the flow moderator cap. 48

Figure 37. An osmotic pump was sutured in place during necropsy. 52

Figure 38. A TAM with a drug delivery needle was still attached to the ileum during necropsy. 52

Figure 39. TAM needles were still in their 30-degree orientation. 53

Figure 40. Adalimumab concentration levels using the kit standard-based samples. Exp 1, Exp 2, and Exp 3 used the TAM/Drug delivery needle and a 1-day osmotic pump. Pos 1

and Pos 2 used the TAM/Drug delivery device but instead of an osmotic pump, a manual syringe pump was used to inject all 200 µL of drug into the intestinal wall. Neg 1 used only an osmotic pump sutured into the intestinal lumen. 54

Figure 41. Adalimumab concentration levels using the modified "adalimumab injection standard" based samples. Exp 1, Exp 2, and Exp 3 used the TAM/Drug delivery needle and a 1-day osmotic pump. Pos 1 and Pos 2 used the TAM/Drug delivery device but instead of an osmotic pump, a manual syringe pump was used to inject all 200 µL of drug into the intestinal wall. Neg 1 used only an osmotic pump sutured into the intestinal lumen..... 55

Figure 42. Schematic of an osmotic pump..... 59

Figure 43. ALZET Osmotic Pump..... 60

Figure 44. Example of a piston-driven osmotic pump..... 61

Figure 45. Schematic of the torus-shaped osmotic pump 63

Figure 46. CAD design of a torus-shaped osmotic pump with a drug injection needle. .. 65

Figure 47. Half-section view of the osmotic pump showing the spherical-shaped piston, drug location, osmotic agent location, and semi-permeable membrane. 65

Figure 48. Drawing of the osmotic pump. Units are in millimeters. 66

Figure 49. Pre-implantation of an osmotic pump with India ink meniscus. 68

Figure 50. Osmotic pump with India ink meniscus after being in a porcine intestine for over 24 hours..... 68

Figure 51. The full concept of the capsule system..... 72

Figure 52. 4-parameter log fit standard curve used to measure adalimumab concentrations for plasma samples from groups 136 (Neg 1), 137 (Exp 1), 139 (Exp 2), 140 (Exp 3), 141 (Pos 1), and 163 (Pos 2). 79

Figure 53. 4-parameter log fit standard curve used to measure adalimumab concentrations for plasma samples from groups 136 (Neg 1), 137 (Exp 1), 139 (Exp 2), 140 (Exp 3), 141 (Pos 1), and 163 (Pos 2). 84

Figure 54. Laser-cut TAM needles. 91

Figure 55. Non-bent TAM needle. 92

Figure 56. Non-bent TAM Needle in bottom 30-degree bending mold. 92

Figure 57. TAM Needle in 30-degree bending molds. 93

Figure 58. Bent TAM Needle in top 30-degree bending mold. 93

Figure 59. 30-degree TAM needle. 94

Figure 60. 1/2 inch 30-gauge hypodermic needle. 94

Figure 61. Hypodermic needle in bending mold. 95

Figure 62. Hypodermic needle bent once. 95

Figure 63. Hypodermic needle bent 90-degrees twice. 96

Figure 64. Hypodermic needle bent and snapped off from Luer lock. 96

Figure 65. TAM with a drug injection needle (shorten arm used). 97

Figure 66. Needle arm bent down and glued to a small catheter. 98

Figure 67. The final device without the osmotic pump. 98

List of Tables

Table 1. Drug delivery evaluation criteria matrix with weights 26

Table 2. Average score (n=6) of the different design concepts. 27

Table 3. Results of Benchtop Study. 31

Table 4. Attachment duration of drug delivery TAM and osmotic pump in study 1. 43

Table 5. Attachment duration of drug delivery TAM and osmotic pump in study 2. 51

Table 6. Function requirement for drug delivery payload. 62

Table 7. List of components, materials, and dimensions for the torus-shaped osmotic pump 66

Table 8. Adalimumab kit standard curve used to measure adalimumab concentrations for plasma samples from Groups 136, 137, 139, 140, 141, and 163. LLOQ (Conc.) = 5 ng/ml. 79

Table 9. Adalimumab ELISA: Group 136. Measured adalimumab concentrations of the samples from Group 136. Values below the LLOQ (5 ng/ml) are marked in red. 80

Table 10. Adalimumab ELISA: Group 137. Measured adalimumab concentrations of the samples from Group 137. Values below the LLOQ (5 ng/ml) are marked in red. 80

Table 11. Adalimumab ELISA: Group 139. Measured adalimumab concentrations of the samples from Group 139. Values below the LLOQ (5 ng/ml) are marked in red. 81

Table 12. Adalimumab ELISA: Group 140. Measured adalimumab concentrations of the samples from Group 140. Values below the LLOQ (5 ng/ml) are marked in **red** and those above the ULOQ (100 ng/ml) are marked in green. 81

Table 13. Adalimumab ELISA: Group 141. Measured adalimumab concentrations of the samples from Group 141. Values below the LLOQ (5 ng/ml) are marked in red and those above the ULOQ (100 ng/ml) are marked in green. 82

Table 14. Adalimumab ELISA: Group 163. Measured adalimumab concentrations of the samples from Group 163. Values below the LLOQ (5 ng/ml) are marked in red and those above the ULOQ (100 ng/ml) are marked in green. 82

Table 15. Additional adalimumab standard curve used to measure adalimumab concentrations for plasma samples from Groups 136, 137, 139, 140, 141, and 163. LLOQ (Conc.) = 0.160 ng/ml. 83

Table 16. Adalimumab ELISA: Group 136. Measured adalimumab concentrations of the samples from Group 136. Values below the LLOQ (0.160 ng/ml) are marked in red. 84

Table 17. Adalimumab ELISA: Group 137. Measured adalimumab concentrations of the samples from Group 137. Values below the LLOQ (0.160 ng/ml) are marked in red. 85

Table 18. Adalimumab ELISA: Group 139. Measured adalimumab concentrations of the samples from Group 139. Values below the LLOQ (0.160 ng/ml) are marked in red. 85

Table 19. Adalimumab ELISA: Group 140. Measured adalimumab concentrations of the samples from Group 140. Values below the LLOQ (0.160 ng/ml) are marked in red. 86

Table 20. Adalimumab ELISA: Group 141. Measured adalimumab concentrations of the samples from Group 141. Values below the LLOQ (0.160 ng/ml) are marked in red. 86

Table 21. Adalimumab ELISA: Group 163. Measured adalimumab concentrations of the samples from Group 163. Values above the ULOQ (500 ng/ml) are marked in green. ... 87

Table 22. List of parts and suppliers. 88

Table 23. List of files with descriptions used to build the TAM. 89

Table 24. List of tools and supplies for the TAM. 89

Chapter 1: Introduction

1.1 Biological Drugs

A biological drug (biologic) is a drug that is derived from any living organism such as humans, animals, or microorganisms [1]–[3]. Compared with conventional synthetic chemical drugs, biologics are relatively large and complex molecules [4]–[6]. They are made up of proteins, carbohydrates, nucleic acids, or a complex composite of these substances [1], [7], [8]. Biological drugs are used to treat various medical conditions such as rheumatoid arthritis, diabetes, or forms of cancers due to their high potency and high selectivity of action [2], [9]–[11]. Some of the most common biological drugs in the United States include adalimumab (Humira®) or rituximab (Rituxan ®) for rheumatoid arthritis, semaglutide (Ozempic®) or dulaglutide (Trulicity®) for treatment of diabetes, or trastuzumab (Herceptin®) for the treatment of breast cancer [9], [12]–[17]. Although these drugs are effective, they must cross numerous obstacles before reaching the pathological site [18]. Specifically, biologics are poorly absorbed in the gastrointestinal (GI) tract because of their physio-chemical properties including size, charge, and hydrophilicity [19]–[22]. Frequently, an orally administered biologic may become inactive or less potent as it might be hydrolyzed or degraded enzymatically before reaching its targeted location [18], [23], [24]. After being degraded, it is excreted rapidly through the urinary system, leaving a minimal amount of drug at the targeted site [25]. Some biologics can be administered via a mucosal route, such as parathyroid hormone [26]. Non-protein biologics (such as steroid hormones) can be administered orally [27]. However, many biological therapeutics typically require parenteral delivery

which includes intravenous (IV) or intramuscular (IM) delivery in hospitals or subcutaneous (SC) injections at the patient's home (e.g. via insulin pen) [28], [29].

Unfortunately, IV, IM, and SC administrations can be painful or psychologically daunting causing many people to fear hypodermic needle placements and potentially drop out of their treatment [30]. It is estimated that 10% of the United States' population has trypanophobia or needle phobia [31]. In a study performed on 12,582 people who were given the option of a free influenza vaccine via intranasal or SC injection, only 1,600 people chose to be vaccinated. Of the 1,600 subjects, 97% of the people selected the nasal route. The subjects were asked the reason for choosing the nasal spray, and 14% responded with fear of injection [32].

Aside from the fear of needles, injections are more challenging to use in a long-acting continuous drug input system outside of the hospital since the patients cannot continuously treat themselves [33]. When investigating new drug delivery methods, pharmacokinetics (PK) and pharmacodynamics (PD) are used to compare delivery methods [34]. Pharmacokinetics is the study and mathematical description of the relationship between the dose of a drug and its concentration in body fluids and tissues over time [35]. Pharmacodynamics, on the other hand, is the quantitative study of the relationship between drug exposure and pharmacologic or toxicologic responses [36]. Simply, PK represents "what the body does to the drug" and PD represents "what the drug does to the body", specifically the targeted site, tissue, organ, etc. [37]. One of the most important pharmacokinetic parameters is bioavailability (F), which is the fraction or percent of an administered drug that reaches systemic circulation [38]. Many times, absolute bioavailability is used to compare different methods of drug delivery (i.e. oral

administration) to an IV injection [39]. Equation (1) shows the formula used to calculate bioavailability.

$$F = \frac{AUC_x}{AUC_{IV}} * \frac{D_x}{D_{IV}} \quad (1)$$

Where the subscripts *x* and *IV* denote the delivery method of interest and intravenous delivery, respectively. Next, AUC means the area under the curve, which represents the area under the plasma concentration curve [40]. The area is defined by the plasma drug concentration on the y-axis and time on the x-axis. Figure 1 shows a generic example of an AUC comparing an oral administration to an IV administration. Lastly, *D* is the dosage of the drug administered, but many times dosages are the same between delivery methods, so it can be removed from the equation.

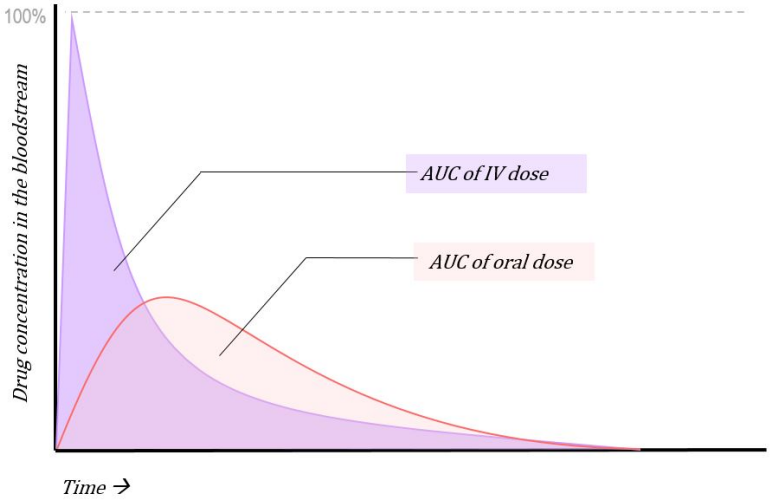

Figure 1. An example graph showing the area under the curve (AUC) of an oral dose and an IV dose [41].

Controlled drug delivery aims to deliver drugs to the target sites at desired rates and times, thus enhancing the drug efficacy, pharmacokinetics, and bioavailability while maintaining minimal side effects [42], [43]. To achieve a controlled drug delivery, many approaches are being explored, such as chemically modifying the biologic, encapsulating or protecting the drug, applying external transdermal microneedle patches, and more recently, novel oral drug delivery devices [44]–[47]. Ingestible drug delivery devices present possibilities for systemic delivery of biological drugs with or without chemical alteration [48], [49]. These easily ingestible devices can carry small electronics, mechanical components, mucoadhesive patches, or dissolvable microneedles which can deliver drug along the GI tract [50]–[53].

1.2 Oral Drug Delivery Devices

In 2002, Eiamtrakarn *et al.* developed a gastrointestinal mucoadhesive patch system (GI-MAPS) to overcome the challenges associated with conventional drug delivery (Figure 2.**)** [54]. The patch system consisted of four layers: (I.) a backing layer made of a water-insoluble polymer to protect biological drugs from enzymatic hydrolysis, (II.) a surface layer made of a polymer sensitive to intestinal pH, (III.) a drug-carrying middle layer, and (IV.) an adhesive layer between the middle and surface layers to create a high concentration gradient between the patch and intestinal enterocytes. In this study, three different surface layer polymers were tested, hydroxypropyl methylcellulose phthalate (HP-55), Eudragit L100, and Eudragit S100. Each device was tested in three fasted beagle dogs using fluorescein as a model drug to track T_{max}, (the time when plasma

concentration reaches its maximum level). Each surface polymer tested with the device demonstrated that the targeting of the device was obtained. In another trial, each device was loaded with 125 μg of recombinant human granulocyte colony-stimulating factor (G-CSF) to detect an increase in total white blood counts. Each device was administered orally to four dogs and 125 μg of G-CSF was delivered intravenously to three dogs for comparison. In comparison to the IV injection, the total increase of white blood cells indicated the bioavailability of G-CSF was 23%, 5.5%, and 6.0% for Eudragit L100, HP-55, and Eudragit S100 systems, respectively [55]. The bioavailability of the device was the highest value achieved compared with other oral drug delivery systems at the time [54].

Figure 2. GI-MAPS oral device comprising mucoadhesive patches and an enterically coated capsule [54].

A group from MIT developed an oral biological delivery system (Figure 3**)** inspired by a leopard tortoise's ability to passively reorient [56]. The self-orienting millimeter-scale applicator (SOMA) autonomously positions itself to interact with GI tissue. The device is designed as a monostatic body, meaning it only has one stable position. This is

accomplished by a shifted center of mass and a high-curvature upper shell that enables self-orientation to the preferred upright position. After correctly orienting itself, the device deploys a microneedle array manufactured from active pharmaceutical ingredients directly through the gastric mucosa while avoiding perforation. By using insulin as the model drug, SOMA was tested in rats and swine to demonstrate safety and efficacy. The study showed that the plasma insulin levels from SOMA were comparable to those with subcutaneous admission [56].

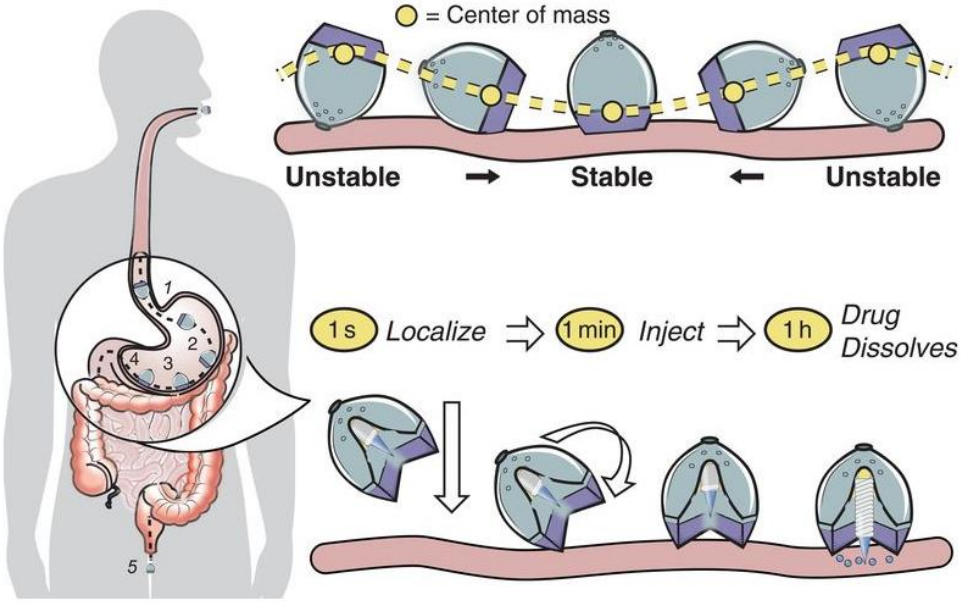

Figure 3. SOMA self-orienting to its stable position and delivering drug [56].

The same MIT group developed another biological drug delivery device termed the luminal unfolding microneedle injector (LUMI) pill (Figure 4**)** [53]. LUMI consists of three degradable arms spring-loaded into a capsule. Each arm consists of a dissolvable drug-loaded microneedle patch. The device utilizes a polymer coating, designed to dissolve at a pH greater than 5.5, in combination with a polyethylene glycol (PEG)

coating to encapsulate a compressed spring that propels the LUMI out of the capsule. After the device is propelled from the capsule, each arm stretches the tissue and presses the microneedle patches into the tissue wall, where they penetrate the epithelial barrier, dissolve and release the encapsulated drug [57]. The researchers used insulin as a model drug and demonstrated that LUMI provided a faster pharmacokinetic uptake profile and a systemic uptake greater than 10% of that of a subcutaneous injection over a 4-h sampling period [53].

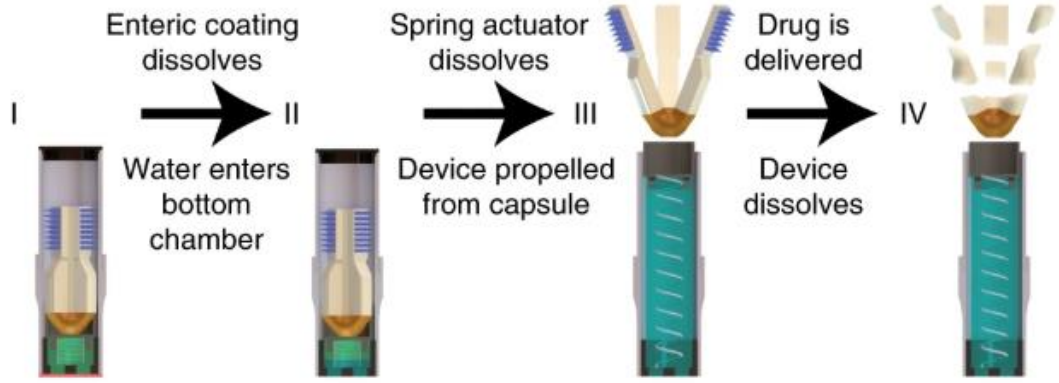

Figure 4. The luminal unfolding microneedle injector (LUMI) actuation scheme [53].

Rani Therapeutics is a private-based company that is developing an ingestible drug delivery system named the RaniPill (Figure 5**)**. From the outside, the Rani Pill appears to be a standard capsule, but several mechanisms occur after ingesting. After entering the GI tract, the outer capsule dissolves exposing a tiny valve that separates two chambers filled with citric acid and bicarbonate. Then the valve dissolves causing the two chemicals to combine which produces carbon dioxide. The carbon dioxide gas inflates a balloon-like structure which drives dissolvable sugar microneedles into the wall of the intestine. The needles then detach from the remaining capsule and slowly dissolve,

introducing the drug into nearby blood vessels. The remaining components either dissolve or pass through the body [58]. Rani Therapeutics is currently testing daily oral insulin pills in human trials [59].

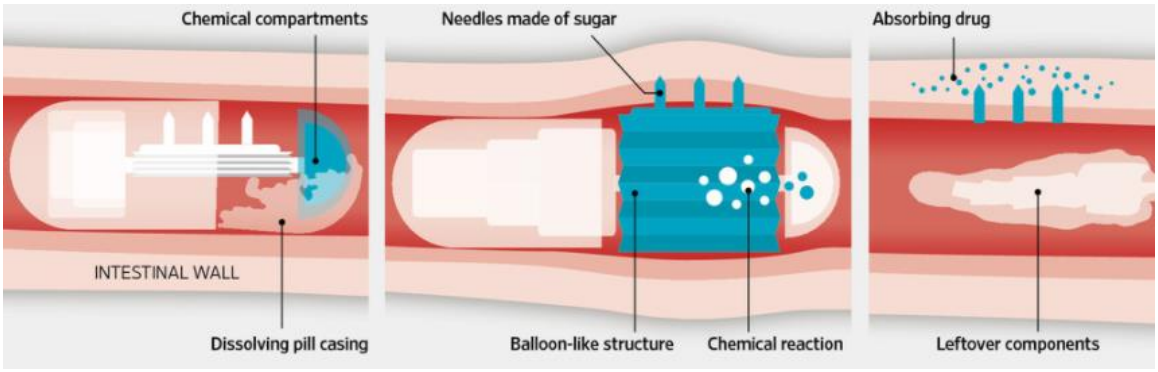

Figure 5. The RaniPill actuation process [59].

1.3 Previous Research and Approach

Although there have been several semi-successful oral biological drug delivery devices produced by multiple groups, they each lack the ability for long-term attachment (greater than 2 weeks). Terry et al had previously been developing a long-term ingestible capsule robot (ICR) for the use of active diagnostics, intervention, and bio-sensing (Figure 6**)** [60]. They designed this with the intention that if physicians can constantly monitor specific elements of the GI tract, better clinical diagnostics could be achieved. For example, the temperature and pH of the intestine have been considered two vital factors that control enzyme activity which thereby affect digestive function [61]. In addition to diagnostics, a long-term attachment may provide other possible functions such as physical tissue manipulation or drug delivery.

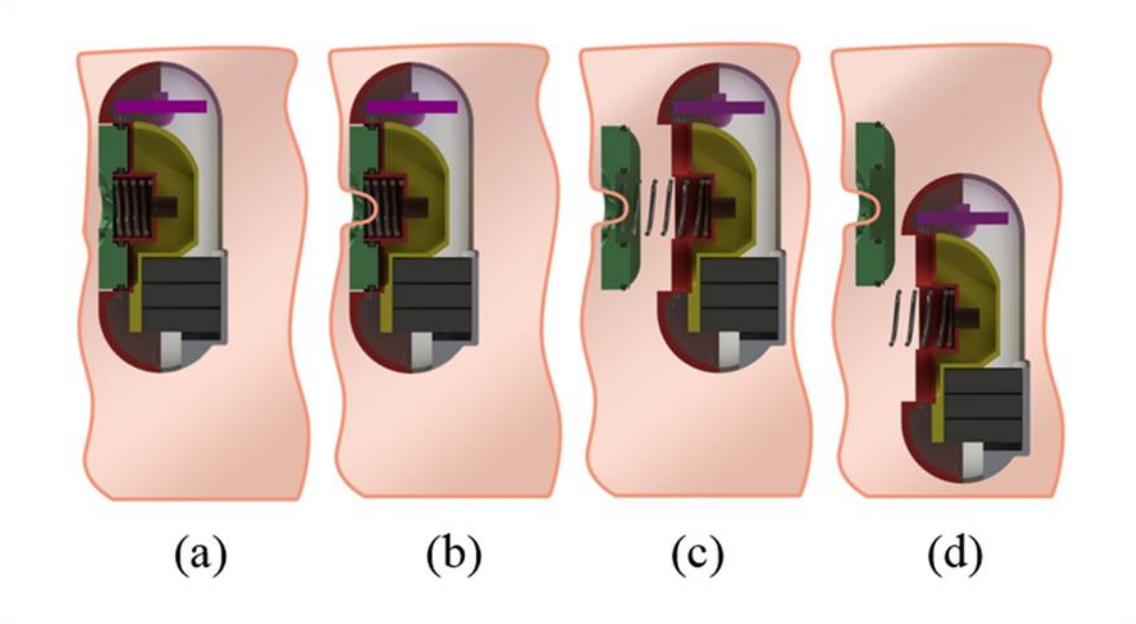

Figure 6. Schematic showing the noninvasive implantation of attachment mechanism on the mucosal lining of the GI tract via a long-term ingestible capsule robot (ICR).

Employing the same design, our current group wanted to use the ICR for systemic delivery of physically and chemically unaltered biological drugs into the submucosa layer of the small intestine. The use of existing, unmodified biological drugs eliminates the cost and complications associated with developing new drugs. It is estimated that new drug development can cost somewhere between $500 million to $2 billion [62], meaning delivery of unaltered biological drugs could save industries money and time. Despite having the capability for systemic drug delivery, the previous ICR had some drawbacks. The dimensions of that ICR were not within the standard ingestible capsule range and contained several electronic components unnecessary for drug delivery. The fabrication process was complicated therefore the device was not mass-producible. Furthermore, all previous optimizations were done on dead, excised porcine intestinal tissue lacking the dynamic properties of live tissue. In this current work, the TRL is developing a mass-

producible, standard capsule sized ICR tailored for long-term drug delivery. The drug delivery ICR is designed so that it passively travels to the small intestine via digestive peristalsis after it is swallowed. The goal is for the ICR to deploy the drug-carrying payload into the submucosa via a novel tissue attachment mechanism referred to as the "TAM".

Inspired by intestinal parasites, the system relies on suction or negative pressure for tissue attachment. Biomimicking the sucking action of a parasite, the TAM consists of an orifice with stainless steel needles angled down and inward, acting as the teeth of a parasite, referred to as the TAM needles (Figure 7A). The stainless steel orifice and needles are mounted on a 3D printed TAM body via ultraviolet (UV) glue. (Figure 7B). Upon reaching the small intestine, the TAM is ejected from the ICR and remains adhered to the mucosa for a prolonged period while maintaining intimate contact with the tissue. An advantage of using the TAM for long-term attachment is the lack of pain receptors along the GI tract [63]. One possible application enabled by this extended intimate contact with tissue is extended-release drug delivery. The payload could be contained inside the TAM unaltered and separate from the ICR, thus enabling the payload to be simple, small, and biocompatible. Like a subcutaneous injection, the drug may be injected directly through the submucosa layer, thus bypassing the barrier function of the small intestine wall.

Figure 7. A) TAM orifice and TAM needles. B) TAM Body

To maximize attachment reliability**,** my collaborator Sunandita Saker**,** designed and optimized a mass-producible miniaturized TAM suited for a drug delivery ICR. Based on previous research, attachment success and duration depends on multiple independent factors related to TAM geometry (orifice diameter, number of needles, needle angle, needle length, needle width), vacuum volume, and small intestine tissue location (duodenum, jejunum, or ileum) [60]. Sunandita implemented a factorial design of experiments in her research to screen and optimize the design with a reduced number of trials for optimal success. Concurrently, the drug delivery portion of the ICR was developed and is the main topic of this thesis. Due to the simultaneous development of the optimized TAM geometry, throughout this work the dimensions of the TAM change. Also, the ICR used in this research does not contain any electronics or robotic functions, therefore it will be referred to as the capsule.

1.4 Research Objectives

The overall scientific objective of the research was to utilize subcutaneous needle injection methodology used for parenteral systemic biologic drug delivery to solve the problem of delivering biologics orally for treating diseases like diabetes, arthritis, or cancers. This was accomplished by showing proof-of-feasibility of biological drug delivery via needle injection into the small intestine. The first goal was to develop a prototype TAM that integrated a commercial off-the-shelf (COTS) drug delivery system for systemic administration of glucagon-like peptide 1 (GLP-1) or a suitable surrogate via the intestinal wall. Specifically, a custom needle was developed for administering drug to the submucosa of the small intestine. A COTS osmotic pump was then integrated with the custom needle and tested for its drug delivery performance using benchtop models. The injection needle and the COTS pump were incorporated into the TAM, and the entire system was tested in a live porcine model for long-term drug delivery using adalimumab as the administered biological drug.

The second goal was to design (without physical implementation) a custom osmotic pump that is compatible with the capsule system. A custom osmotic pump was designed using dimensions and specifications from a commercial manufacturer of these types of pumps. The custom pump design met the criteria for use in the complete capsule system but was not fabricated or tested in this current work.

Chapter 2: Drug Delivery System

2.1 Functional Requirements of Drug Delivery System

1. Location of Delivery

The drug shall be delivered to the small intestine, ideally near the ileum region. The ileum region is where most GLP-1 is naturally secreted from enteroendocrine cells (L cells). Systemic delivery shall be administered to the submucosa.

2. Duration of Administration

The drug injection needle and osmotic pump should deliver GLP-1 (or a suitable surrogate) for 4-7 days at a minimum bioavailability of 10%.

3. Success Rate

Although this project was designed to assess feasibility, we created a design that targets a success rate of greater than 90%, i.e. at least four days of sufficient drug is administered in 9 out of 10 TAM trials in different animals (to be studied in future work).

4. Animal

The TAM shall function properly in a fed, watered, and awake pig without harming one animal.

5. Component Materials and Properties

The drug injection needle and the osmotic pump will be made with non-toxic parts. The osmotic pump used in experiments will be a commercially available osmotic pump.

6. MRI Compatibility

The osmotic pump and drug delivery needle shall be compatible with MRI.

7. Cost

The cost of the capsule system should be less than $50 (based on 50,000 units/year).

8. Manufacturability

The system shall be manufacturable in a timely fashion on a scale of 100,000 units/year. Note: this quantity is different from the cost quantity to make a conservative case in both categories.

2.2 Initial design of the Drug Injection Needle

The purpose of this task was to design and fabricate a custom injection needle for implementation on the TAM to administer a biological drug to the submucosa. The initial approach was to modify a 30-gauge brain infusion needle (BIN) available from Alzet (Figure 8). The cannula was a 3 mm long stainless steel tube with a 0.16 mm inner diameter and 0.31 mm outer diameter (the cannula was not hypodermic). The cannula was selected as a preliminary approach since it could easily be attached to the Alzet osmotic pumps that would be used for drug delivery later in this work. The cannula is attached to the osmotic pump via a thin, small, plastic tube referred to as a catheter in this work. The infusion kit was modified by removing the pedestal to expose the low-profile L-shaped steel tubing. The TAM and drug delivery needle required space in the capsule for tissue suction. To accommodate the BIN, a special capsule for benchtop testing was designed and 3D printed (Figure 9-11). The vacuum aspiration port was necessary to create a negative pressure but in the final design, the negative pressure will be carried on board. After the capsule was created, varying lengths of BINs were inserted through the capsule hole and each BIN's base was glued to the bottom of the capsule. The complete assembly is shown in Figure 12-15.

A preliminary experiment was set up to determine if the BIN could deliver a drug into the submucosa of excised intestinal tissue. The goal of the experiment was to determine a criterion that showed drug delivery into the intestinal tissue with a needle. For the tests, drug injection needle lengths varied from 0.5 mm to 2.5 mm (the tip of the canula was 4.5 mm to 2.5 mm away from the top of the TAM body, respectively). In the experiment, intestinal tissue was placed over the orifice of the TAM and drug injection needle. Next, the vacuum valve was opened exposing the tissue to 600 μL of -25 mmHg air. The negative pressure causes the intestinal tissue to aspirate into the space of the capsule. When tissue is aspirated into the capsule, the TAM needles penetrate the mucosa layer causing a firm attachment to the intestinal wall. During the aspiration of the intestinal tissue, the drug injection needle could also penetrate the submucosa. After a strong aspiration and attachment, colored water (mimicking drug) was pushed through the drug injection needle and potentially into the intestinal tissue by a syringe pump and catheter. Approximately 2 mL were injected into the intestinal tissue so that one could easily visualize delivery, fulfilling the goal of finding a criterion to confirm delivery. The experimental setup is shown in Figure 16.

After the preliminary experiments with the BIN integrated with the device, it was decided using a 30-gauge needle to penetrate the submucosa and deliver a drug bolus was feasible (Figure 17 and Figure 18). This experimental setup was used later in this work and the results are explained in more detail. Although the Alzet BIN showed benchtop drug delivery, it proved difficult to modify due to size constraints, so it was decided to make custom drug injection needles using a 30-gauge needle. Another downside to using the BIN was its inconsistency in piercing the mucosa. This was likely due to the BIN

being a non-hypodermic needle, so succeeding experiments were tested with a hypodermic needle. Figure 19 shows the difference between a blunt canula and a beveled hypodermic needle.

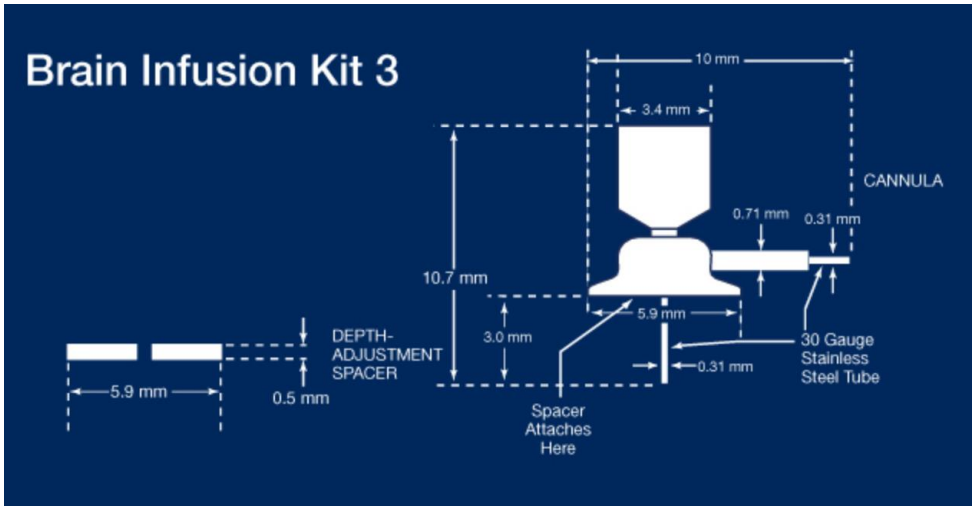

Figure 8. Schematic of the brain infusion kit from ALZET.

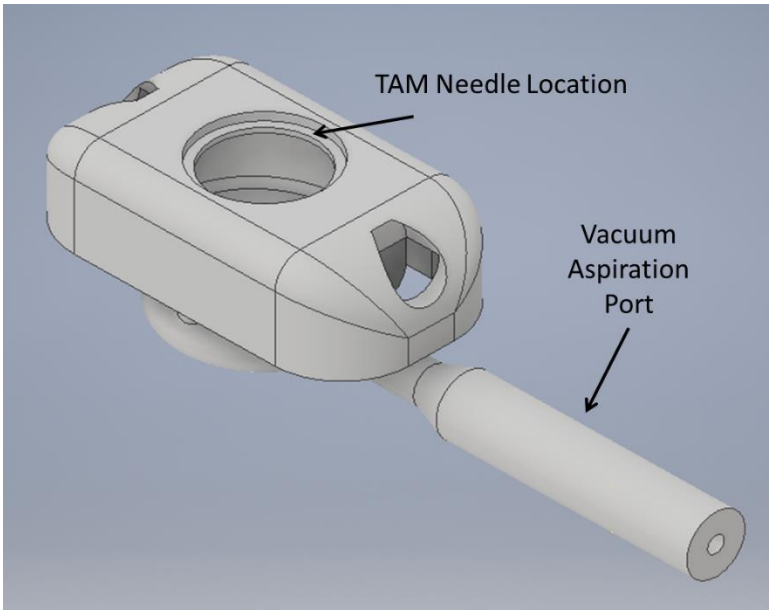

Figure 9. CAD design of a capsule compatible with the BIN.

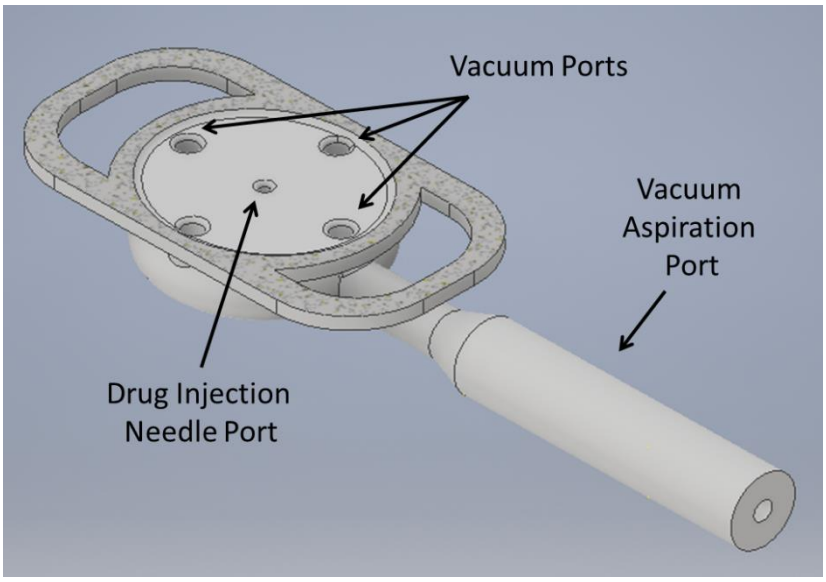

Figure 10. CAD design of a capsule compatible with the BIN (cross-section).

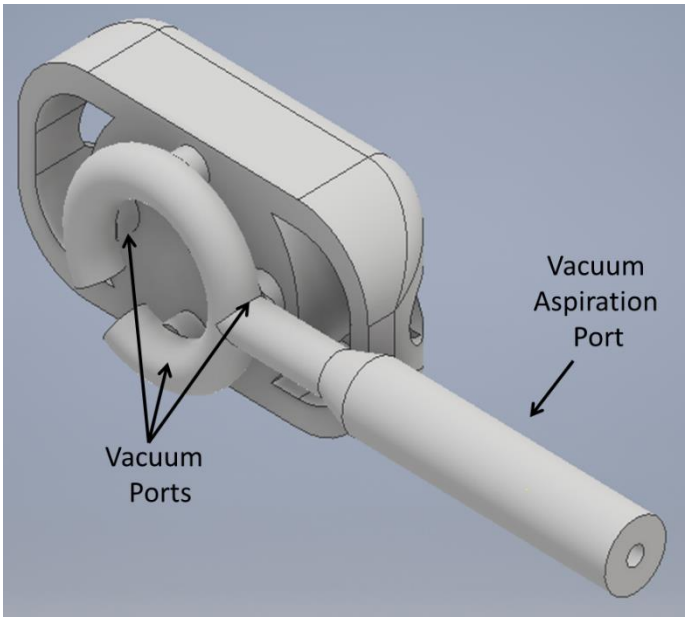

Figure 11. CAD design of a capsule compatible with the BIN (bottom-view).

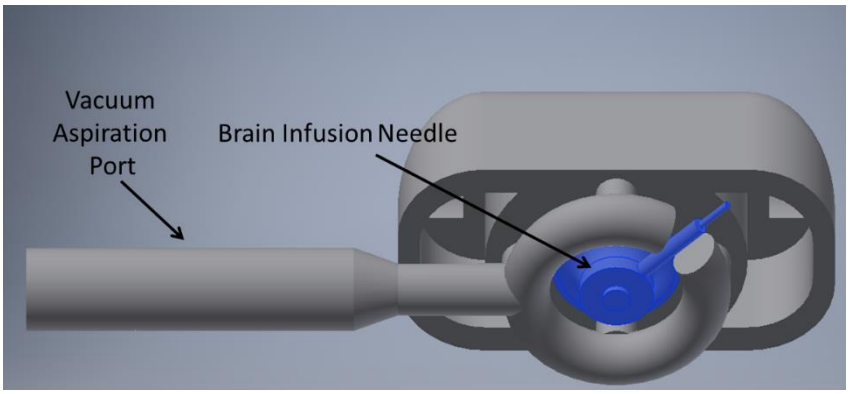

Figure 12. CAD assembly of a capsule with the BIN.

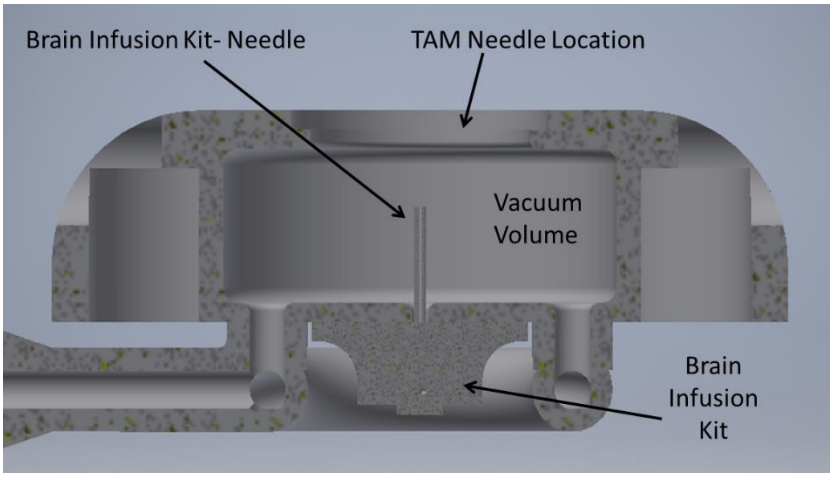

Figure 13. CAD assembly of a capsule with the BIN (cross-section).

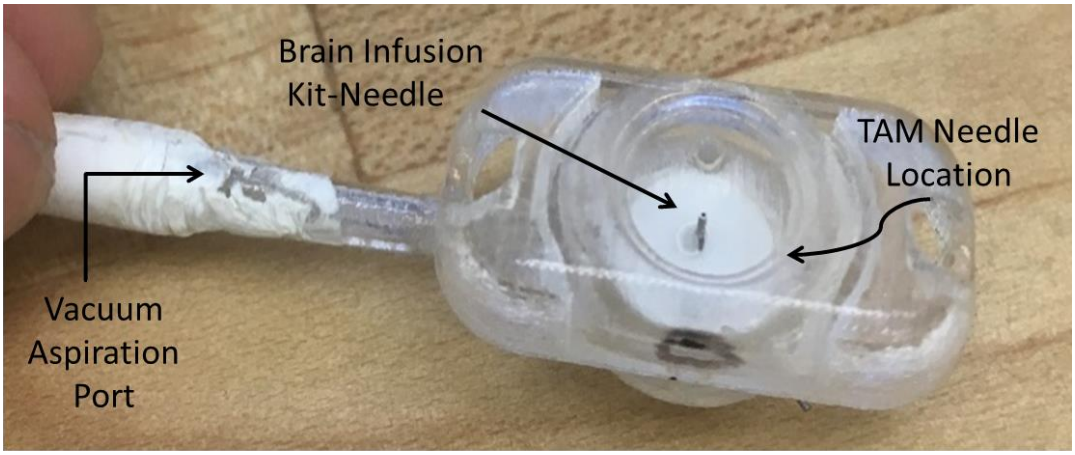

Figure 14. Assembly of a capsule with the BIN.

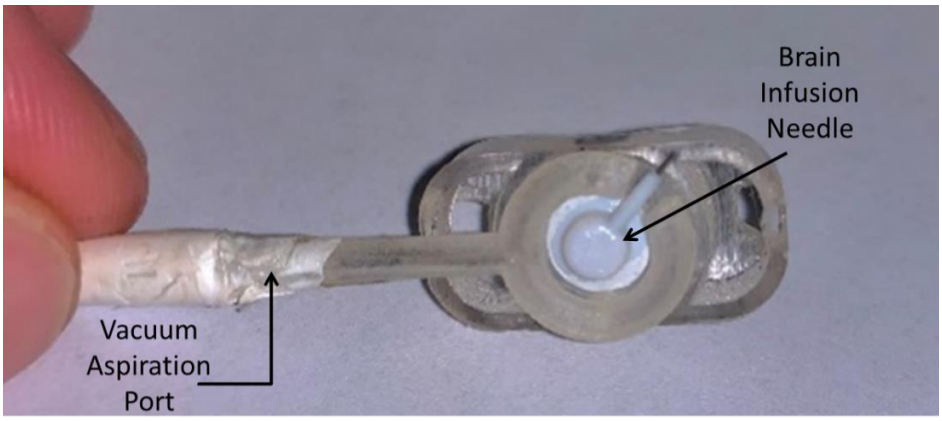

Figure 15. Assembly of a capsule with the BIN (bottom-view).

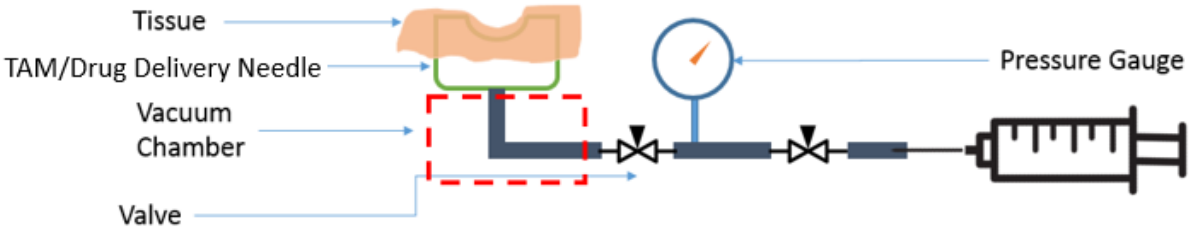

Figure 16. Aspiration system with TAM/drug delivery needle.

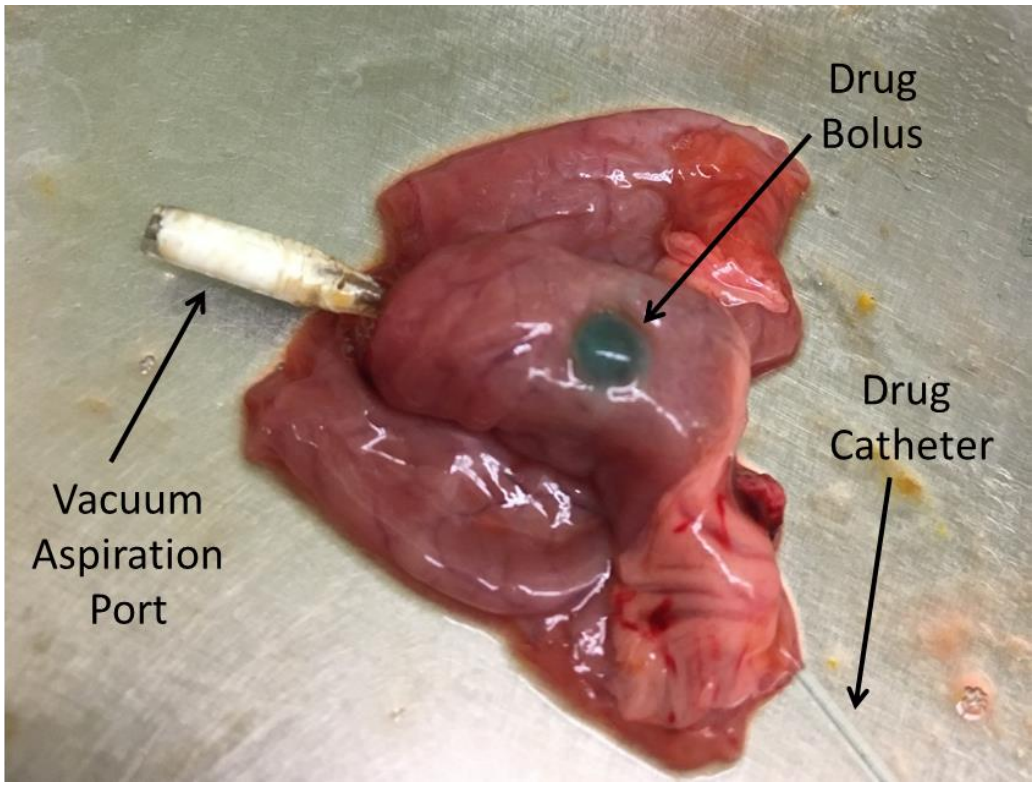

Figure 17. A representative image of BIN delivering a "drug" bolus. Colored (green) water was used in this benchtop study.

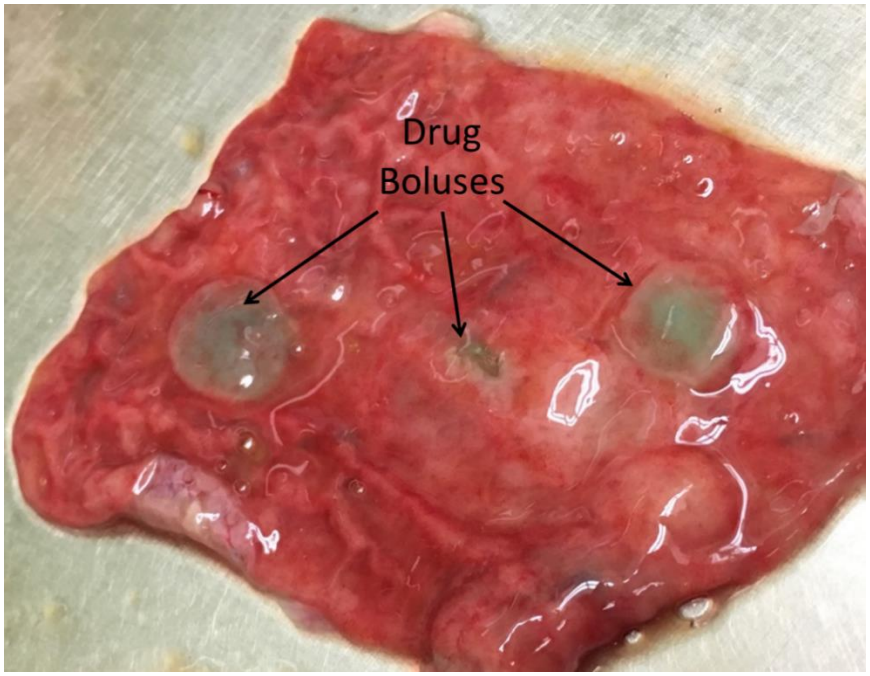

Figure 18. Several “drug” boluses showing successful drug delivery using the BIN prototype.

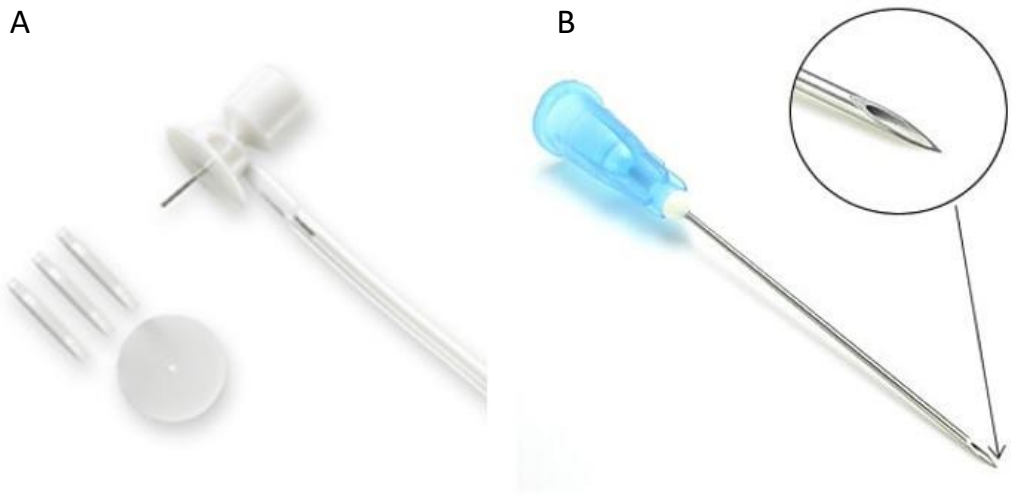

Figure 19. A) ALZET's blunt canula (needle) and B) a beveled hypodermic needle.

2.3 Alternative Designs for Drug Delivery

To achieve reliable drug delivery, alternative design concepts were brainstormed (Figure 21). The previously described bench-top experiments helped determine feasibility and gain knowledge of the newly introduced concepts. Designs 2-4 required the needle to connect to the osmotic pump via a catheter (or some other channel). In the concepts below, the designed osmotic pump is shaped like a torus and is explored later in Chapter 3. The five alternative designs for attachment are described below and variations of the capsule are shown in Figure 20.

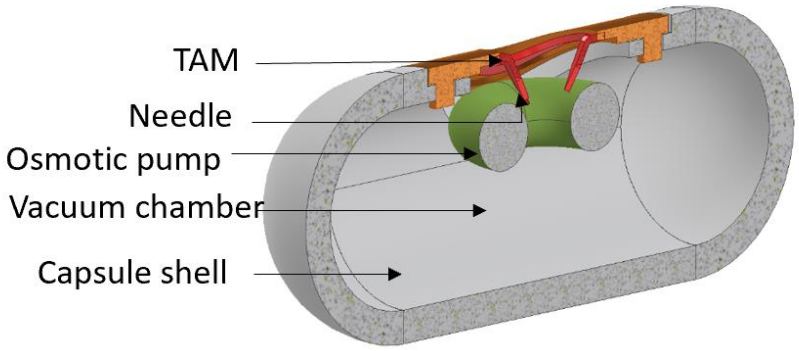

Figure 20. Concept model of capsule illustrating a torus-shaped osmotic pump.

Design 1: Perpendicular Needle

In the perpendicular needle design, the drug injection needle is within the torus-shaped osmotic pump. The injection needle is connected directly to the osmotic pump with 2-4 ports. The needle perpendicularly pierces the tissue upon aspiration. This design was similar to the benchtop test described above with the BIN.

Design 2: Spring-Loaded Needle Outside Capsule

In the spring-loaded needle design, the injection needle is offset from the orifice of the TAM, therefore away from the aspirated tissue. The drug needle penetrates the tissue via a pre-loaded spring during the attachment sequence. The advantage of this design is that it mitigates the possible problem of reduced blood flow to aspirated tissue because the needle is outside the aspiration zone.

Design 3: Dual-Purpose Needle

In the dual-purpose needle design, the injection needle replaces one of the TAM's needles and thus has dual purposes: to perform tissue attachment as well as provide a channel for the drug. This concept would require no extra injection needles.

Design 4: Spring-loaded Needle within Capsule

In the spring-loaded needle within the capsule design, the injection needle is within the capsule at some undetermined orientation. In this design, the needle approaches horizontally. The injection needle is spring-loaded and independent of tissue aspiration.

Design 5: Drug pool through TAM hole

In the drug pool design, the concept is to create a reservoir of drug between the pump and the tissue. The drug is pumped out of the osmotic pump over time and stored in a closed capsule to prevent leakage into the lumen. The drug then enters the submucosa through the channels created by the TAM needles. With this concept, there is no direct drug injection, therefore no need to rely on drug needle penetration depth.

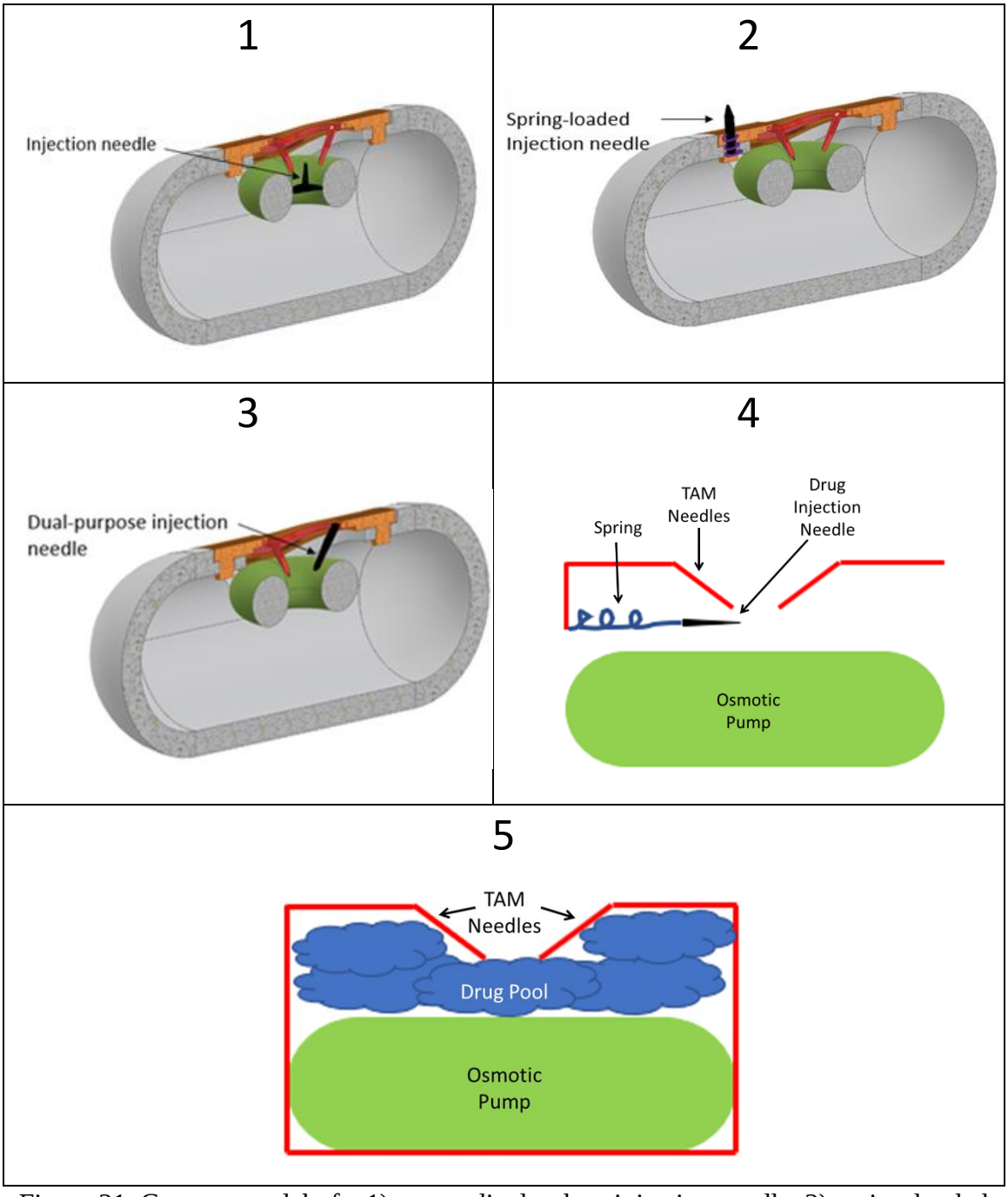

Figure 21. Concept model of a 1) perpendicular drug injection needle, 2) spring-loaded drug injection needle, 3) dual-purpose drug injection needle, 4) spring-loaded drug injection needle within the capsule, 5) drug pool within the capsule

2.4 Down Selection Process

To determine which approaches to drug delivery were better suited to the application, the six team members scored each design in a Pugh Matrix. After several iterations of scoring, the concept with the highest score was the “drug pool” concept. However, due to the novelty of this concept, it was decided to not use this idea in initial testing but rather use the second-highest scoring and third-highest scoring concepts, the dual-purpose needle, and the perpendicular drug injection needle, respectively.

Below are the evaluation parameters and weights (Table 2 and Table 3) for the last iteration of the Pugh Matrix. The perpendicular drug injection needle was the reference, so it received “0” for every parameter. The devices were scored based on the following scale:

+2: much better than the baseline.
+1: somewhat better than the baseline.
0: equal to the baseline.
-1: somewhat worse than the baseline.
-2: much worse than the baseline.

Table 1. Drug delivery evaluation criteria matrix with weights

	Evaluation Parameters	Weight (1,3,9)
	Development risk/complexity	
1	Technical feasibility	9
2	Development time	9
3	Development expense (technologies employed, cost to integrate)	3
	Robustness of penetration	
4	Reliability of tissue penetration	9
5	Risk of penetrating too far	9
6	Needle engagement robustness	9
	Robustness of drug delivery	
7	Bioavailability performance	9
	Size profile	
8	Size Profile	9
	Cost	
9	Part complexity, tolerances required	3
10	Labor (manual vs automation)	3
11	IP favorability	1
12	Dead volumes and/or material use efficiency	1
	Manufacturability	
13	Assembly complexity	9
14	Manufacturability, chemical and/or wet processes	3
15	Scalability	9
	Durability	
16	Reliability over shelf life	9
17	Sterilization materials compatibility and risks	9

Table 2. Average score (n=6) of the different design concepts.

Attachment Concepts

Evaluation Parameters	Weight (1,3,9)	Perpendicular Needle	Spring-Loaded Needle	Dual Purpose Needle	Spring-Loaded within Capsule	Drug Pool
1	9	0.0	-1.5	-1.0	-1.8	0.3
2	9	0.0	-1.3	-1.0	-1.3	0.8
3	3	0.0	-1.3	-1.3	-1.3	1.3
4	9	0.0	1.5	1.2	0.2	-0.5
5	9	0.0	-0.3	1.2	0.5	1.8
6	9	0.0	0.5	1.3	0.2	-1.2
7	9	0.0	1.2	0.0	0.3	-1.3
8	9	0.0	-0.3	0.5	-0.5	0.3
9	3	0.0	-1.8	0.5	-1.7	1.3
10	3	0.0	-0.5	-0.2	-0.5	0.5
11	1	0.0	0.0	0.8	0.0	0.5
12	1	0.0	-0.7	0.8	-0.8	-0.5
13	9	0.0	-1.8	0.2	-1.8	0.3
14	3	0.0	-0.7	-0.5	-0.8	0.0
15	9	0.0	-0.5	-0.5	-0.5	0.3
16	9	0.0	-0.7	0.0	-0.7	0.0
17	9	0.0	-0.5	-0.2	-0.2	0.7
	Total	0.0	-8.8	1.8	-10.8	4.8
	Weighed Total	0.0	-48.2	12.2	-64.8	24.5
		Legend				
		much worse	worse	neutral	improved	much improved
		-2	-1	0	1	2

2.5 Design

The dual-purpose needle (Figure 22. A, C, and E) and perpendicular needle (Figure 22 B, D, and F-H) TAMs were designed and created to be tested with intestinal tissue on the benchtop. All drug injection needles used in the experiment were 30-gauge hypodermic needles. The dual-purpose needle had the same dimensions as the TAM needles at the time, as shown in Figure 22 A and C. The needle was 3 mm long at a 30-degree angle relative to the top of the TAM. The perpendicular needle concept had two different versions created, referred to as the non-flush perpendicular needle (Figure 22 F and H) and the flush perpendicular needle (Figure 22 G). The flush perpendicular needle design was designed to have a smaller profile after attachment. This design was introduced after preliminary successes with the non-flush perpendicular needle. In either design, the 30-gauge hypodermic needle is inserted through a 0.5 mm hole in the TAM, bent towards the center of the TAM, and then bent again up towards the top of the TAM orifice (Appendix B shows the full manufacturing process). For both versions, the vertical length of the needle could be modified if needed. After ad-hoc benchtop testing, each version performed best when the hypodermic needle was even with the top of the TAM orifice. To be at the orifice's height, the vertical length of the non-flush and flush perpendicular needle was 5 mm and 2 mm, respectively.

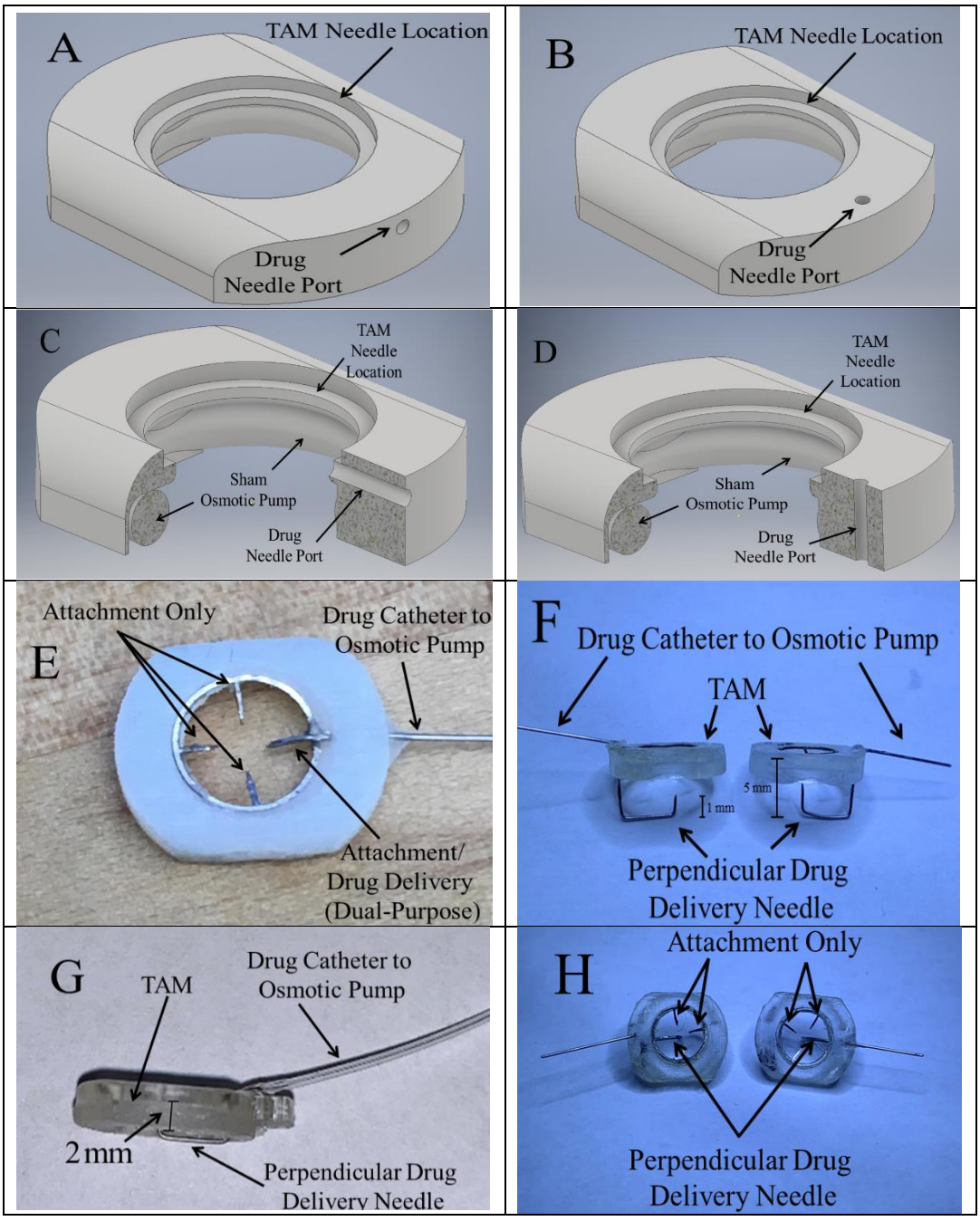

Figure 22. A) CAD design of dual-purpose needle TAM. B) CAD design of perpendicular needle TAM. C) Cross-section CAD design of dual-purpose TAM. D) Cross-section CAD design of perpendicular TAM. E) Top view of the dual-purpose needle TAM. F) Side view of perpendicular needles TAMs. 1 mm needle on the left and 5 mm needle on the right. The heigh of the needles could be altered. G) Side view of perpendicular needle flush to TAM. H) Top view of perpendicular needles TAMs.

2.6 Benchtop Experiments

Following the creation of the devices, they were tested with intestinal tissue on the benchtop**.** Each device was tested in the ileum and jejunum regions of the intestine. The ileum was selected for several reasons, its nutrient absorbent properties, thick wall layer, and is the longest section of the human small intestine [64], [65]. The thicker the tissue is, the easier it is to penetrate without perforating completely through the intestinal wall. The jejunum was also used to see how the devices would perforate the thin wall of the jejunum. The duodenum was excluded from the test because it had a similar thickness to the ileum but less nutrient absorbing properties. The setup and attachment sequence was the same as described earlier, Figure 16. However, with this setup, the TAM and drug injection needle could be removed from the aspiration system. This was a major advantage over the BIN assembly, creating a smaller attachment profile. After manually injecting the sham drug (colored water) through the drug delivery needle via a syringe, one of three results occurred: 1- The drug injection needle penetration was insufficient and did not deliver the sham drug (Figure 23); 2- The drug injection needle sufficiently penetrated (Figure 24) and formed a bolus of colored water within the intestinal tissue (Figure 25). Occasionally when the bolus was delivered, colored water was visible around the capillaries (Figure 25 and Figure 26); 3- The drug injection needle penetrated too far and perforated the tissue. Each device type was tested 10 times at the jejunum and ileum and recorded as a successful or unsuccessful delivery (Table 3**)**. After running the test, the flush perpendicular needle performed the best at the ileum, followed by the other perpendicular device at the ileum. The dual-purpose device did not perform well at either location. Each failed perpendicular device drug delivery at the jejunum occurred because

the needle perforated too far. All other failures occurred because the needle did not penetrate enough.

Table 3. Results of Benchtop Study.

Needle Type	Tissue Location	Number of Successful Deliveries (10 Trials)	Reason for Failures
Flush Perpendicular	Ileum	10	N/A
Non-Flush Perpendicular	Ileum	7	Penetration Short
Dual Purpose	Ileum	3	Penetration Short
Flush Perpendicular	Jejunum	6	Full Perforation
Non-Flush Perpendicular	Jejunum	5	Full Perforation
Dual Purpose	Jejunum	3	Penetration Short

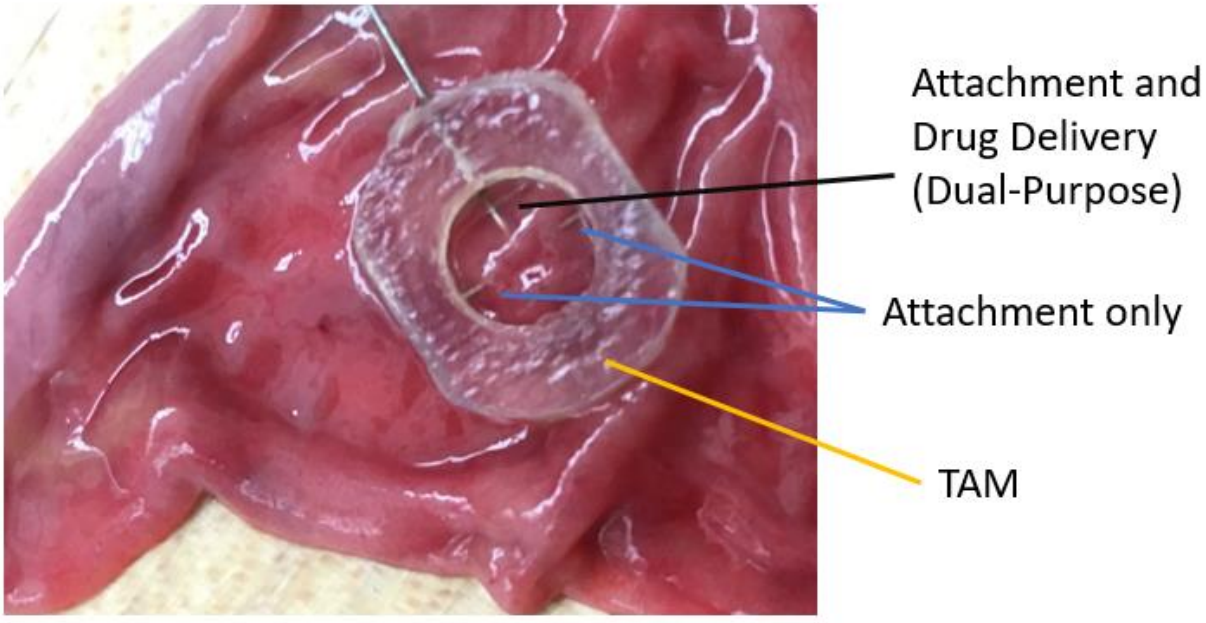

Figure 23. Attached dual-purpose needle.

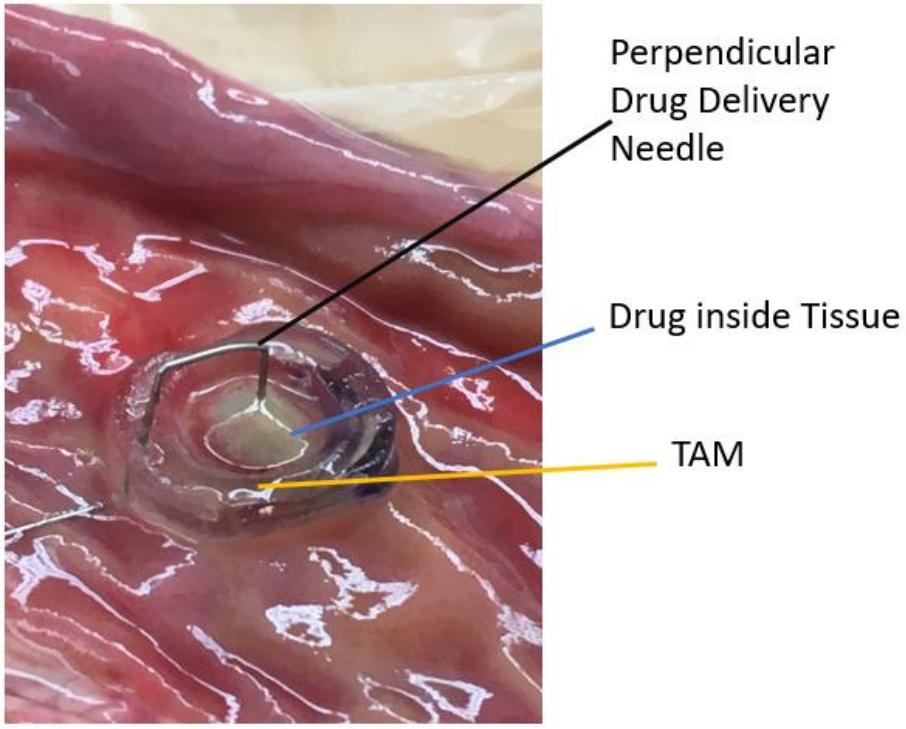

Figure 24. Perpendicular needle delivering drug.

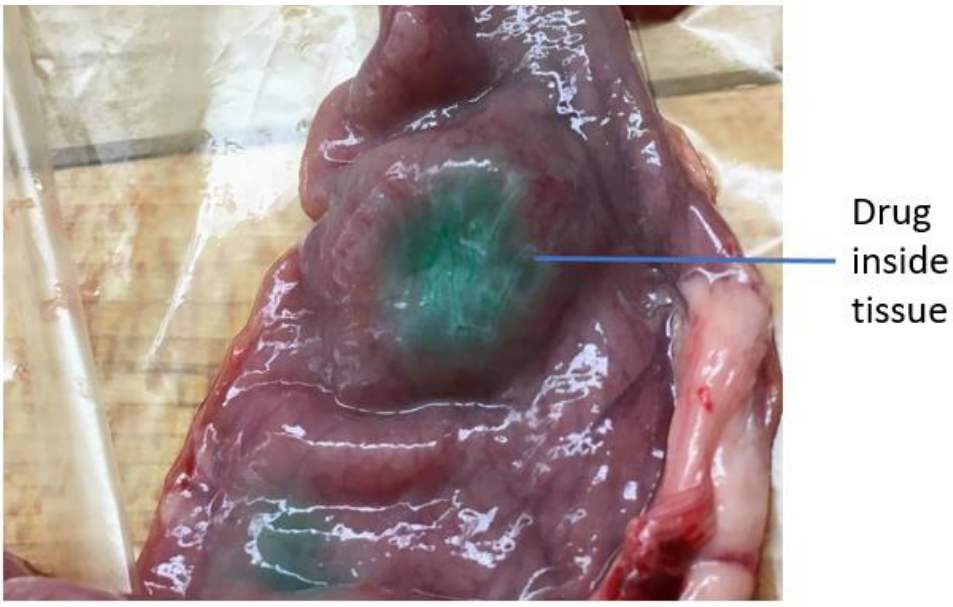

Figure 25. Colored water is shown in/around vessels of the small intestine after delivery from the perpendicular drug injection needle.

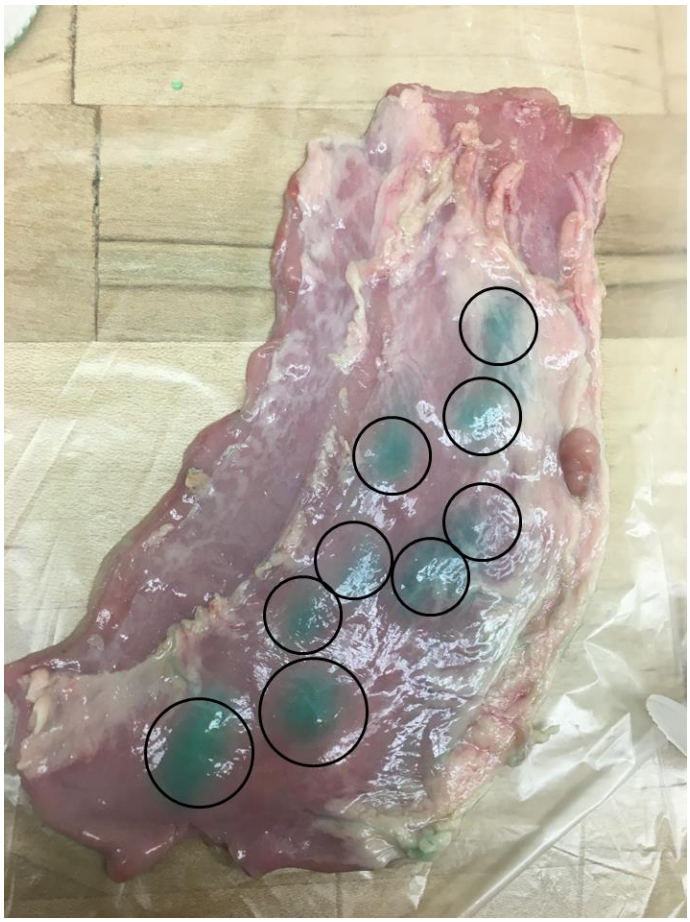

Figure 26. Several boluses of colored water were delivered into the small intestine from the perpendicular needle.

2.7 In vivo Experiment 1

2.7.1 Introduction

Based on the benchtop results, an in vivo experiment was designed. The flush perpendicular drug delivery needle (referred to simply as the perpendicular needle hereafter) was used in the ileum region. Adalimumab (PGN-001) was selected to be delivered based on the guidance of our sponsor, Progenity. Adalimumab is a biological drug used to treat arthritis and is detected in the blood at small concentrations: however, it is nonabsorbable in the small intestine, making it an appropriate surrogate drug to GLP-

1. Essentially, adalimumab is only detected in plasma samples if it is injected into the submucosa. It does not show up on plasma samples if it is simply injected into the lumen of the intestine.

2.7.2 Objectives

1) Penetrate small intestinal tissue with the drug injection needle without gastrointestinal perforation

2) Deliver drug systemically via the submucosa of the small intestine for at least four days.

2.7.3 Hypothesis

The drug delivery capsule will deliver non-absorbent biologics into the submucosa of the small intestine and systemically thereafter. This was a methods development study, so the number of pigs outlined in the procedure did not meet the power for statistical significance.

2.7.4 Materials and Methods

After selecting the perpendicular drug delivery needle as the method to deliver the drug, the design of the needle was slightly altered so that it had a smaller profile. This design was tested and confirmed with benchtop testing. The final TAM/drug delivery needle is shown in Figure 27. The capsule chamber was used to aspirate tissue and after attachment, the TAM was manually removed from the capsule, leaving behind only the TAM and drug delivery hypodermic needle. This device was attached via catheters to a 200 μL osmotic pump as shown in Figure 28.

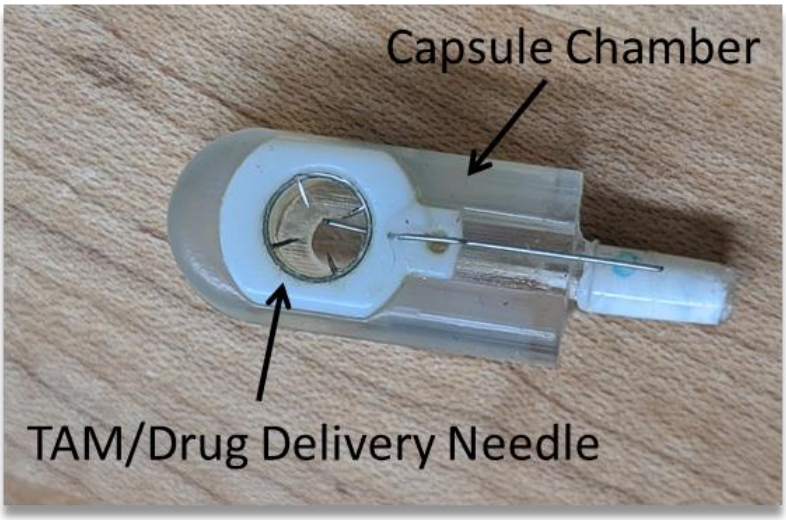

Figure 27. TAM/Drug delivery needle and the capsule chamber for tissue aspiration

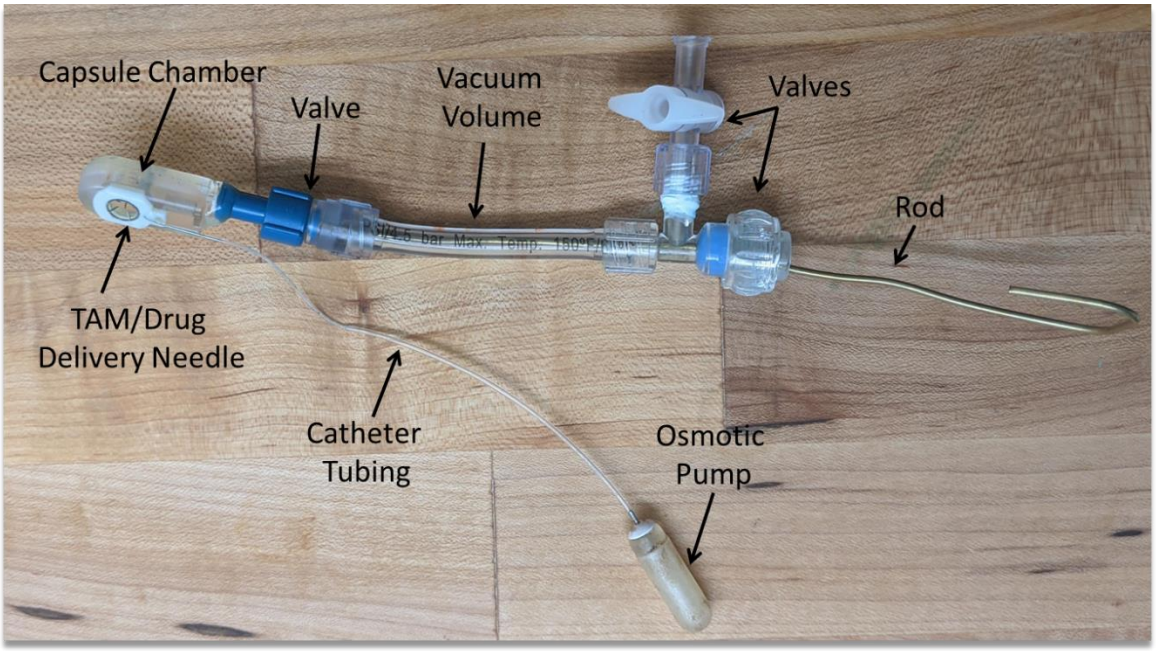

Figure 28. Capsule chamber/TAM/drug delivery needles connected to a 200 ul osmotic pump via catheters. Note: The device is attached to the vacuum system.

The 200 µL osmotic pumps were purchased from ALZET and were primed according to the manufacturer's procedure [66]. This was done to ensure osmotic

pumping would begin as soon as the pump was placed into the intestine after the TAM/drug delivery needle was attached.

During the study, we switched from a 7-day delivery pump to a 1-day delivery pump due to shorter than expected attachment times (results shown later in the chapter). By switching to the 1-day pump, the osmotic pump would ideally have had enough time to deliver all its volume into the intestine before TAM detachment.

Experimental Design

- Animal model: Yorkshire-domestic cross
- Animal size: 20-35 kg (8-10 weeks old)
- Dose delivered: 20 mg adalimumab
- Volume delivered via osmotic pump: 200 μL
- Sample: serum
- Number of animals: 6 animals
- Study duration: 14 days (7 delivery + 7 pharmacokinetics) or 7 days after device detaches
- Sampling frequency: 0, 6, 12, 24 hours and then once daily to necropsy
- Gross pathology
- Histopathology of the site (H&E)

Experimental Groups

1) Negative control (n=1): This pig had drug injected into the lumen of the small intestine via an osmotic pump for 7 days. There was no TAM/drug delivery needle in this animal, only an osmotic pump.

2) Positive control (n=1): This pig had drug fully injected into the submucosa of the small intestine manually with a needle and syringe.

3) Experimental groups (n=4): These pigs received injections into the submucosa of the small intestine using the drug delivery device with an osmotic pump sutured downstream of the intestine. The drug was injected after the tissue was aspirated into a

special "tissue capture mechanism" (TAM). In this study, the experimental groups were separated into:

a. (n=2) 7-day drug delivery osmotic pumps

b. (n=2) 1-day drug delivery osmotic pumps

Surgery/Experimental Procedure

Step 1. Weigh the animal, record weight (in lbs and kg).

Step 2. Administer the anesthetics (TKX shot) and atropine (to decrease salivation).

Step 3. Place the animal on the surgery table. Trim the hair over the abdomen of the pig and clean the skin with isopropyl alcohol and povidone-iodine to create a sterile field.

Step 4. Once the pig is anesthetized, place a jugular catheter for blood samples.

Step 5. Collect 1ml of jugular venous blood samples into an EDTA blood collection tube before capsule deployment. (t=0)

Step 6. Cut the skin of the abdomen using scissors for several centimeters over the region of the intestinal tissue.

Step 7. Bring and secure the desired intestinal tissue (duodenum, jejunum, or ileum) up into the incision field.

Step 8. Cut open the intestine a few centimeters to gain access into the small intestine lumen.

Step 9. Suture osmotic pump within the intestinal lumen. The osmotic pump is to be connected to the capsule device via a 15 cm catheter.

Step 10. Once the osmotic pump is sutured in place (step 9 and step 10 can be reversed), place capsule inside the lumen of the intestine and aspirate tissue to allow for attachment.

a. Place the device against the intestinal tissue and feels for intimate contact.

b. With no air pockets surrounding the device, open the vacuum valve. This will cause intestinal tissue to aspirate into the device (Figure 29).

c. The attachment needles will now be attached to the intestinal tissue (through the submucosa but stopping before puncturing the serosa) Note: This was proven in previous experiments.

d. Remove the device from the vacuum system (Figure 30).

e. Over the next few days, the submucosa will die and slough off causing the device to naturally be released from the tissue.

Step 11. Check for strong attachment by giving a slight tug on the capsule. Make note if it does not attach but continue to attempt attachment up to 5 times.

Step 12. Once the capsule has successfully attached to the small intestine, seal the injection site with skin glue/sutures to prevent leakage of the intestinal fluid into the peritoneal cavity. Suture marker beads next to the attachment site to allow reference for X-ray (Figure 31).

Step 13. Close the skin of the pig using sutures in a running fashion.

Step 14. Give the animal a subcutaneous injection of buprenorphine (0.05 mg/kg) for analgesia.

Step 15. Remove the swine from anesthesia and place it into a clean, warm area for recovery.

Step 16. Using the indwelling jugular catheter, collect 1 ml of jugular venous samples into EDTA blood collection tubes at the following time points post capsule deployment. (t= 6, 12, 24 hours, and once daily to necropsy).

Step 17. After 1 day, allow the pig to return to normal eating habits.

Step 18. Continue collecting blood samples up until necropsy on day 14, or once the device detaches collect blood for 7 days after.

Step 19. On day 14, if the animal is still alive, euthanize it using Fatal-Plus. Collect tissues for histology if desired.

Step 20. Send blood samples to a laboratory for analysis.

Blood Collection:

- Blood Sample Site/Volume: Jugular vein or other accessible veins, ~2 mL
- Type of Blood Tubes: K2EDTA
- Type of Sample: Plasma (~400 µL)
- Sample Storage and Shipment: -60 to -80°C
- Each blood sample is collected from the pig jugular vein, or another suitable vessel via direct venipuncture, placed into a chilled tube containing K2EDTA as the anticoagulant, and inverted several times to mix. Blood samples are kept on wet ice until centrifugation.

Plasma Preparation and Storage:

Blood samples were centrifuged at a temperature of 4°C, at 3,000 x g, for 5 minutes. All samples were maintained chilled throughout processing. Plasma was collected into pre-labeled polypropylene tubes and placed in a freezer at -60 to -80°C until delivered to PBL Assay Science for analysis. The assay work is described in the in vivo study 2 section.

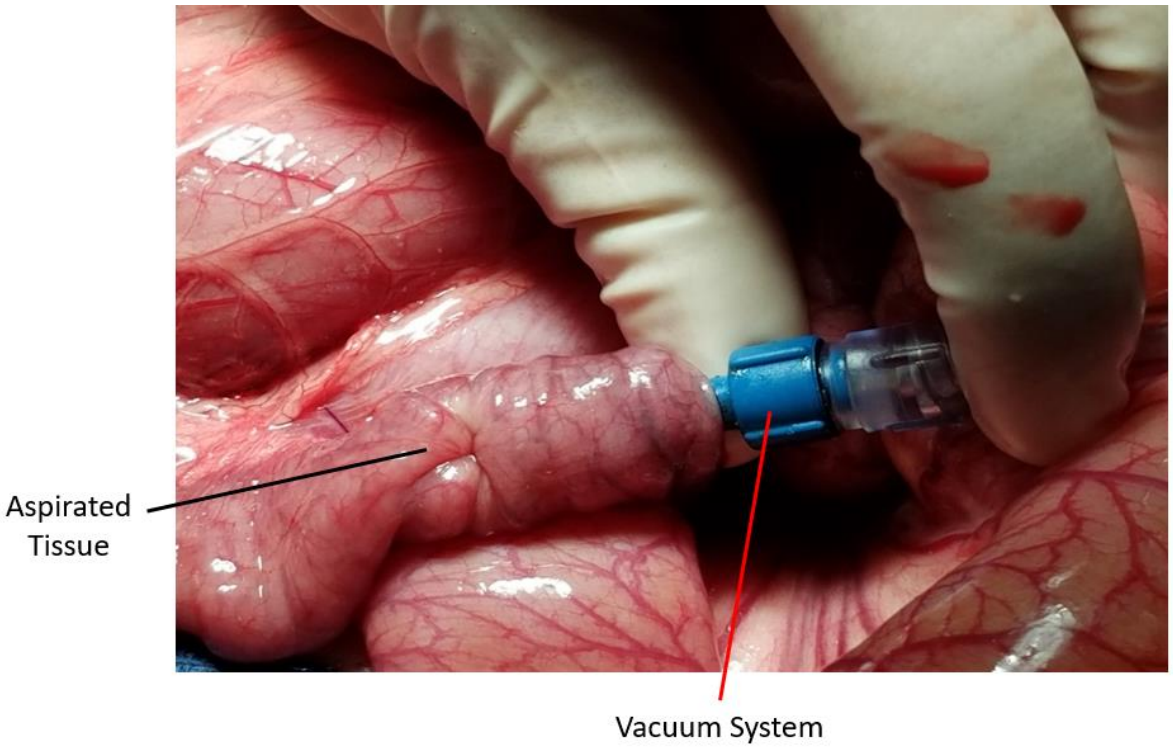

Figure 29. Tissue aspirated into TAM/drug delivery needle

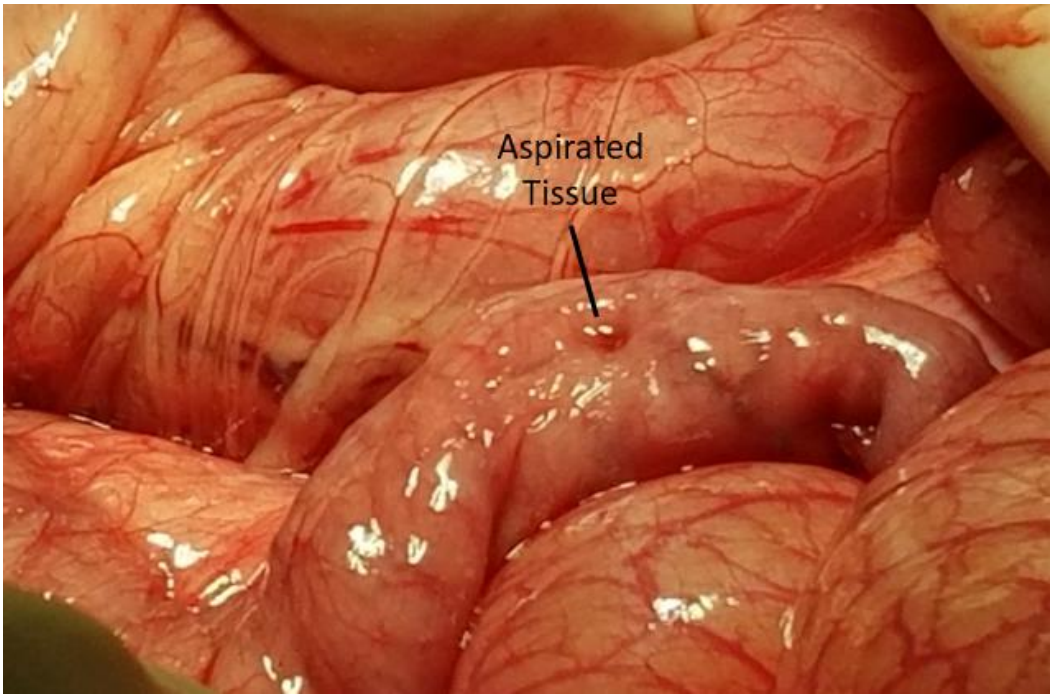

Figure 30 Tissue still aspirated after TAM/drug delivery needle has been removed from the aspiration system

Figure 31. Sutured marker beads for reference of TAM/drug delivery needle during radiographs

Animal Housekeeping Information

Radiographs: The animals were X-rayed at t= 0, 6, 12, 24 hours, and once daily until the device was determined to be detached. The device was considered detached by using the marker beads as a relative position of the device. Radiographs were not taken over the weekends. The radiographs were taken from either lateral side of the animal. These were attempted without snaring of the animal but sometimes snaring was required. Occasionally the hind leg was superimposed on a radiograph. To counter this, the hind leg was pulled back by a technician, while the other took the radiograph.

Blood Draws: Blood draws were taken at the same time points as the radiographs but continued seven days after the device detached because the half-life of adalimumab is seven days. Blood draws were not taken on the weekends, hence the gap in data in the results section. The blood draws in this study were taken from the indwelling jugular vein by one staff member, while another snared the animal. The catheter was first flushed with heparinized saline, the blood was then drawn, and lastly, the catheter was flushed again.

Medications: Meloxicam was administered every 24 hours for 2-5 days post-procedure.

2.7.5 Results

TAM/Drug Delivery Needle Attachment and Pump Duration

As described in the design, the TAM and drug delivery needle were integrated into a single device, so they attached and detached together. The osmotic pump was sutured downstream of the device. In commercial versions of the device, the pump will be integrated into the TAM. The device attachment times were determined via X-rays. By using the marker beads as a reference, the device's attachment/detachment status could be determined. The results of the attachment of this study are shown here (Table 4):

Table 4. Attachment duration of drug delivery TAM and osmotic pump in study 1.

Pig ID	Description	TAM Attachment Duration	Pump Attachment Duration
Exp 1: 7-Day	7 Day Pump/TAM	52 - 100 hours (~2.2 - 4.2 days)	52 - 100 hours (~2.2 - 4.2 days)
Exp 2: 7-Day	7 Day Pump/TAM	24-52 hours (~1-2.2 days)	24-52 hours (~1-2.2 days)
Neg 1	Pump Only- Negative Control	NA	52- 75 hours (~2.2-3.2 days)
Pos 1	Direct Syringe Injection- Positive Control	NA	NA
Exp 3: 1-Day	1 Day Pump/TAM	53-76 hours (~2.2-3.2 days)	53-76 hours (~2.2-3.2 days)
Exp 4: 1-Day	1 Day Pump/TAM	53-76 hours (~2.2-3.2 days)	53-76 hours (~2.2-3.2 days)

Since the facilities are shut down on weekends and X-rays are only taken once a day, the attachment time is shown as a range of time. The early time is the last known time of attachment (Figure 32) and the later time is the next time checked that showed certain detachment (Figure 33**).** All devices were attached to the distal ileum.

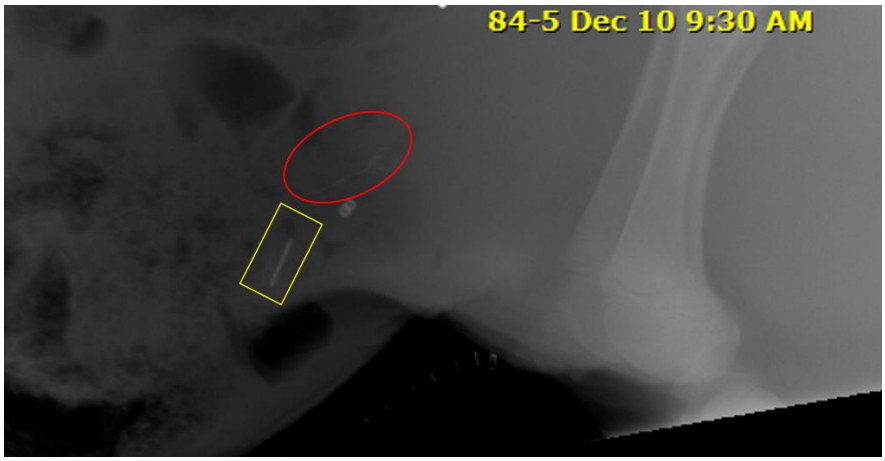

Figure 32. A representative x-ray of an attached TAM/Drug delivery needle. The yellow square outlines the osmotic pump and the red circle outlines the TAM/Drug delivery needle. Between the two are the marker beads.

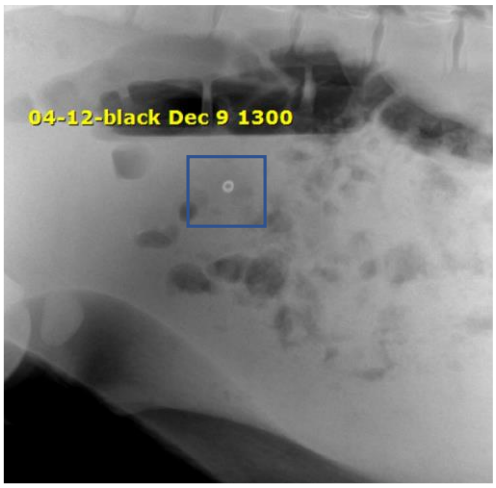

Figure 33. A representative x-ray of a detached TAM. Only the marker beads are shown in the x-ray.

Drug Delivery

The plasma concentration levels for the six different animals are shown below **(**Figure 34).

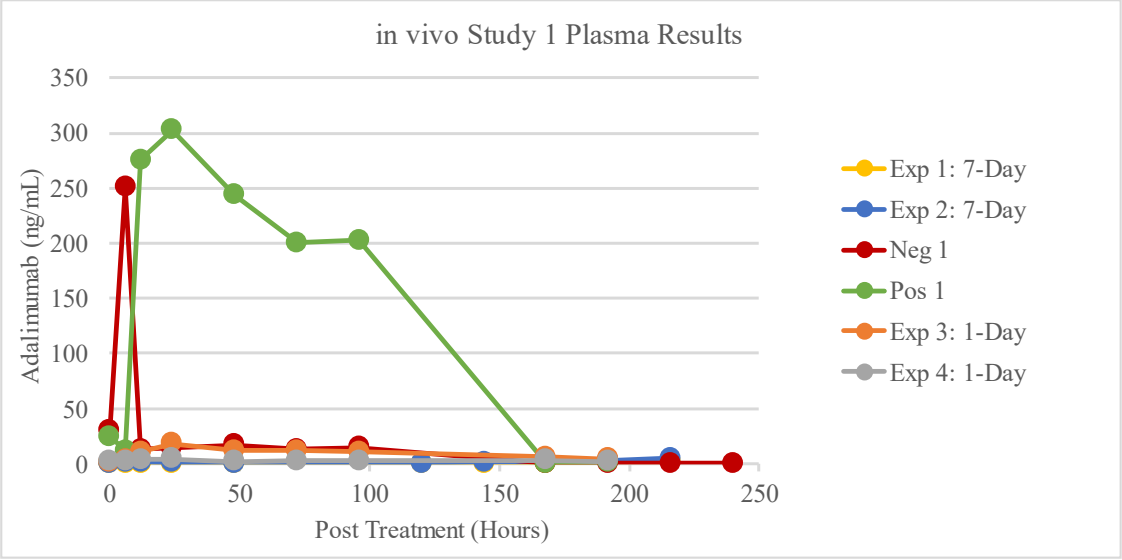

Figure 34. Adalimumab plasma concentration levels from in vivo study 1. Exp 1, Exp 2, Exp 3, and Exp 4 used the TAM/Drug delivery needle and either a 7-day osmotic pump or a 1-day osmotic pump. Pos 1 used a direct needle injection using a manual syringe pump (No TAM/Drug delivery device). Neg 1 used only an osmotic pump sutured into the intestinal lumen.

2.7.6 Complications/Conclusions

This work enabled the veterinarian, staff, and members of the Terry Research Lab (TRL) to refine the procedures and analysis of the drug delivery experiments.

Due to attachment times being shorter than expected, 1-day osmotic pumps were used for the last two animals. Another problem was that the pumps detached from the suture, so a later experiment was performed with a new suturing method and this pump remained intact for at least five days (directly before holiday shutdown so the pig had to be euthanized after five days). This new suture method is explained in more detail in the second study.

Regarding TAM attachment times, all but one TAM was successful in attaching for at least two days. During this study, work was being done to optimize the TAM attachment time for longer durations. As noted in the x-ray results, the osmotic pump detached from the sutures, but a new method has been tested that improves pump attachment times to exceed the TAM attachment time (used in vivo Experiment 2).

The concentration of adalimumab in systemic blood had mixed results. The positive control showed relatively high levels of the drug in the blood, which demonstrates that adalimumab can be delivered in the submucosa of the small intestine and systemically thereafter via a hypodermic needle. Neg 1 showed higher drug concentration in the blood than Exp 1 and Exp 2 (7-day pumps) and Exp 4 (1-day pump) but had similar results to Exp 3 (1-day pump). The results of the negative control were puzzling. Adalimumab may be absorbed across a mucosal surface to some degree, which is a reason for the second in vivo experiment. Exp 3 (1-day pump) showed drug in the

blood but was at least 10 times less concentrated than the positive control and similar in concentration to the negative control. This was a methods development study, so the number of pigs in the results did not meet the power for statistical significance.

We identified several possible reasons for poor drug delivery from the experimental groups and explored them in the next trial. These were:

1. The osmotic function does not perform as anticipated in the small bowel.
2. The drug injection needle possibly does not penetrate deeply enough.
3. The TAM and/or osmotic pump possibly detaches early.
4. Catheter possibly disconnects from the injection needle.

2.8 In vivo Experiment 2

2.8.1 Introduction

Improvements were made to address the above problems and potential problems and the experiment was repeated. Before running the experiment, testing on pig carcasses was performed to further optimize attachment and drug delivery. Many portions of the in vivo experiment 2 were the same as the previous study, so unless otherwise noted, assume the same procedure.

2.8.2 Objectives

1) Penetrate small intestinal tissue with the drug injection needle without gastrointestinal perforation

2) Deliver drug systemically via the submucosa of the small intestine for at least one day. This objective is different than the previous study in that we were looking for less

time delivering drug and were more focused on proving any drug delivery, even over a shorter period.

2.8.3 Hypothesis

The hypothesis for this study is the same as the previous study: The drug delivery capsule will deliver non-absorbent biologics into the submucosa of the small intestine and systemically thereafter. This was a methods development study, so the number of pigs outlined in the procedure did not meet the power for statistical significance.

2.8.4 Materials and Methods

The perpendicular drug delivery device was used again for this experiment, with slight modifications to make the profile smaller **(**Figure 35**).** The rigid arm of the drug needle that attaches to the catheter was shortened. The overall catheter length from the device to the osmotic pump was shortened to about five centimeters.

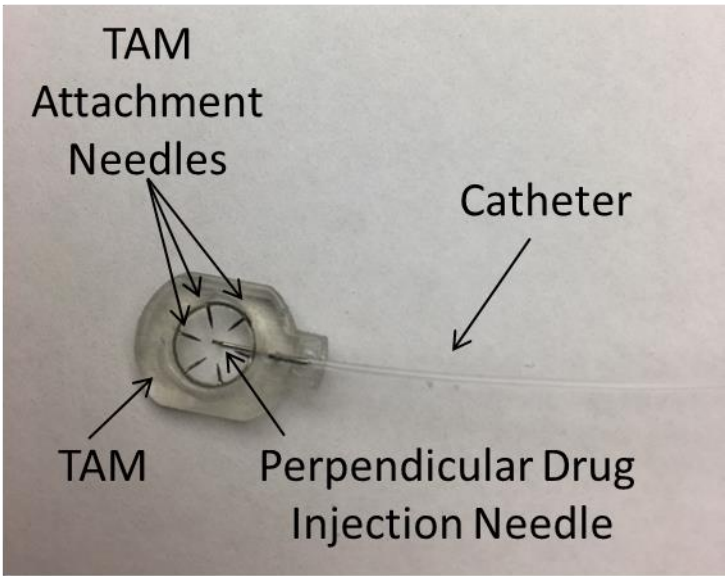

Figure 35. Smaller profile TAM and drug delivery needle device connected to a catheter.

For this experiment, only 1-day 200 µL osmotic pumps were used for the experimental groups. The 1-day pumps were used to ensure the best chance of systemic drug delivery. Due to the osmotic pumps detaching early in the first study, they were sutured differently in this study. This new suture method allowed the pump to attach to the intestine for an extended period and not impact the TAM detachment. The method required drilling a hole in the osmotic pump flow moderator cap to create an extra and more secure anchoring point (Figure 36). This method was tested in animals and was attached for at least five days, meaning the TAM would be the limiting factor since it detaches before five days.

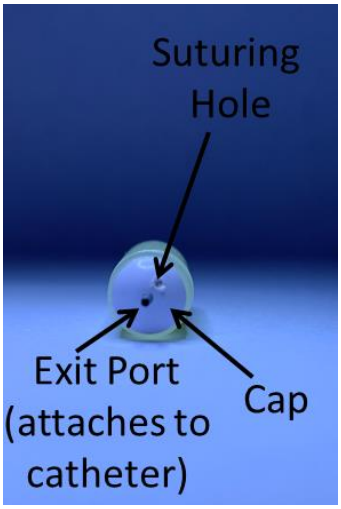

Figure 36. Osmotic pump with a hole drilled into the flow moderator cap.

Experimental Design

The experimental design was the same as the previous study with some exceptions. The breed of pigs was changed to a Duroc Landrace cross breed because the previous breed was unavailable. The duration for this study was shortened to about 36 hours for the inspection of the hardware and tissue in situ following delivery and to

collect hardware and tissue. Due to the shorter study length, blood draws were taken more frequently. Blood was drawn every six hours during the day. To accommodate the more frequent blood draws, arterial catheters were implanted into the animals.

Experimental Groups

The animal groups for this study were:

1) Negative control (n=1): A 1-day delivery pump was used to directly deliver the drug into the lumen of the intestine. Also, an osmotic pump with a long-coiled catheter (~ 75 cm) was implanted to measure the function of the pump. This was used to show how far the meniscus of the fluid had traveled, thus verifying osmotic function (results in Chapter 3).
2) Positive controls (n=2): The TAM/Drug delivery needle was used in combination with a syringe. The device was attached as normal, and then the drug was injected manually with a syringe. This is different from the previous approach where only a hypodermic needle and a syringe were used, and no TAM.
3) Experimental groups (n=3): These animals received injections into the submucosa using the altered TAM shown in Figure 35. All devices were attached to a 1-day osmotic pump sutured with the new method.

Surgery/Experimental Procedure

The procedure was the same as the previous study except for the following alterations to these steps:

Step 9: Use the new suture method and the shorter catheter length.

Step 16: Blood collections are collected every six hours during the day.

Step 18 and 19: The study will only last 36 hours.

Blood Collection

This time the studies were performed to avoid the weekends so that blood draws were taken more often. The total number of blood draws was limited because of the available funds for one Enzyme-linked immunosorbent assay (ELISA) kit. Each ELISA kit contains 96 wells to tests for adalimumab plasma concentration, however several of those wells are occupied for standards and each plasma sample was duplicated. Based on this, 34 total blood draws were taken. Due to the limited number of blood draws, each animal received five blood draws and the positive controls received an extra two blood draws each.

Plasma Preparation and Storage

Same as the previous study

Animal Housekeeping Information

The same as the previous study, but with different duration of housing based on the blood samples described in the blood collection paragraph.

2.8.5 Results

TAM/Drug Delivery Needle Attachment and Pump Duration

The results of the TAM and osmotic pump attachment times are shown in Table 5.

Table 5. Attachment duration of drug delivery TAM and osmotic pump in study 2.

Pig ID	Description	Duration until Necropsy	TAM Attached during Necropsy?	Pump Attached during Necropsy?
Neg 1	Negative Control	34 hours (~1.4 days)	N/A	YES
Exp 1	1-day osmotic pump	33.5 hours (~1.4 days)	SLIGHTLY	YES
Exp 2	1-day osmotic pump	31.25 hours (~1.3 days)	NO	YES
Exp 3	1-day osmotic pump	30 hours (~1.3 days)	YES	YES
Pos 1	Positive Control	48 hours (~2 days)	NO	N/A
Pos 2	Positive Control	46 hours (~1.9 days)	NO	N/A

As shown in Table 5 all the devices and osmotic pumps were placed in the ileum region of the small intestine. All six pigs were healthy and survived to the end of the study. All four osmotic pumps placed into an animal stayed sutured in place for the entire study (Figure 37). Out of the five animals that had a TAM attached to the small intestine during surgery, one (Figure 38) still had the TAM strongly attached during necropsy, while another had the TAM slightly attached. All the devices recovered were completely intact. The TAM needles used for attachment were still UV glued to the TAM body, they kept their appropriate needle angle (Figure 39**)**, and the catheter connecting the drug needle and osmotic pump was undamaged.

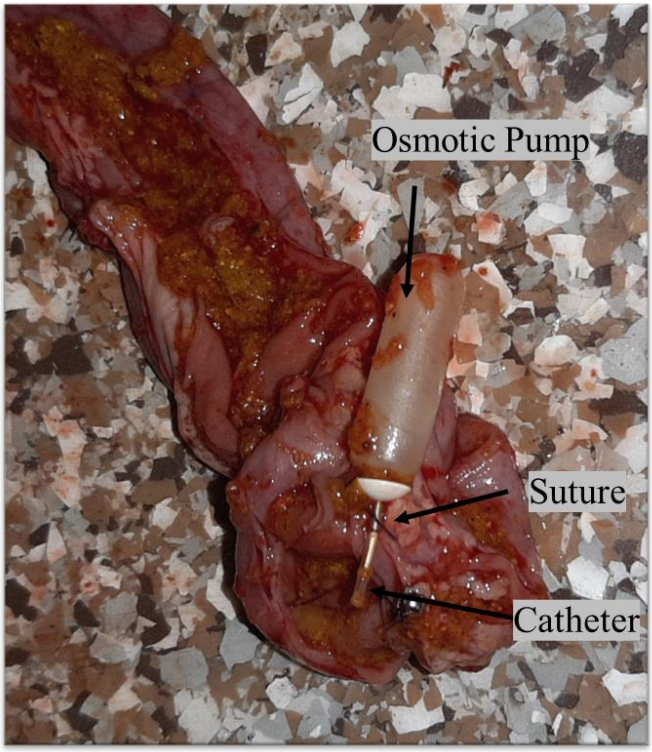

Figure 37. An osmotic pump was sutured in place during necropsy.

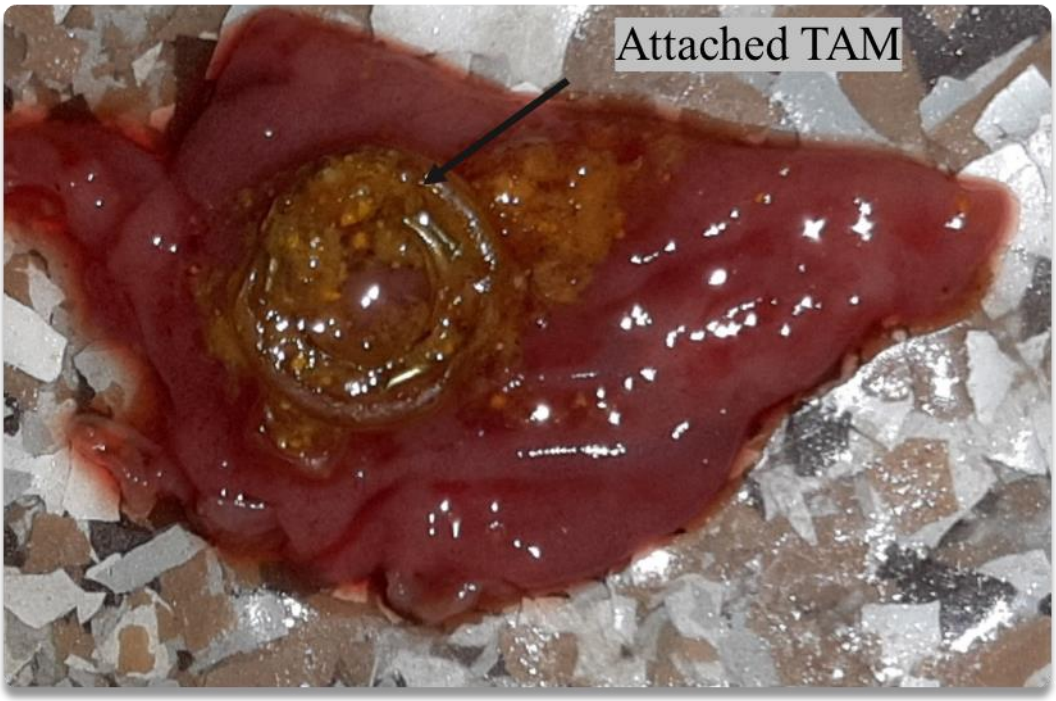

Figure 38. A TAM with a drug delivery needle was still attached to the ileum during necropsy.

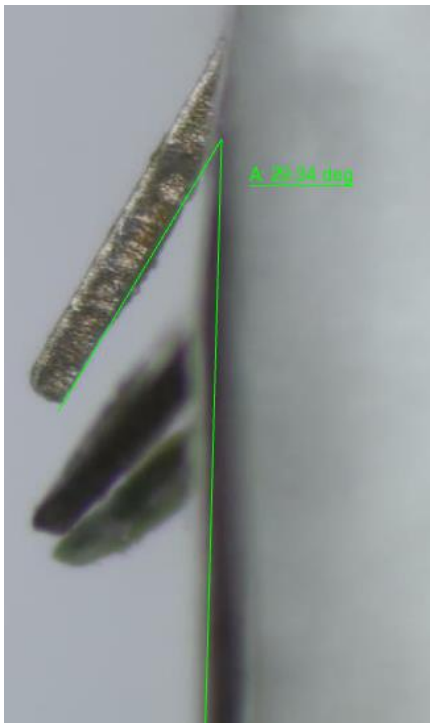

Figure 39. TAM needles were still in their 30-degree orientation.

Drug Delivery

The plasma results for the six different animals are shown below (Figure 40 and Figure 41). The samples were run using two different standards. Figure 40 used kit standard concentration samples of 0, 5, 10, 25, 50, 100 ng/mL while Figure 41 used a more specialized dynamic range of standard samples called “adalimumab injection

standards" and they included sample concentrations from 0, 0.032, 0.16, 0.8, 4, 20, 100 and 500 ng/mL (Appendix A).

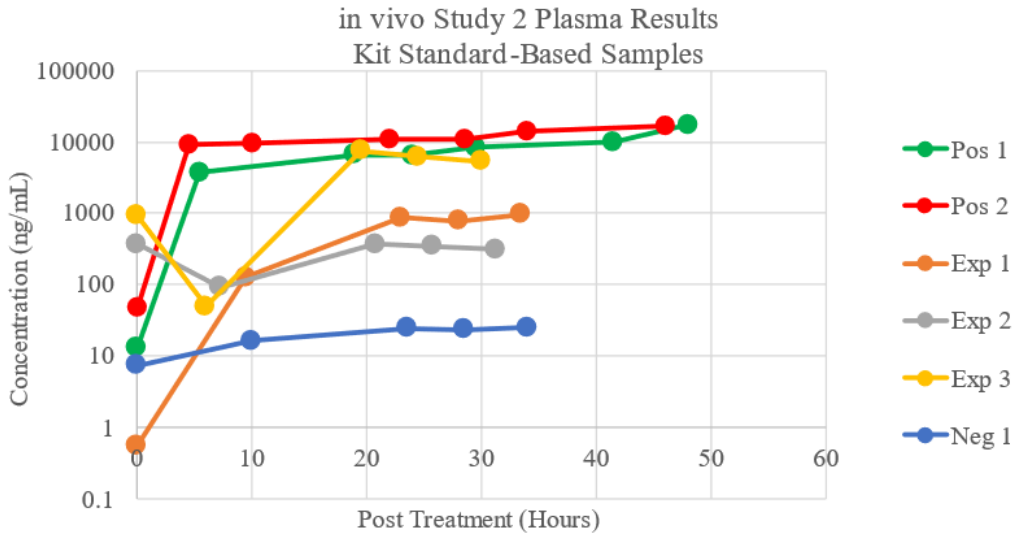

Figure 40. Adalimumab concentration levels using the kit standard-based samples. Exp 1, Exp 2, and Exp 3 used the TAM/Drug delivery needle and a 1-day osmotic pump. Pos 1 and Pos 2 used the TAM/Drug delivery device but instead of an osmotic pump, a manual syringe pump was used to inject all 200 µL of drug into the intestinal wall. Neg 1 used only an osmotic pump sutured into the intestinal lumen.

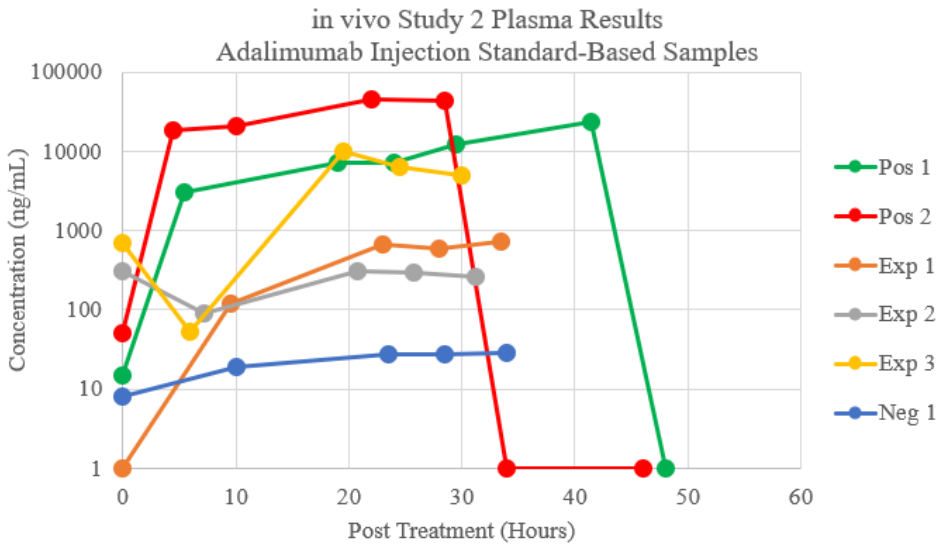

Figure 41. Adalimumab concentration levels using the modified "adalimumab injection standard" based samples. Exp 1, Exp 2, and Exp 3 used the TAM/Drug delivery needle and a 1-day osmotic pump. Pos 1 and Pos 2 used the TAM/Drug delivery device but instead of an osmotic pump, a manual syringe pump was used to inject all 200 µL of drug into the intestinal wall. Neg 1 used only an osmotic pump sutured into the intestinal lumen.

Overall, the two graphs had similar trends. Both positive groups showed relatively high levels of adalimumab in the plasma, especially Pos 2. Exp 3 showed comparable drug levels, suggesting successful systemic biological drug delivery. Neg 1 showed an insignificant level of drug and Exp 1 and Exp 2 showed little to no drug delivery.

2.8.6 Discussion/Conclusions

Based on the plasma results and hardware finding during necropsy, it was evident that this study performed better than the previous study. The plasma results from study 2 indicated successful drug delivery for both positive controls and one experimental treatment while study 1 had no drug delivery for any group. By reducing the post

treatment time for study 2, all the components were located easily. This made it easy to inspect the hardware for any signs of failure. In the previous study, the radiographs were used to determine if the TAM device or osmotic pump was still attached. The images gave a general idea if the TAM or osmotic pump was still attached or at least in the general area. However, this method was difficult to confidently say the device was still attached. Since this study was shorter than the previous, the device and pump were checked for attachment during necropsy. The duration until necropsy varied slightly per animal because of different initial surgery times and the amount of blood draws available to use in the ELISA kit was limited. Overall, the hardware stayed intact throughout the whole study, meaning the catheter disconnecting from the injection needle was eliminated as one of the identified possible reasons for poor drug delivery in study 1.

Generally, the plasma samples are diluted at 1:100, but based on the previous study, it turned out most of the samples were falling below the lower limit of quantification (LLOQ). Therefore, samples were run in a more concentrated form (1:50). Also, there was a possibility that some of the samples would fall above the assay upper limit of quantification (ULOQ) of kit standard and a more concentrated standard would allow one to measure these samples. To avoid being below the LLOQ and above the ULOQ, the assay was run with the additional "adalimumab injection standard."

To find the drug concentration levels in the plasma, the optical densities (O.D) of the standards were taken and two 4-parameter log fit standard curves were created. The formulas were designed to get the standard curves only. The curve fit formula was not used to get the sample concentrations directly, but a program called Softmax fitted the

samples' O.D. values to get their respective concentrations. Concentrations obtained from the back-interpolation were multiplied by their respective dilution factors to get the final analyte concentration per sample. The raw O.D. values are found in appendix A**.**

Although the two graphs showed a similar trend for most groups, Pos 2 had an unexplainable difference between the 10-hour and 22-hour timepoints. Figure 41 shows a more drastic increase in concentration compared to Figure 40**.** Also, the last two timepoints for Pos 2 and the last time point for Pos 1 were above the ULOQ, therefore the software could not calculate their actual concentrations. Similarly, the first time point of Exp 1 was lower than the LLOQ. Each in vivo study was performed without statistical power to draw conclusions, but there is evidence that suggests further progress is merited.

Although the drug delivery device showed successful delivery of a biological drug in the small intestine, it used a relatively large commercially manufactured osmotic pump. To fit an osmotic pump into the final capsule design, a theoretical custom osmotic pump was designed.

Chapter 3: Osmotic Pump

3.1 Introduction

One of the most important aspects of drug delivery, besides the drug itself, is the correct dosage. Underdosing gives poor therapeutic activity, and overdosing can cause adverse events [67], [68]. Rate-controlled release systems allow maintaining the drug concentration within the body at an optimum level [69], [70]. One of the most successful

release systems in recent years is the osmotic pump [71]. Osmotic micropumps require no electrical energy, thus enabling drug delivery systems of the smallest size[72]. For these reasons, an osmotic pump was chosen for drug delivery. One of the only commercially available loadable osmotic pumps today is produced by ALZET and is the model for the theoretical custom osmotic pump.

3.2 Theory of Osmotic Pumps

Osmosis is one of the most fundamental phenomena in biology, allowing cells to balance solute concentrations [73], [74]. Osmosis occurs when two solutions contain different concentrations of solutes and are separated by a selectively permeable membrane [75], [76]. Solvent molecules travel along a gradient from low concentration to high concentration, if the membrane allows [77]. The transfer of molecules continues until equilibrium in concentration occurs [78]. If the membrane is semi-permeable, only certain molecules can pass, usually the water molecules [79]. In the case of an osmotic pump, water flows through the semi-permeable membrane, but the solute (osmotic agent) is unable to pass through the semi-permeable membrane [80]. Consequently, it results in a hydrostatic pressure difference across the membrane [81]. Osmotic pumps utilize this hydrostatic pressure to “push” out the drug from the other end of the pump/capsule [82].

There are three primary components to an osmotic pump: osmotic agent, solvent, and the drug [72]. In our case, the solvent is the water molecules from the intestinal chyme, mucous, etc. The drug that is loaded into the osmotic pump could ideally be any drug with a reasonable viscosity. ALZET claims their pumps can deliver any viscosity up to ketchup (~50,000 cps).[83] This means we are left with the osmotic agent used to

"drive" the osmosis. To calculate the osmotic pressure, the van't Hoff equation (2) is used [84].

$$\boldsymbol{\pi = iCRT} \tag{2}$$

This equation shows the osmotic pressure (π) of a solution is proportional to the solute concentration (osmotic agent) and temperature, where *C* stands for the corresponding osmotic agent solute concentration (mol/L), *R* is the molar gas constant (8314 J mol^{-1} K^{-1}), and *T* the absolute temperature (K). The van't Hoff factor *i* represents the number of moles of solute dissolved in a solution per mole of added solid solute (this value is 1 if a solute does not dissociate). When the osmotic pressure is known, one can calculate the flow rate of a fluid using equation (3) [85].

$$\boldsymbol{J = K \times A \times (\sigma \Delta \pi - \Delta P)} \tag{3}$$

where J is the volume transported per unit time, K is the permeability of the membrane, A is the effective surface area of the membrane, σ is the osmotic reflection coefficient of the membrane, $\Delta\pi$ is the difference in osmotic pressure, and ΔP is the difference in hydrostatic pressure. Figure 42 shows the components of a simple osmotic pump [85].

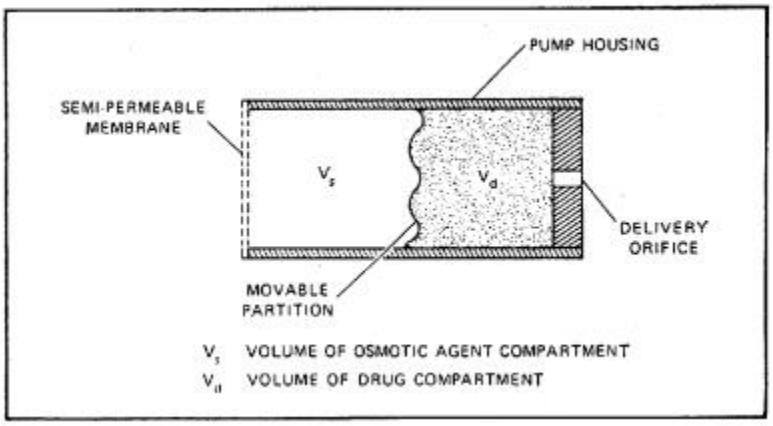

Figure 42. Schematic of an osmotic pump.

Knowing the components and the theory of an osmotic pump, we can now take a closer look at ALZET's osmotic pump (Figure 43.) They have three different sizes of pumps, a 100 μL, 200 μL, and 2 mL reservoir. Each of these pumps has several different release times ranging from one day to four weeks. Our goal was to deliver a drug for 4-7 days, so these pumps were an excellent product to model. However, we had a very strict size constraint and all three of these models were too large. Consequently, we needed to design a pump that would be compatible with our TAM design.

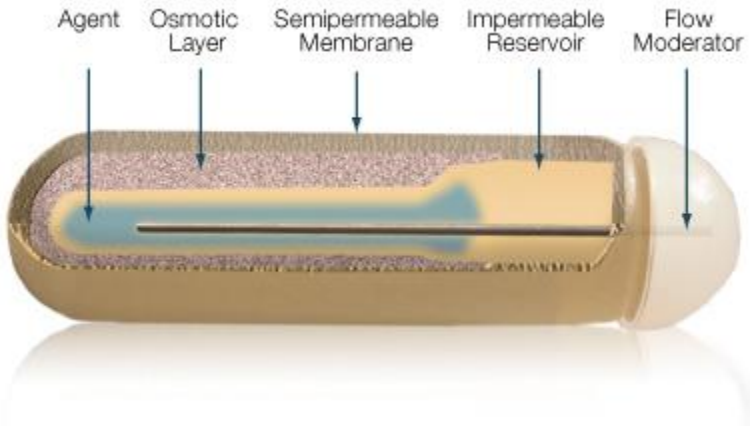

Figure 43. ALZET Osmotic Pump.

Our theoretical pump would use the same components that the ALZET pump uses, just with different shapes and sizes. First, their pump uses sodium chloride as an osmotic agent, so that would be used in our theoretical pump. The osmotic pressure created from sodium chloride at body temperature is over 270,000 mmHg [71]. For our system, the drug injection needle was around a total of 6 mm long with an inner diameter of 0.159 mm (30 gauge) and two 90-degree elbows. Using these dimensions and a velocity of 1 μL/day to calculate the pressure loss in the system, the total loss would be negligible, nearly 0. The pressure within capillaries is only around 20 mmHg [86],

meaning the pressure generated from the pump would certainly overcome any pressure loss from the tubing and needle bends and therefore would pump drug into the bloodstream.

ALZET uses a cellulose ester blend as a semi-permeable membrane. They do not specify exactly the contents of the blend due to intellectual property, but there is much literature about different cellulose ester blends including cellulose acetate, cellulose diacetate, cellulose triacetate, cellulose propionate, cellulose acetate butyrate, and cellulose ethers [71]. We anticipate our custom pump would use one of the blends.

ALZET's design is different than the simple schematic in Figure 43 in that their movable portion does not push from one direction, but rather radially contracts to push the drug out. The movable portion is a thermoplastic hydrocarbon elastomer. Some designs use a piston to push the drug out (Figure 44) [87]. We used this piston-driven device for our theoretical pump.

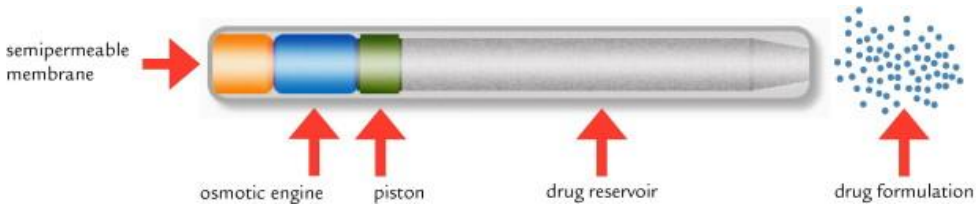

Figure 44. Example of a piston-driven osmotic pump.

3.3 Functional Requirements of Osmotic Pump

1. Component Materials and Properties

The osmotic pump used in the final will be designed with non-toxic parts and the osmotic pump used in experiments will be a commercially available osmotic pump.

2. Drug Chemistry, Manufacturing, and Controls (CMC)

Parts or materials of the TAM in contact with the drug shall be stable. A limited drug shelf life shall not limit the TAM shelf life, and vice versa.

3. Drug Loading

The TAM should contain a feature that allows the loading of a drug before going in-vivo.

4. Manufacturability

The system shall be manufacturable in a timely fashion on a scale of 100,000 units/year. Note: this quantity is different from the cost quantity to make a conservative case in both categories.

5. Drug Payload Description

The theoretical osmotic pump should work for the following payloads.

Table 6. Function requirement for drug delivery payload.

Payload Type	Target Concentration	Delivery Rate	Duration	Total Volume
GLP-1	10 μg/μL	10 μg/day	4-7 days	4-7 μL/week

6. Drug Payload Material and Viscosity

The drug will be in a liquid format with viscosity and fluid properties based on the commercially available formulation.

3.4 Design of Osmotic Pump

After each of the components has been selected, the shape and size of the osmotic pump were modified to fit within the final capsule design. Based on ALZET's dimensions, the drug reservoir volume is at a minimum of 20% of the pump's total

volume. If the volume of the drug we are trying to deliver in a week is 7 µl, and we follow ALZETs drug reservoir to pump volume ratio, our pump size would be about 35 mm^3. As a safety factor, a 30% clearance was given in the design making the total pump volume 45 mm^3. To satisfy these conditions, a torus-shaped, piston-driven, osmotic pump was designed (Figure 45).

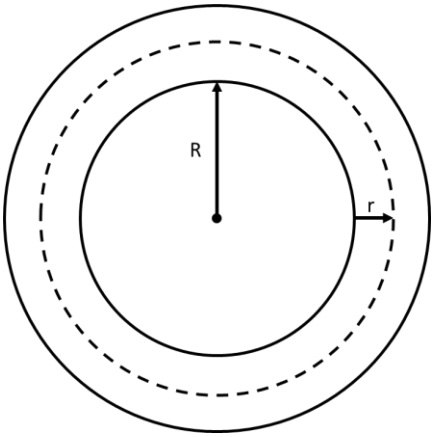

Figure 45. Schematic of the torus-shaped osmotic pump

The volume of a torus is:

$$\boldsymbol{V = (\pi r^2)(2\pi R)} \quad (4)$$

where *R* is the major radius and *r* is the minor radius. In our design, R is 4 mm and r is 0.75 mm resulting in a total pump volume of approximately 45 mm^3. The thickness of the outer shell is 0.15 mm. To insert the drug injection needle a small arc (30-degrees or about 8% of the total volume) of the torus was removed (Figure 46), resulting in a final pump volume of about 41 mm^3. ALZET's 100 µL pump has a semi-permeable membrane thickness of 0.45 mm and an osmotic agent thickness of 0.30 mm. The regions that contain the semi-permeable membrane, osmotic agent, and drug are illustrated in the half-section view in Figure 47. In our design, the semi-permeable region was about 20-

degrees of the pump, which is around 1 mm thick, with a radius of 0.6 mm. The osmotic agent is filled between the semi-permeable layer and the piston. The amount of osmotic agent required should be tested to determine the delivery rate and duration. The biological drug fills the remaining volume from the piston to the hypodermic needle. The 30-gauge hypodermic needle consists of two 90-degree bends with a total length of around 6 mm. Table 7 shows all the components, materials, and dimensions required to construct the custom osmotic pump. ALZET's 100 µL pumps are sold at around $24.00, with a lowered assumed unit cost. The components, materials, and overall size of our custom osmotic pump are similar to ALZET's 100 µL pump, therefore we expect our unit cost to be lower than $24.00. The file for the osmotic pump is found here: https://unl.box.com/s/wxb06ud6dox4bw222rivbc3po5vaf0zb or Wankum_Ben\Capsule Project\Final Device Files for Progenity\osmotic_Pump_file. A detailed drawing with dimensions is shown in Figure 48 and the file is found here: https://unl.box.com/s/u1yyhetpcx08ovdrmhkplle3mzwgyaar or Wankum_Ben\Capsule Project\Final Device Files for Progenity\osmotic_Pump_file_drawing.

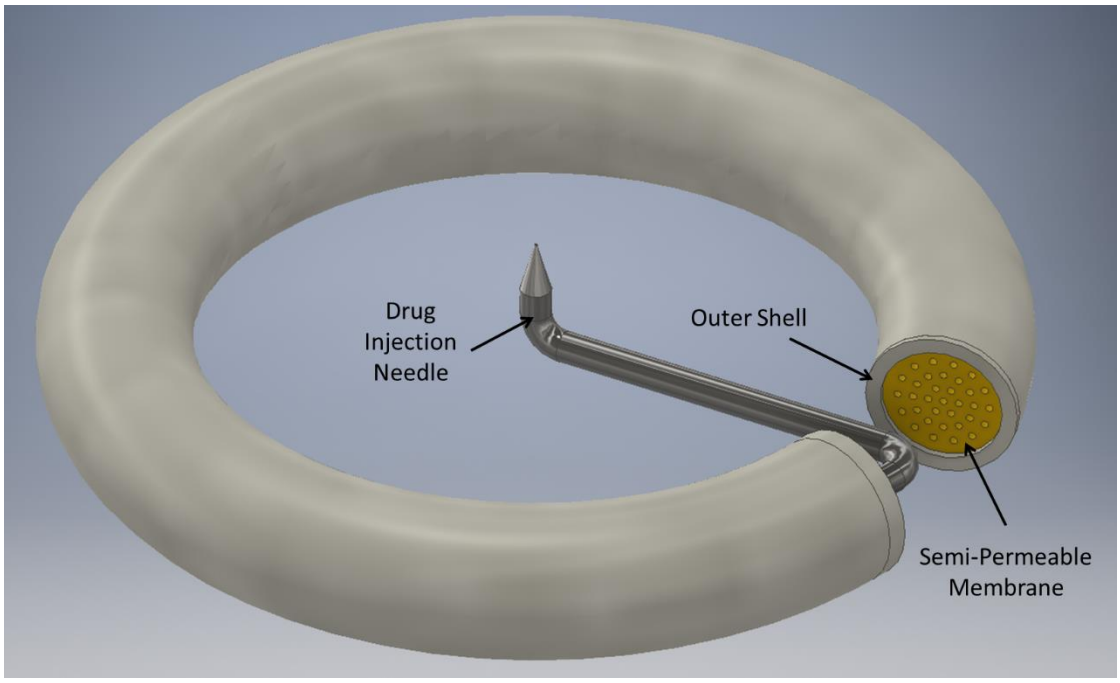

Figure 46. CAD design of a torus-shaped osmotic pump with a drug injection needle.

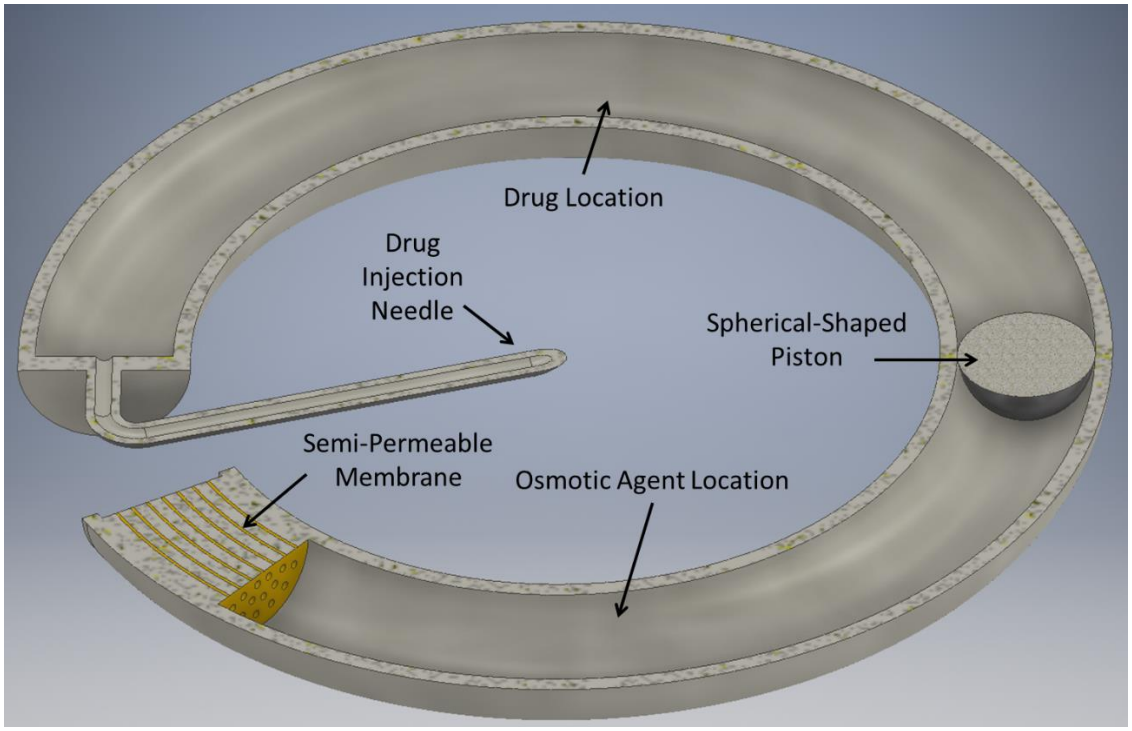

Figure 47. Half-section view of the osmotic pump showing the spherical-shaped piston, drug location, osmotic agent location, and semi-permeable membrane.

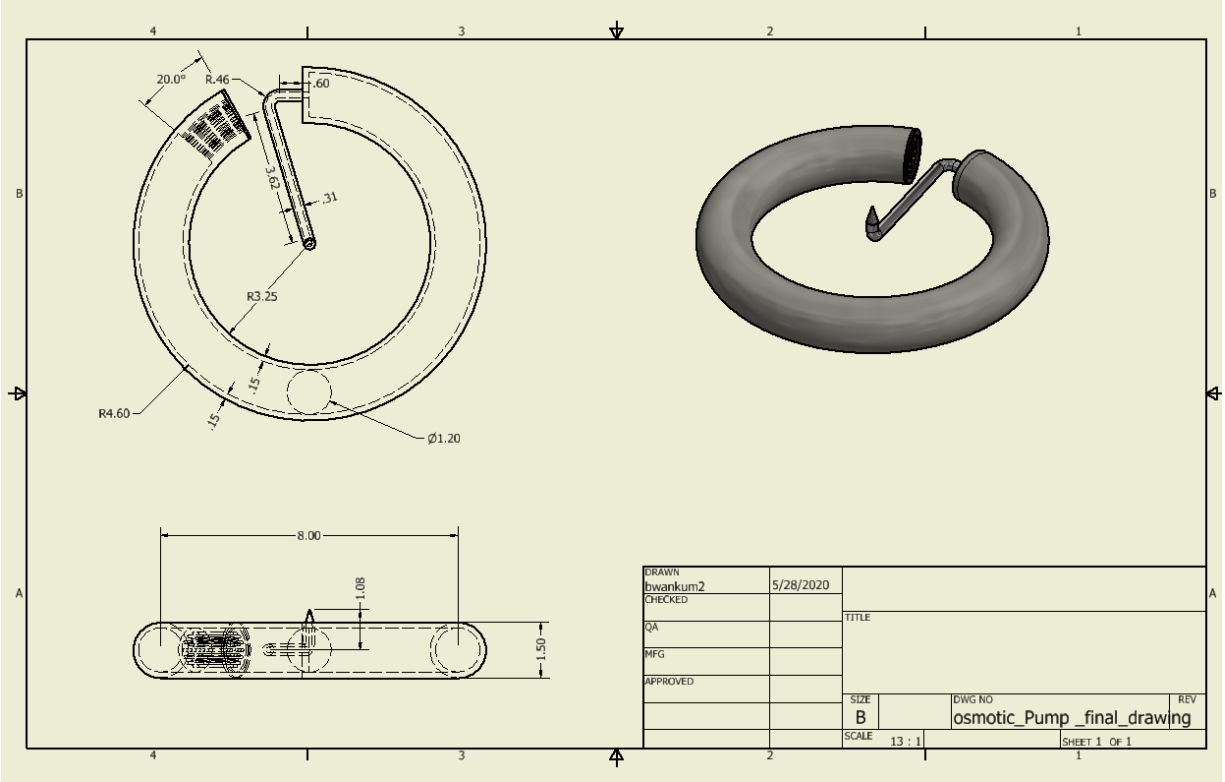

Figure 48. Drawing of the osmotic pump. Units are in millimeters.

Table 7. List of components, materials, and dimensions for the torus-shaped osmotic pump

Component	Material	Dimension
30 gauge Hypodermic Needle	Stainless Steel or PLA	~ 0.5 mm then 90-degree bend towards the center, 3.5 mm then 90-degree bend up, 0.75 mm to the tip of the needle, 30 gauge = ID of 0.159 mm
Semi-Permeable Membrane	Cellulose Ester Blend	0.6 mm radius, 20-degrees (~5%) of pump
Osmotic Agent	Sodium Chloride	Fill in the void between the semi-permeable membrane and the piston
Spherical-Shaped Piston	Stainless Steel or PLA	0.6 mm radius
Drug	Preference	N/A
Outershell	Stainless Steel or PLA	R = 4 mm, r = 0.75 mm, and 0.15 mm wall thickness

3.5 Function of Osmotic Pump in the Intestine

To our knowledge, there has been no proof of ALZET's osmotic pumps being used in any portion of the small or large intestine. To prove the feasibility of osmotic drug delivery in the intestine, an ALZET 1-day, 200 μL osmotic pump was sutured into the ileum. The osmotic pump was loaded with black India ink, primed in saline at 37^{o} C for 3 hours, and a 75 cm tube was attached. The meniscus of the ink was measured before implantation (Figure 49). The pump and tubing were then sutured into a porcine intestine via enterotomy. After surgery, the animal recovered and resumed its normal diet and activity for over a day, until it was euthanized for inspection. The pump was found sutured in place, the meniscus of India ink was measured (Figure 50), and the volume of ink delivered was calculated. The total volume of ink delivered was approximately 220 μL, which was close to the expected 200 μL for the lot we received. This experiment strongly suggests that an osmotic pump can be used in the intestine for accurate drug delivery.

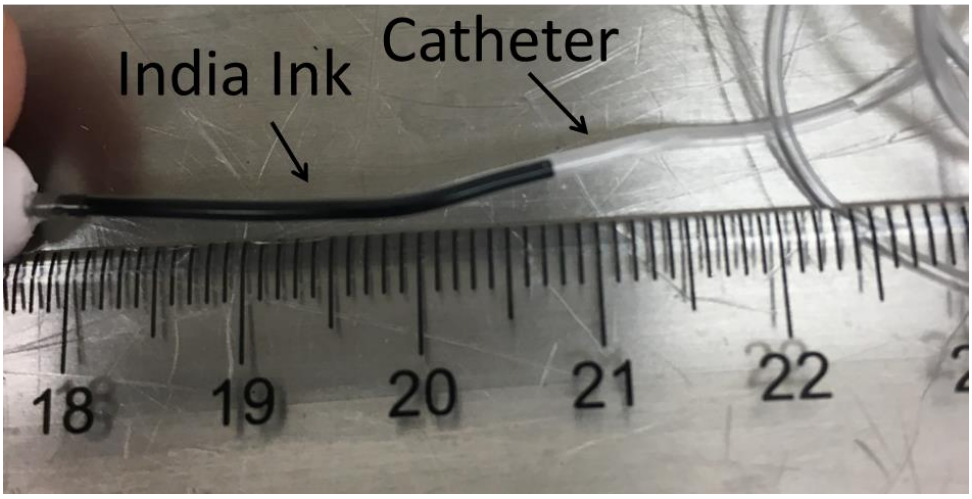

Figure 49. Pre-implantation of an osmotic pump with India ink meniscus.

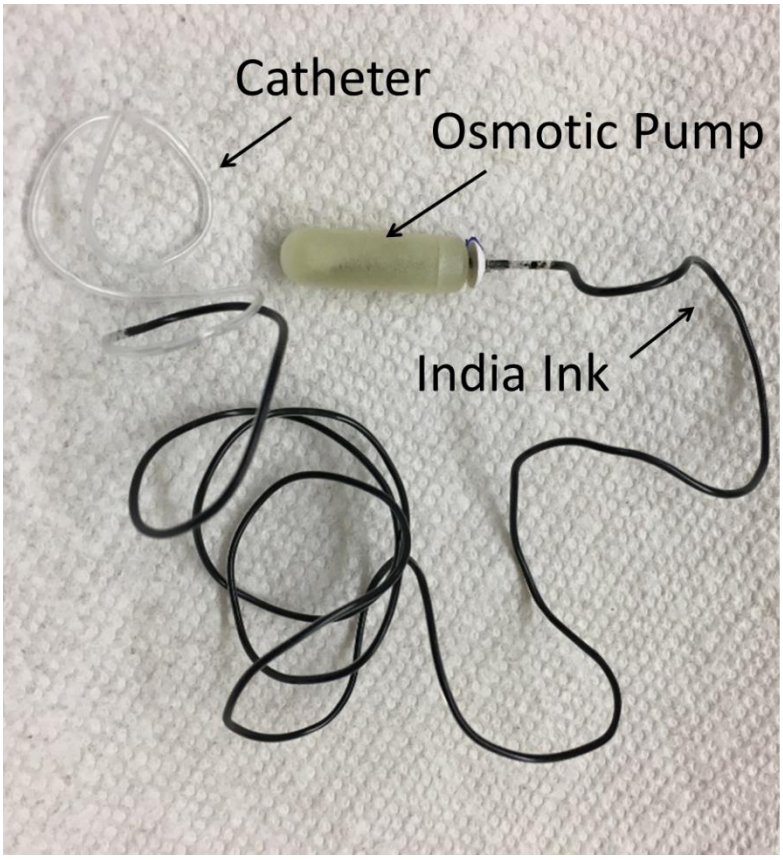

Figure 50. Osmotic pump with India ink meniscus after being in a porcine intestine for over 24 hours.

Chapter 4: Discussion and Conclusions

The overall scientific goal of the research was to utilize subcutaneous needle injection methodology used for parenteral systemic biologic drug delivery to solve the problem of delivering biologics orally for treating diseases like diabetes, arthritis, or cancers. This was to be accomplished by demonstrating proof-of-feasibility of systemic biological drug delivery via a needle injection into the submucosa of the small intestine. This was completed by integrating the TAM with a commercial off-the-shelf (COTS) drug delivery system. The COTS system used to deliver the drug in this work was AZLET's osmotic pumps. The pumps were connected to a hypodermic drug delivery needle via a thin, tubed catheter. The drug delivery needle was developed to administer the drug into the submucosa of the small intestine. The drug delivery needle was designed and integrated into the TAM body and tested on the benchtop. The final design of the drug delivery needle was a needle that perpendicularly pierced the intestinal tissue upon actuation of the attachment sequence.

After the delivery needle consistently and successfully performed on excised swine tissue, it was tested in live pigs. Two separate tests were performed on six animals each. The goal of the studies was to deliver a biological drug (adalimumab) with the TAM and drug delivery needle via an osmotic pump. Positive and negative controls were used for comparisons. The first study did not go as planned, since the TAM was detaching sooner than expected, but the experimental procedure was learned and there were still questions to be answered, so the experiment was repeated with modifications.

The second study showed much stronger evidence of drug delivery, with both positive controls and an experimental group showing adalimumab in the plasma results. Both studies were a methods development study, so the number of pigs in the results did not meet the power for statistical significance.

The other goal of this project was to design a custom osmotic pump that could theoretically be introduced into the full device. The theory of osmotic pumps was studied and ALZET's commercial osmotic pumps were used as a reference in the design of the custom pump. A torus-shaped, piston-driven, osmotic pump was designed to fit within the capsule. An ALZET osmotic pump was tested with India ink in the small intestine and showed evidence of accurate drug delivery. Although there was no statistical power in these experiments, the animal studies showed drug delivery, suggesting an osmotic pump can be used for drug delivery, but a full-scale study with statistical power should be performed.

4.1 Future Work

Drug delivery using injection into the intestinal submucosa with an ingestible device is a radical approach for the administration of agents with poor oral bioavailability. However, with this approach, the innovation potential is large. Specifically, the ability to deliver unmodified drugs, which take years and billions of dollars to develop. Although the drug delivery needle showed proof of feasibility to systemically deliver drug via injection into the intestinal wall, there were drawbacks to the study design. As stated, this study was a methods development study, so future

studies should include additional animals to draw more conclusions. Numerous technical and regulatory hurdles need to be negotiated before patient trials can be performed.

One of the main concerns of the capsule designs is how will a swallowed device latch on strongly enough to the mucosal surface so that it can perform its complete task. At the time of this writing, TRL is working on a coil spring system to provide intimate contact with the intestinal wall. There are risks of full perforation, obstruction, and other mechanical complications. These complications will occur but the key is to keep the incidence very low during studies.

As discussed in the introduction of this work, bioavailability is a major benchmark to determine the success of a device. A future study should include an animal being administered adalimumab via IV. This would allow one to calculate the bioavailability of the device by comparing the AUC of the device to the AUC of an IV administration.

Since attachment times were shorter than expected, future work should be done on optimizing TAM attachment time. Once a reliable long-term attachment is achieved, it would be interesting to run another drug delivery test. In vivo study 1 was designed to accomplish this and might be useful to rerun after attachment time is lengthened.

After my work was complete, the new injection needle and TAM were integrated into the capsule system that was designed in another phase of the project (Figure 51). The capsule system implemented all aspects of the final design, except for the custom osmotic pump; a sham pump was used instead. The semi-complete capsule system should be evaluated in vivo to test its ability to perform the full attachment and voiding sequence.

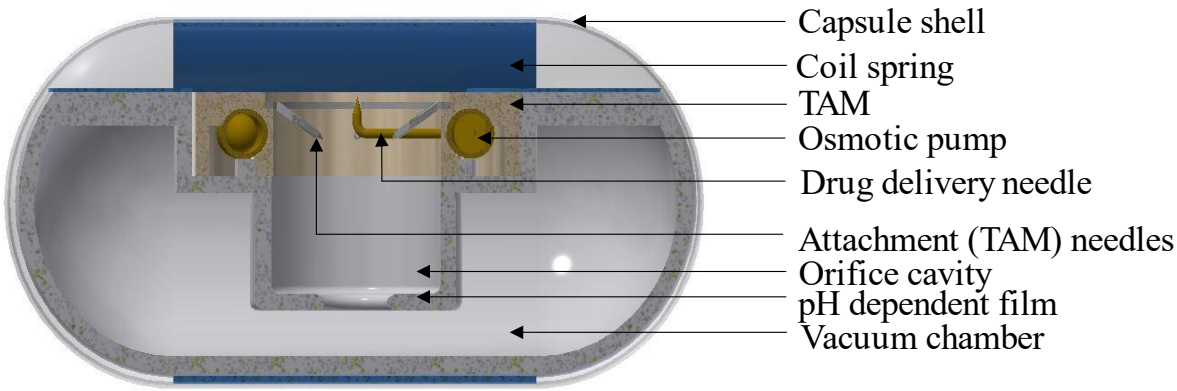

Figure 51. The full concept of the capsule system.

References

[1] A. Dabrowska, “Biologics and Biosimilars: Background and Key Issues,” p. 31.

[2] H. Chen and Q. Wang, “An Overview of Hypoglycemic Biological Drugs,” in *Structure and Health Effects of Natural Products on Diabetes Mellitus*, H. Chen and M. Zhang, Eds. Singapore: Springer, 2021, pp. 33–55.

[3] J. V. Pham *et al.*, “A Review of the Microbial Production of Bioactive Natural Products and Biologics,” *Front. Microbiol.*, vol. 10, 2019, doi: 10.3389/fmicb.2019.01404.

[4] P. A. O’Malley, “Large Molecule Pharmacotherapy: Biologics in Clinical Nurse Specialist Practice,” *Clinical Nurse Specialist*, vol. 31, no. 3, pp. 134–137, Jun. 2017, doi: 10.1097/NUR.0000000000000297.

[5] T. Morrow and L. H. Felcone, “Defining the difference: What Makes Biologics Unique,” *Biotechnol Healthc*, vol. 1, no. 4, pp. 24–29, Sep. 2004.

[6] P. K. Patel, C. R. King, and S. R. Feldman, “Biologics and biosimilars,” *Journal of Dermatological Treatment*, vol. 26, no. 4, pp. 299–302, Jul. 2015, doi: 10.3109/09546634.2015.1054782.

[7] K. Morihiro, Y. Kasahara, and S. Obika, “Biological applications of xeno nucleic acids,” *Molecular BioSystems*, vol. 13, no. 2, pp. 235–245, 2017, doi: 10.1039/C6MB00538A.

[8] S. T. Sharfstein, “Non-protein biologic therapeutics,” *Current Opinion in Biotechnology*, vol. 53, pp. 65–75, Oct. 2018, doi: 10.1016/j.copbio.2017.12.014.

[9] J. R. Maneiro, A. Souto, and J. J. Gomez-Reino, “Risks of malignancies related to tofacitinib and biological drugs in rheumatoid arthritis: Systematic review, meta-analysis, and network meta-analysis,” *Seminars in Arthritis and Rheumatism*, vol. 47, no. 2, pp. 149–156, Oct. 2017, doi: 10.1016/j.semarthrit.2017.02.007.

[10] P. Ruscitti, F. Ursini, P. Cipriani, G. D. Sarro, and R. Giacomelli, “Biologic drugs in adult onset Still’s disease: a systematic review and meta-analysis of observational studies,” *Expert Review of Clinical Immunology*, vol. 13, no. 11, pp. 1089–1097, Nov. 2017, doi: 10.1080/1744666X.2017.1375853.

[11] M. A. Nauck, D. R. Quast, J. Wefers, and J. J. Meier, “GLP-1 receptor agonists in the treatment of type 2 diabetes – state-of-the-art,” *Molecular Metabolism*, p. 101102, Oct. 2020, doi: 10.1016/j.molmet.2020.101102.

[12] D. J. Hodgson, H. Ghasriani, and Y. Aubin, “Assessment of the higher order structure of Humira®, Remicade®, Avastin®, Rituxan®, Herceptin®, and Enbrel® by 2D-NMR fingerprinting,” *Journal of Pharmaceutical and Biomedical Analysis*, vol. 163, pp. 144–152, Jan. 2019, doi: 10.1016/j.jpba.2018.09.056.

[13] D. G. Ribaldone *et al.*, “Adalimumab Therapy Improves Intestinal Dysbiosis in Crohn’s Disease,” *Journal of Clinical Medicine*, vol. 8, no. 10, Art. no. 10, Oct. 2019, doi: 10.3390/jcm8101646.

[14] F. Puppo, G. Murdaca, M. Ghio, and F. Indiveri, “Emerging biologic drugs for the treatment of rheumatoid arthritis,” *Autoimmunity Reviews*, vol. 4, no. 8, pp. 537–541, Nov. 2005, doi: 10.1016/j.autrev.2005.04.016.

[15] J. H. Lee, K. Paek, J. H. Moon, S. Ham, J. Song, and S. Kim, “Biological Characterization of SB3, a Trastuzumab Biosimilar, and the Influence of Changes in Reference Product Characteristics on the Similarity Assessment,” *BioDrugs*, vol. 33, no. 4, pp. 411–422, Aug. 2019, doi: 10.1007/s40259-019-00362-5.

[16] J. S. Geiser *et al.*, “Clinical Pharmacokinetics of Dulaglutide in Patients with Type 2 Diabetes: Analyses of Data from Clinical Trials,” *Clin Pharmacokinet*, vol. 55, no. 5, pp. 625–634, May 2016, doi: 10.1007/s40262-015-0338-3.

[17] D. Peiris *et al.*, “Cellular glycosylation affects Herceptin binding and sensitivity of breast cancer cells to doxorubicin and growth factors,” *Scientific Reports*, vol. 7, no. 1, Art. no. 1, Feb. 2017, doi: 10.1038/srep43006.

[18] S. T. Sanjay *et al.*, “Recent advances of controlled drug delivery using microfluidic platforms,” *Advanced Drug Delivery Reviews*, vol. 128, pp. 3–28, Mar. 2018, doi: 10.1016/j.addr.2017.09.013.

[19] V. Truong-Le, P. M. Lovalenti, and A. M. Abdul-Fattah, “Stabilization Challenges and Formulation Strategies Associated with Oral Biologic Drug Delivery Systems,” *Advanced Drug Delivery Reviews*, vol. 93, pp. 95–108, Oct. 2015, doi: 10.1016/j.addr.2015.08.001.

[20] M. Vertzoni *et al.*, “Impact of regional differences along the gastrointestinal tract of healthy adults on oral drug absorption: An UNGAP review,” *European Journal of Pharmaceutical Sciences*, vol. 134, pp. 153–175, Jun. 2019, doi: 10.1016/j.ejps.2019.04.013.

[21] B. Homayun, X. Lin, and H.-J. Choi, “Challenges and Recent Progress in Oral Drug Delivery Systems for Biopharmaceuticals,” *Pharmaceutics*, vol. 11, no. 3, Mar. 2019, doi: 10.3390/pharmaceutics11030129.

[22] R. Singh, S. Singh, and J. W. Lillard, “Past, present, and future technologies for oral delivery of therapeutic proteins,” *J Pharm Sci*, vol. 97, no. 7, pp. 2497–2523, Jul. 2008, doi: 10.1002/jps.21183.

[23] T. D. Brown, K. A. Whitehead, and S. Mitragotri, “Materials for oral delivery of proteins and peptides,” *Nature Reviews Materials*, vol. 5, no. 2, Art. no. 2, Feb. 2020, doi: 10.1038/s41578-019-0156-6.

[24] M. Moros, S. G. Mitchell, V. Grazu, and J. M. de l. Fuente, “The Fate of Nanocarriers As Nanomedicines In Vivo: Important Considerations and Biological Barriers to Overcome,” *Current Medicinal Chemistry*, vol. 20, no. 22, pp. 2759–2778, Jul. 2013.

[25] S. T. Sanjay, M. Dou, G. Fu, F. Xu, and X. Li, “Controlled Drug Delivery Using Microdevices,” *Curr Pharm Biotechnol*, vol. 17, no. 9, pp. 772–787, 2016.

[26] D. Wang *et al.*, “Development and in vivo evaluation of intranasal formulations of parathyroid hormone (1-34),” *Drug Deliv*, vol. 28, no. 1, pp. 487–498, doi: 10.1080/10717544.2021.1889718.

[27] A. Leone-Bay *et al.*, “Oral Delivery of Biologically Active Parathyroid Hormone,” *Pharm Res*, vol. 18, no. 7, pp. 964–970, Jul. 2001, doi: 10.1023/A:1010936227570.

[28] N. Škalko-Basnet, “Biologics: the role of delivery systems in improved therapy,” *Biologics*, vol. 8, pp. 107–114, Mar. 2014, doi: 10.2147/BTT.S38387.

[29] J. Jin *et al.*, “The optimal choice of medication administration route regarding intravenous, intramuscular, and subcutaneous injection,” *Patient Prefer Adherence*, vol. 9, pp. 923–942, Jul. 2015, doi: 10.2147/PPA.S87271.

[30] K. A. Birnie, M. Noel, C. T. Chambers, L. S. Uman, and J. A. Parker, “Psychological interventions for needle-related procedural pain and distress in children and adolescents,” *Cochrane Database Syst Rev*, vol. 2018, no. 10, Oct. 2018, doi: 10.1002/14651858.CD005179.pub4.

[31] J. G. Hamilton, “Needle phobia: a neglected diagnosis,” *J Fam Pract*, vol. 41, no. 2, pp. 169–175, Aug. 1995.

[32] P. Sendi, R. Locher, B. Bucheli, and M. Battegay, “Intranasal Influenza Vaccine in a Working Population,” *Clinical Infectious Diseases*, vol. 38, no. 7, pp. 974–980, Apr. 2004, doi: 10.1086/386330.
[33] R. K. Sivamani, D. Liepmann, and H. I. Maibach, “Microneedles and transdermal applications,” *Expert Opinion on Drug Delivery*, vol. 4, no. 1, pp. 19–25, Jan. 2007, doi: 10.1517/17425247.4.1.19.
[34] D. R. Owens, T. S Bailey, C. G. Fanelli, J.-F. Yale, and G. B. Bolli, “Clinical relevance of pharmacokinetic and pharmacodynamic profiles of insulin degludec (100, 200 U/mL) and insulin glargine (100, 300 U/mL) – a review of evidence and clinical interpretation,” *Diabetes & Metabolism*, vol. 45, no. 4, pp. 330–340, Sep. 2019, doi: 10.1016/j.diabet.2018.11.004.
[35] E. Flynn, “Pharmacokinetic Parameters,” in *xPharm: The Comprehensive Pharmacology Reference*, S. J. Enna and D. B. Bylund, Eds. New York: Elsevier, 2007, pp. 1–3.
[36] M. Marian and W. Seghezzi, “Chapter 4 - Novel Biopharmaceuticals: Pharmacokinetics, Pharmacodynamics, and Bioanalytics,” in *Nonclinical Development of Novel Biologics, Biosimilars, Vaccines and Specialty Biologics*, L. M. Plitnick and D. J. Herzyk, Eds. San Diego: Academic Press, 2013, pp. 97–137.
[37] D. W. Nebert and G. Zhang, “16 - Pharmacogenomics,” in *Emery and Rimoin’s Principles and Practice of Medical Genetics and Genomics (Seventh Edition)*, R. E. Pyeritz, B. R. Korf, and W. W. Grody, Eds. Academic Press, 2019, pp. 445–486.
[38] G. Price and D. A. Patel, “Drug Bioavailability,” in *StatPearls*, Treasure Island (FL): StatPearls Publishing, 2020.
[39] R. Tardif and J. Brodeur, “Pharmacokinetics/Toxicokinetics,” in *Encyclopedia of Toxicology (Second Edition)*, P. Wexler, Ed. New York: Elsevier, 2005, pp. 383–390.
[40] J. R. Turner, “Area Under the Curve (AUC),” in *Encyclopedia of Behavioral Medicine*, M. D. Gellman and J. R. Turner, Eds. New York, NY: Springer, 2013, pp. 125–126.
[41] D. P. Vaughan, “A model-independent proof of Dost’s law of corresponding areas,” *Journal of Pharmacokinetics and Biopharmaceutics*, vol. 5, no. 3, pp. 271–276, May 1977, doi: 10.1007/BF01065400.
[42] S. Senapati, A. K. Mahanta, S. Kumar, and P. Maiti, “Controlled drug delivery vehicles for cancer treatment and their performance,” *Signal Transduction and Targeted Therapy*, vol. 3, no. 1, Art. no. 1, Mar. 2018, doi: 10.1038/s41392-017-0004-3.
[43] K. Park, “The Controlled Drug Delivery Systems: Past Forward and Future Back,” *J Control Release*, vol. 190, pp. 3–8, Sep. 2014, doi: 10.1016/j.jconrel.2014.03.054.
[44] X. He, J. Sun, J. Zhuang, H. Xu, Y. Liu, and D. Wu, “Microneedle System for Transdermal Drug and Vaccine Delivery: Devices, Safety, and Prospects,” *Dose Response*, vol. 17, no. 4, Oct. 2019, doi: 10.1177/1559325819878585.
[45] E. M. Pridgen, F. Alexis, and O. C. Farokhzad, “Polymeric Nanoparticle Technologies for Oral Drug Delivery,” *Clinical Gastroenterology and Hepatology*, vol. 12, no. 10, pp. 1605–1610, Oct. 2014, doi: 10.1016/j.cgh.2014.06.018.
[46] M. Joseph, H. M. Trinh, K. Cholkar, D. Pal, and A. K. Mitra, “Recent perspectives on the delivery of biologics to back of the eye,” *Expert Opinion on Drug Delivery*, vol. 14, no. 5, pp. 631–645, May 2017, doi: 10.1080/17425247.2016.1227783.
[47] M. R. Prausnitz, “Engineering Microneedle Patches for Vaccination and Drug Delivery to Skin,” *Annu. Rev. Chem. Biomol. Eng.*, vol. 8, no. 1, pp. 177–200, Jun. 2017, doi: 10.1146/annurev-chembioeng-060816-101514.

[48] E. Caffarel-Salvador, A. Abramson, R. Langer, and G. Traverso, “Oral delivery of biologics using drug-device combinations,” *Current Opinion in Pharmacology*, vol. 36, pp. 8–13, Oct. 2017, doi: 10.1016/j.coph.2017.07.003.
[49] B. Homayun, X. Lin, and H.-J. Choi, “Challenges and Recent Progress in Oral Drug Delivery Systems for Biopharmaceuticals,” *Pharmaceutics*, vol. 11, no. 3, Mar. 2019, doi: 10.3390/pharmaceutics11030129.
[50] A. Banerjee and S. Mitragotri, “Intestinal patch systems for oral drug delivery,” *Current Opinion in Pharmacology*, vol. 36, pp. 58–65, Oct. 2017, doi: 10.1016/j.coph.2017.08.005.
[51] R. Goffredo, A. Pecora, L. Maiolo, A. Ferrone, E. Guglielmelli, and D. Accoto, “A Swallowable Smart Pill for Local Drug Delivery,” *Journal of Microelectromechanical Systems*, vol. 25, no. 2, pp. 362–370, Apr. 2016, doi: 10.1109/JMEMS.2016.2524542.
[52] G. Dranitsaris, E. Amir, and K. Dorward, “Biosimilars of Biological Drug Therapies,” *Drugs*, vol. 71, no. 12, pp. 1527–1536, Aug. 2011, doi: 10.2165/11593730-000000000-00000.
[53] A. Abramson *et al.*, “A luminal unfolding microneedle injector for oral delivery of macromolecules,” *Nature Medicine*, vol. 25, no. 10, Art. no. 10, Oct. 2019, doi: 10.1038/s41591-019-0598-9.
[54] S. L. Tao and T. A. Desai, “Gastrointestinal patch systems for oral drug delivery,” *Drug Discovery Today*, vol. 10, no. 13, pp. 909–915, Jul. 2005, doi: 10.1016/S1359-6446(05)03489-6.
[55] S. Eiamtrakarn *et al.*, “Gastrointestinal mucoadhesive patch system (GI-MAPS) for oral administration of G-CSF, a model protein,” *Biomaterials*, vol. 23, no. 1, pp. 145–152, Jan. 2002, doi: 10.1016/S0142-9612(01)00089-8.
[56] A. Abramson *et al.*, “An ingestible self-orienting system for oral delivery of macromolecules,” *Science*, vol. 363, no. 6427, pp. 611–615, Feb. 2019, doi: 10.1126/science.aau2277.
[57] M. R. Prausnitz, Y. Gomaa, and W. Li, “Microneedle patch drug delivery in the gut,” *Nature Medicine*, vol. 25, no. 10, Art. no. 10, Oct. 2019, doi: 10.1038/s41591-019-0606-0.
[58] N. K. Mandsberg, J. F. Christfort, K. Kamguyan, A. Boisen, and S. K. Srivastava, “Orally ingestible medical devices for gut engineering,” *Advanced Drug Delivery Reviews*, vol. 165–166, pp. 142–154, Jan. 2020, doi: 10.1016/j.addr.2020.05.004.
[59] *Rani Therapeutics*. https://www.ranitherapeutics.com/ (accessed Jan. 04, 2021).
[60] W. Xie, V. Kothari, and B. S. Terry, “A bio-inspired attachment mechanism for long-term adhesion to the small intestine,” *Biomed Microdevices*, vol. 17, no. 4, p. 68, Jun. 2015, doi: 10.1007/s10544-015-9972-7.
[61] M. C. Carey, D. M. Small, and C. M. Bliss, “Lipid Digestion and Absorption,” *Annu. Rev. Physiol.*, vol. 45, no. 1, pp. 651–677, Oct. 1983, doi: 10.1146/annurev.ph.45.030183.003251.
[62] C. P. Adams and V. V. Brantner, “Estimating The Cost Of New Drug Development: Is It Really $802 Million?,” *Health Affairs*, vol. 25, no. 2, pp. 420–428, Mar. 2006, doi: 10.1377/hlthaff.25.2.420.
[63] M. Knopp, “Encapsulation innovation: The new and novel in hard and soft capsules,” p. 6.
[64] K. Nylund, T. Hausken, S. Ødegaard, G. E. Eide, and O. H. Gilja, “Gastrointestinal wall thickness measured with transabdominal ultrasonography and its relationship to demographic factors in healthy subjects,” *Ultraschall Med*, vol. 33, no. 7, pp. E225–E232, Dec. 2012, doi: 10.1055/s-0031-1299329.

[65] J. S. Karthikeyan, D. Salvi, and M. V. Karwe, “Modeling of fluid flow, carbohydrate digestion, and glucose absorption in human small intestine,” *Journal of Food Engineering*, vol. 292, p. 110339, Mar. 2021, doi: 10.1016/j.jfoodeng.2020.110339.

[66] “Filling & Priming ALZET Pumps,” *ALZET® Osmotic Pumps*. https://www.alzet.com/guide-to-use/filling-priming-alzet-pumps/ (accessed Jan. 31, 2021).

[67] C. Carvajal, “Poor response to treatment: beyond medication,” *Dialogues Clin Neurosci*, vol. 6, no. 1, pp. 93–103, Mar. 2004.

[68] A. S. B. Bohnert *et al.*, “Overdose and adverse drug event experiences among adult patients in the emergency department,” *Addict Behav*, vol. 86, pp. 66–72, Nov. 2018, doi: 10.1016/j.addbeh.2017.11.030.

[69] D. Jain, R. Raturi, V. Jain, P. Bansal, and R. Singh, “Recent technologies in pulsatile drug delivery systems,” *Biomatter*, vol. 1, no. 1, pp. 57–65, Jul. 2011, doi: 10.4161/biom.1.1.17717.

[70] M. Bayat and S. Nasri, “Chapter 12 - Injectable microgel–hydrogel composites ‘plum pudding gels’: new system for prolonged drug delivery,” in *Nanomaterials for Drug Delivery and Therapy*, A. M. Grumezescu, Ed. William Andrew Publishing, 2019, pp. 343–372.

[71] R. A. Keraliya *et al.*, “Osmotic Drug Delivery System as a Part of Modified Release Dosage Form,” *ISRN Pharm*, vol. 2012, Jul. 2012, doi: 10.5402/2012/528079.

[72] S. Herrlich, S. Spieth, S. Messner, and R. Zengerle, “Osmotic micropumps for drug delivery,” *Advanced Drug Delivery Reviews*, vol. 64, no. 14, pp. 1617–1627, Nov. 2012, doi: 10.1016/j.addr.2012.02.003.

[73] B. Kim, G. Gwak, and S. Hong, “Review on methodology for determining forward osmosis (FO) membrane characteristics: Water permeability (A), solute permeability (B), and structural parameter (S),” *Desalination*, vol. 422, pp. 5–16, Nov. 2017, doi: 10.1016/j.desal.2017.08.006.

[74] A. Yaroshchuk, “‘Breakthrough’ osmosis and unusually high power densities in Pressure-Retarded Osmosis in non-ideally semi-permeable supported membranes,” *Scientific Reports*, vol. 7, no. 1, Art. no. 1, Mar. 2017, doi: 10.1038/srep45168.

[75] T. Y. Cath, A. E. Childress, and M. Elimelech, “Forward osmosis: Principles, applications, and recent developments,” *Journal of Membrane Science*, vol. 281, no. 1, pp. 70–87, Sep. 2006, doi: 10.1016/j.memsci.2006.05.048.

[76] H. Patel and V. Parikh, “An overview of Osmotic Drug Delivery System: An update review,” *International Journal of Bioassays*, vol. 6, pp. 5426–5436, Jul. 2017, doi: 10.21746/ijbio.2017.07.001.

[77] K. M. Fisher, K. S. Williams, and J. E. Lineback, “Osmosis and Diffusion Conceptual Assessment,” *CBE Life Sci Educ*, vol. 10, no. 4, pp. 418–429, 2011, doi: 10.1187/cbe.11-04-0038.

[78] I. L. Minkov, E. D. Manev, S. V. Sazdanova, and K. H. Kolikov, “Equilibrium and Dynamic Osmotic Behaviour of Aqueous Solutions with Varied Concentration at Constant and Variable Volume,” *ScientificWorldJournal*, vol. 2013, Dec. 2013, doi: 10.1155/2013/876897.

[79] N. J. Yang and M. J. Hinner, “Getting Across the Cell Membrane: An Overview for Small Molecules, Peptides, and Proteins,” *Methods Mol Biol*, vol. 1266, pp. 29–53, 2015, doi: 10.1007/978-1-4939-2272-7_3.

[80] J. Morelle *et al.*, “Mechanisms of Crystalloid versus Colloid Osmosis across the Peritoneal Membrane,” *J Am Soc Nephrol*, vol. 29, no. 7, pp. 1875–1886, Jul. 2018, doi: 10.1681/ASN.2017080828.
[81] R. K. Verma, D. M. Krishna, and S. Garg, “Formulation aspects in the development of osmotically controlled oral drug delivery systems,” *Journal of Controlled Release*, vol. 79, no. 1, pp. 7–27, Feb. 2002, doi: 10.1016/S0168-3659(01)00550-8.
[82] Z. Zhao, C. Wu, Y. Zhao, Y. Hao, Y. Liu, and W. Zhao, “Development of an oral push–pull osmotic pump of fenofibrate-loaded mesoporous silica nanoparticles,” *Int J Nanomedicine*, vol. 10, pp. 1691–1701, Mar. 2015, doi: 10.2147/IJN.S76755.
[83] “Viscosity Tables.” http://www.vp-scientific.com/Viscosity_Tables.htm (accessed Apr. 22, 2020).
[84] J. H. van’t Hoff, “Die Rolle des osmotischen Druckes in der Analogie zwischen Lösungen und Gasen,” *Zeitschrift für Physikalische Chemie*, vol. 1U, no. 1, pp. 481–508, Feb. 1887, doi: 10.1515/zpch-1887-0151.
[85] F. Theeuwes and S. I. Yum, “Principles of the design and operation of generic osmotic pumps for the delivery of semisolid or liquid drug formulations,” *Ann Biomed Eng*, vol. 4, no. 4, pp. 343–353, Dec. 1976, doi: 10.1007/BF02584524.
[86] A. C. Shore, “Capillaroscopy and the measurement of capillary pressure,” *Br J Clin Pharmacol*, vol. 50, no. 6, pp. 501–513, Dec. 2000, doi: 10.1046/j.1365-2125.2000.00278.x.
[87] E. Montanya, “Future and emerging therapies,” in *Handbook of Incretin-based Therapies in Type 2 Diabetes*, S. Gough, Ed. Cham: Springer International Publishing, 2016, pp. 77–92.

Appendices

Appendix A: Standard Curves and Raw Data from In Vivo Experiment 2

The following tables and figures were provided by PBL Assay Science:

Table 8. Adalimumab kit standard curve used to measure adalimumab concentrations for plasma samples from groups 136 (Neg 1), 137 (Exp 1), 139 (Exp 2), 140 (Exp 3), 141 (Pos 1), and 163 (Pos 2). LLOQ (Conc.) = 5 ng/ml.

Standard	Conc. (ng/ml)	O.D.	Mean O.D.	Std. Dev.	CV%	Calculated Conc.	% Recovery
Standard 1	100	1.399	1.374	0.035	2.6	100.409	100.409
		1.349					
Standard 2	50	1.139	1.116	0.033	2.9	49.963	99.926
		1.093					
Standard 3	25	0.834	0.826	0.012	1.5	24.52	98.082
		0.817					
Standard 4	10	0.497	0.516	0.027	5.2	10.595	105.953
		0.535					
Standard 5	5	0.308	0.299	0.013	4.5	4.7	93.996
		0.289					
Blank	0	0.012	0.011	0.001	12.9	0.011	NaN
		0.01					

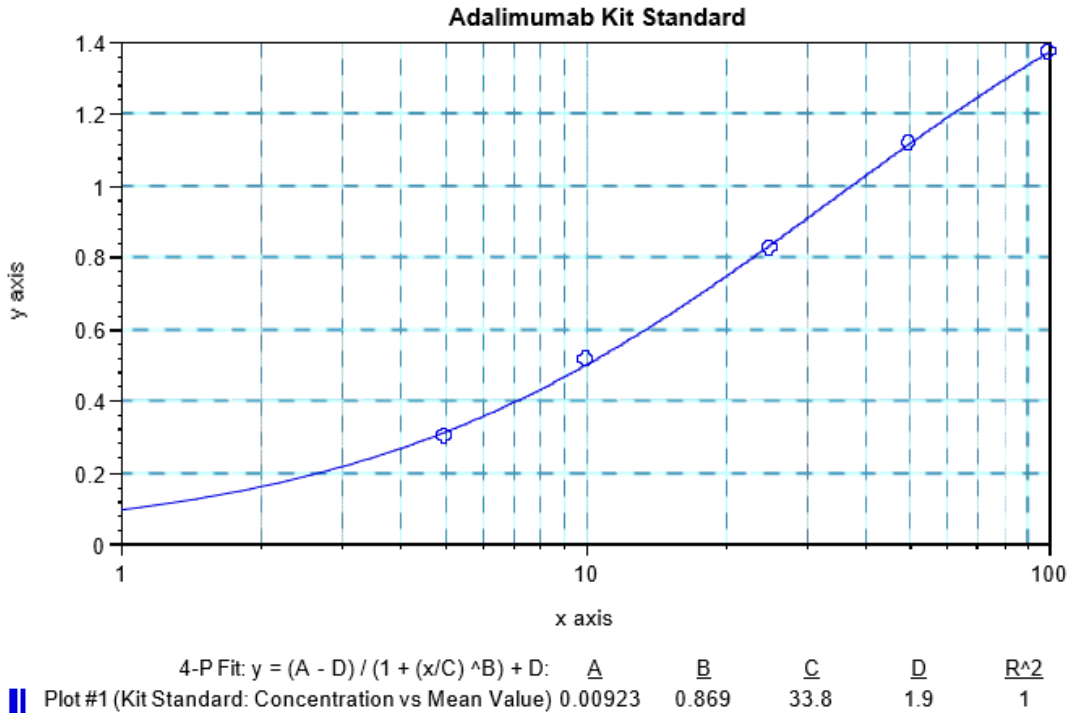

Figure 52. 4-parameter log fit standard curve used to measure adalimumab concentrations for plasma samples from groups 136 (Neg 1), 137 (Exp 1), 139 (Exp 2), 140 (Exp 3), 141 (Pos 1), and 163 (Pos 2).

Table 9. Adalimumab ELISA: Group 136 (Neg 1). Measured adalimumab concentrations of the samples from group 136 (Neg 1). Values below the LLOQ (5 ng/ml) are marked in **red**.

Sample	O.D.	Mean O.D.	Std. Dev.	CV%	Concentration	Final Conc.
136 A	0.027	0.026	0.001	5.4	0.148	7.402
	0.025					
136 B	0.044	0.043	0.002	5	0.329	16.449
	0.041					
136 C	0.057	0.056	0.001	2.5	0.491	24.547
	0.055					
136 D	0.056	0.055	0.002	3.9	0.472	23.621
	0.053					
136 E	0.056	0.057	0.001	2.5	0.503	25.168
	0.058					

Table 10. Adalimumab ELISA: Group 137 (Exp 1). Measured adalimumab concentrations of the samples from group 137 (Exp 1). Values below the LLOQ (5 ng/ml) are marked in **red**.

Sample	O.D.	Mean O.D.	Std. Dev.	CV%	Concentration	Final Conc.
137 A	0.012	0.011	0.001	12.9	0.011	0.553
	0.01					
137 B	0.202	0.191	0.016	8.5	2.546	127.319
	0.179					
137 C	0.714	0.692	0.032	4.6	17.432	871.582
	0.669					
137 D	0.646	0.647	0.001	0.2	15.474	773.702
	0.648					
137 E	0.747	0.735	0.017	2.3	19.521	976.047
	0.723					

Table 11. Adalimumab ELISA: Group 139 (Exp 2). Measured adalimumab concentrations of the samples from group 139 (Exp 2). Values below the LLOQ (5 ng/ml) are marked in **red**.

Sample	O.D.	Mean O.D.	Std. Dev.	CV%	Concentration	Final Conc.
139 A	0.419	0.407	0.017	4.2	7.35	367.48
	0.395					
139 B	0.149	0.151	0.002	1.4	1.861	93.056
	0.152					
139 C	0.421	0.409	0.018	4.3	7.39	369.502
	0.396					
139 D	0.412	0.392	0.029	7.4	6.938	346.91
	0.371					
139 E	0.364	0.364	0.001	0.2	6.224	311.19
	0.363					

Table 12. Adalimumab ELISA: Group 140 (Exp 3). Measured adalimumab concentrations of the samples from group 140 (Exp 3). Values below the LLOQ (5 ng/ml) are marked in **red** and those above the ULOQ (100 ng/ml) are marked in **green**.

Sample	O.D.	Mean O.D.	Std. Dev.	CV%	Concentration	Final Conc.
140 A	0.718	0.716	0.003	0.4	18.586	929.286
	0.714					
140 B	0.097	0.093	0.006	6.1	0.983	49.137
	0.089					
140 C	1.499	1.499	0	0	**151.412**	**7570.61**
	1.499					
140 D	1.372	1.439	0.095	6.6	**123.165**	**6158.244**
	1.506					
140 E	1.293	1.395	0.144	10.3	**107.061**	**5353.028**
	1.497					

Table 13. Adalimumab ELISA: Group 141 (Pos 1). Measured adalimumab concentrations of the samples from group 141 (Pos 1). Values below the LLOQ (5 ng/ml) are marked in **red** and those above the ULOQ (100 ng/ml) are marked in **green**.

Sample	O.D.	Mean O.D.	Std. Dev.	CV%	Concentration	Final Conc.
141 A	0.036	0.037	0.001	1.9	0.261	13.036
	0.037					
141 B	1.228	1.27	0.059	4.7	74.563	3728.156
	1.312					
141 C	1.372	1.459	0.122	8.4	**131.429**	**6571.474**
	1.545					
141 D	1.508	1.454	0.076	5.3	**129.452**	**6472.613**
	1.4					
141 E	1.487	1.524	0.052	3.4	**166.098**	**8304.901**
	1.561					
141 F	1.459	1.571	0.158	10.1	**200.317**	**10015.83**
	1.683					
141 G	1.703	1.684	0.027	1.6	**350.093**	**17504.668**
	1.665					

Table 14. Adalimumab ELISA: Group 163 (Pos 2). Measured adalimumab concentrations of the samples from group 163 (Pos 2). Values below the LLOQ (5 ng/ml) are marked in **red** and those above the ULOQ (100 ng/ml) are marked in **green**.

Sample	O.D.	Mean O.D.	Std. Dev.	CV%	Concentration	Final Conc.
163 A	0.088	0.092	0.005	5.4	0.962	48.08
	0.095					
163 B	1.524	1.556	0.045	2.9	**187.914**	**9395.716**
	1.587					
163 C	1.558	1.563	0.007	0.5	**193.761**	**9688.074**
	1.568					
163 D	1.513	1.595	0.116	7.3	**222.22**	**11110.981**
	1.677					
163 E	1.567	1.594	0.037	2.4	**220.742**	**11037.106**
	1.62					
163 F	1.668	1.643	0.035	2.2	**279.389**	**13969.457**
	1.618					
163 G	1.663	1.679	0.022	1.3	**338.978**	**16948.898**
	1.694					

Table 15. Additional adalimumab standard curve used to measure adalimumab concentrations for plasma samples from groups 136 (Neg 1), 137 (Exp 1), 139 (Exp 2), 140 (Exp 3), 141 (Pos 1), and 163 (Pos 2). LLOQ (Conc.) = 0.160 ng/ml.

Standard	Conc. (ng/ml)	O.D.	Mean O.D.	Std. Dev.	CV%	Calculated Conc.	% Recovery
Standard 1	500	1.766	1.555	0.299	19.2	362.648	72.53
		1.343					
Standard 2	100	1.595	1.424	0.242	17	118.166	118.166
		1.253					
Standard 3	20	0.921	0.838	0.117	14	18.866	94.331
		0.755					
Standard 4	4	0.339	0.309	0.043	14	4.294	107.352
		0.278					
Standard 5	0.8	0.081	0.081	0.001	0.9	0.885	110.577
		0.08					
Standard 6	0.16	0.025	0.024	0.002	9	0.131	81.956
		0.022					
Standard 7	0.032	0.011	0.011	0	0	NaN	NaN
		0.011					
Blank	0	0.009	0.009	0.001	8.3	NaN	NaN
		0.008					

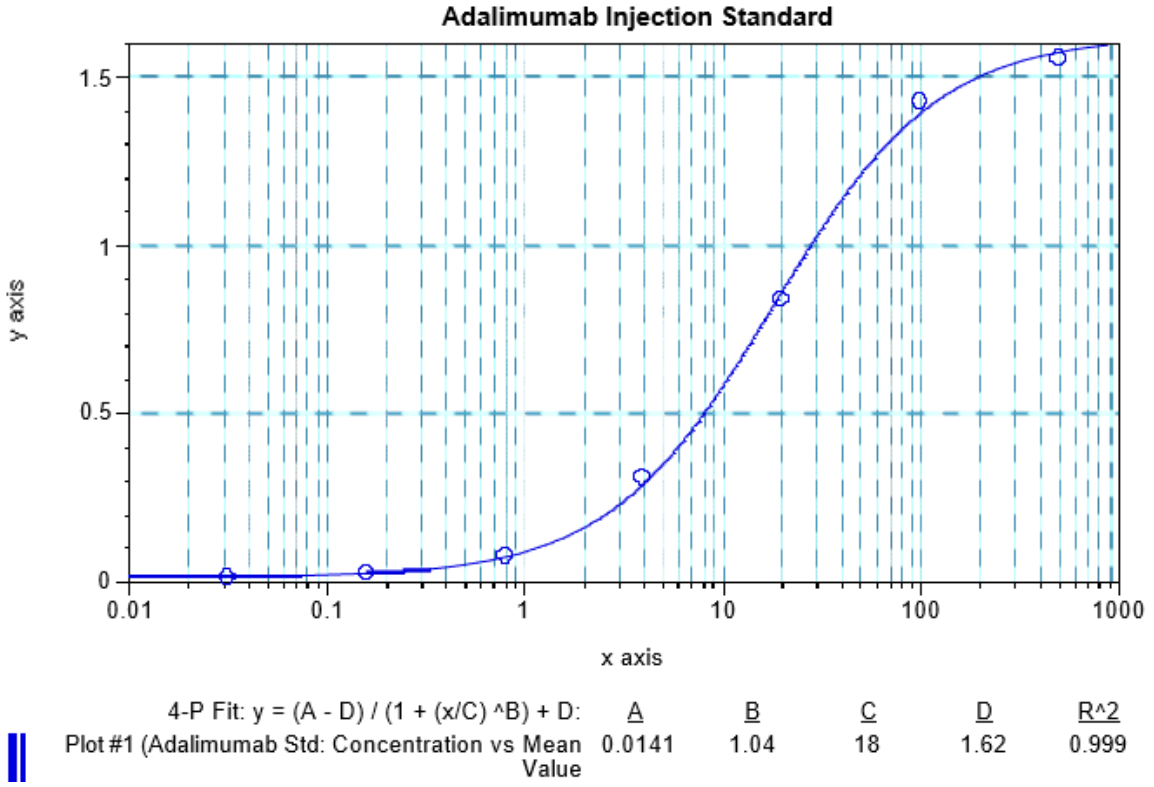

Figure 53. 4-parameter log fit standard curve used to measure adalimumab concentrations for plasma samples from groups 136 (Neg 1), 137 (Exp 1), 139 (Exp 2), 140 (Exp 3), 141 (Pos 1), and 163 (Pos 2).

Table 16. Adalimumab ELISA: Group 136 (Neg 1). Measured adalimumab concentrations of the samples from group 136 (Neg 1). Values below the LLOQ (0.160 ng/ml) are marked in red.

Sample	O.D.	Mean O.D.	Std. Dev.	CV%	Concentration	Final Conc.
136 A	0.027	0.026	0.001	5.4	0.165	8.234
	0.025					
136 B	0.044	0.043	0.002	5	0.383	19.15
	0.041					
136 C	0.057	0.056	0.001	2.5	0.561	28.028
	0.055					
136 D	0.056	0.055	0.002	3.9	0.541	27.041
	0.053					
136 E	0.056	0.057	0.001	2.5	0.574	28.686
	0.058					

Table 17. Adalimumab ELISA: Group 137 (Exp 1). Measured adalimumab concentrations of the samples from group 137 (Exp 1). Values below the LLOQ (0.160 ng/ml) are marked in red.

Sample	O.D.	Mean O.D.	Std. Dev.	CV%	Concentration	Final Conc.
137 A	0.012	0.011	0.001	12.9	NaN	NaN
	0.01					
137 B	0.202	0.191	0.016	8.5	2.421	121.058
	0.179					
137 C	0.714	0.692	0.032	4.6	13.272	663.613
	0.669					
137 D	0.646	0.647	0.001	0.2	11.892	594.579
	0.648					
137 E	0.747	0.735	0.017	2.3	14.749	737.443

Table 18. Adalimumab ELISA: Group 139 (Exp 2). Measured adalimumab concentrations of the samples from group 139 (Exp 2). Values below the LLOQ (0.160 ng/ml) are marked in red.

Sample	O.D.	Mean O.D.	Std. Dev.	CV%	Concentration	Final Conc.
139 A	0.419	0.407	0.017	4.2	6.1	305.018
	0.395					
139 B	0.149	0.151	0.002	1.4	1.843	92.162
	0.152					
139 C	0.421	0.409	0.018	4.3	6.13	306.496
	0.396					
139 D	0.412	0.392	0.029	7.4	5.799	289.941
	0.371					
139 E	0.364	0.364	0.001	0.2	5.271	263.561
	0.363					

Table 19. Adalimumab ELISA: Group 140 (Exp 3). Measured adalimumab concentrations of the samples from group 140 (Exp 3). Values below the LLOQ (0.160 ng/ml) are marked in red.

Sample	O.D.	Mean O.D.	Std. Dev.	CV%	Concentration	Final Conc.
140 A	0.718	0.716	0.003	0.4	14.087	704.365
	0.714					
140 B	0.097	0.093	0.006	6.1	1.052	52.587
	0.089					
140 C	1.499	1.499	0	0	196.28	9813.987
	1.499					
140 D	1.372	1.439	0.095	6.6	128.757	6437.836
	1.506					
140 E	1.293	1.395	0.144	10.3	101.585	5079.237
	1.497					

Table 20. Adalimumab ELISA: Group 141 (Pos 1). Measured adalimumab concentrations of the samples from group 141 (Pos 1). Values below the LLOQ (0.160 ng/ml) are marked in red.

Sample	O.D.	Mean O.D.	Std. Dev.	CV%	Concentration	Final Conc.
141 A	0.036	0.037	0.001	1.9	0.304	15.198
	0.037					
141 B	1.228	1.27	0.059	4.7	60.883	3044.143
	1.312					
141 C	1.372	1.459	0.122	8.4	145.365	7268.227
	1.545					
141 D	1.508	1.454	0.076	5.3	141.197	7059.838
	1.4					
141 E	1.487	1.524	0.052	3.4	248.241	12412.032
	1.561					
141 F	1.459	1.571	0.158	10.1	480.591	24029.547
	1.683					
141 G	1.703	1.684	0.027	1.6	NaN	NaN
	1.665					

Table 21. Adalimumab ELISA: Group 163 (Pos 2). Measured adalimumab concentrations of the samples from group 163 (Pos 2). Values above the ULOQ (500 ng/ml) are marked in **green**.

Sample	O.D.	Mean O.D.	Std. Dev.	CV%	Concentration	Final Conc.
163 A	0.088	0.092	0.005	5.4	1.032	51.58
	0.095					
163 B	1.524	1.556	0.045	2.9	368.148	18407.405
	1.587					
163 C	1.558	1.563	0.007	0.5	415.26	20763.02
	1.568					
163 D	1.513	1.595	0.116	7.3	**906.42**	**45320.985**
	1.677					
163 E	1.567	1.594	0.037	2.4	**858.859**	**42942.952**
	1.62					
163 F	1.668	1.643	0.035	2.2	NaN	NaN
	1.618					
163 G	1.663	1.679	0.022	1.3	NaN	NaN
	1.694					

Appendix B: Drug delivery TAM fabrication process

Following are the materials, files, and instructions for building the drug delivery TAM:

Bill of Materials for Device

Table 22. List of parts and suppliers.

Description	Supplier
30 Gauge, ½ inch hypodermic needle	Global Medical Products (#48-2015)
Laser-cut TAM needle 316 Full Hard Stainless, .008" thickness	Micron Laser, Hillsboro, OR
Small Catheter- Medical grade micro vinyl catheter tubing (I.D. x O.D.: 0.027″ x 0.045″ / 0.69mm x 1.14mm)	Scientific Commodities Inc. (SCI) (cat.# bb31785-v/3a-50′ roll)
Large- Catheter- Medical grade micro vinyl catheter tubing (I.D. x O.D.: 0.011″ x 0.025″ / 0.28mm x 0.64mm)	Scientific Commodities Inc. (SCI) (cat.# bb31785-v/1-50′ roll)
200 µL 1-day delivery osmotic pump (other pumps from ALZET may be used depending on the volume and duration of the study).	Alzet Osmotic Pumps- 2001D
PGN-001 (adalimumab)	Progenity

List of Files for Device

All files for the fabrication of the drug delivery TAM are found here: https://unl.box.com/s/h6evar1gy8prq3eha0vvu18xgptvicxj

Table 23. List of files with descriptions used to build the TAM.

File	Description
TAM_with_sham_osmotic_pump_wgroove_perpindicular_needleV3 https://unl.box.com/s/x4r9dbslauuft5hmzdbagfpd5j1e6n80	Inventor model - TAM device with hole for drug delivery hypodermic needle
6.5 mm 90-degree bend .2 mm bend radius https://unl.box.com/s/d6tzdkgwk1rg11dch0nkus6mllbdtau6	Inventor model- 6.5mm length, 90-degree bend, 0.2mm bend radius mold
2mm 90-degree bend .2 mm bend radius https://unl.box.com/s/b1f52e8kmsy7foq5r7c2entrnvaevb9y	Inventor model- 2 mm length, 90-degree bend, 0.2mm bend radius mold
6mmdia_30d_bend_die https://unl.box.com/s/v87def8nmay28m5a3ij5bq2ghsvr0rvb	Inventor model- 6 mm diameter, 30-degree die
6mmdia_30d_bend_punch https://unl.box.com/s/emrfk0s1v72sdgl62rs4otj95j76eufj	Inventor model- 6 mm diameter, 30-degree punch

List of Tools and Supplies for Device

Table 24. List of tools and supplies for the TAM.

Tool/Supplies	Description
UV glue	Hold together TAM needles and drug delivery needle to TAM device
UV light	Cure UV glue
Microscope	Confirm bend angles for TAM needles and drug delivery needle
VeroClear (Stratasys-OBJ-03271)	3D print material for TAM device
RGD450 (Stratasys-OBJ- 03308)	3D print material for hypodermic needle and TAM needle bending molds

Assembly Procedure

Step 1. 3D print the following files with their specified material:

a. TAM (VeroClear)- https://unl.box.com/s/x4r9dbslauuft5hmzdbagfpd5j1e6n80
b. 6.5 mm bending mold (RGD450)- https://unl.box.com/s/d6tzdkgwk1rg11dch0nkus6mllbdtau6
c. 2.0 mm bending mold (RGD450)- https://unl.box.com/s/b1f52e8kmsy7foq5r7c2entrnvaevb9y
d. 30-degree TAM needle bending mold punch and die- https://unl.box.com/s/v87def8nmay28m5a3ij5bq2ghsvr0rvb https://unl.box.com/s/emrfk0s1v72sdgl62rs4otj95j76eufj

Bending TAM needle

Step 2. Remove the TAM needle from the laser cut sheet (Figure 54).

Step 3. Place the non-bent TAM needle (Figure 55) onto the bottom 30-degree TAM needle bending mold. (Figure 56).

Step 4. Place the top 30-degree TAM needle bending mold over the TAM needle and press down (Figure 57).

Step 5. Separate the two molds and remove the bent TAM needles from the top bending mold (Figure 58).

Step 6. Take the 30-degree bent TAM needle (Figure 59) and confirm its angle with a microscope.

Bending drug delivery needle

Step 7. Bend the ½ inch 30-gauge hypodermic needle (Figure 60) 6.5 mm at 90-degrees by using the 3D printed mold (Figure 61). Confirm the 90-degree bend with a microscope (Figure 62).

Step 8. Next, bend the hypodermic needle 90-degrees again with the 2 mm mold (Figure 63). The needle should now have two 90-degree bends. Confirm the angles with a microscope.

Step 9. Snap off the yellow Luer lock from the hypodermic needle (Figure 64).

Assembling Device

Step 10. Place UV glue onto the bottom of the bent TAM needle and set it in the slot on the TAM device. Cure the UV glue with a UV light (Figure 65).

Step 11. Slide the bent hypodermic needle into the TAM device's pre-existing hole (Figure 65).

Step 12. Cut 2 cm of the small catheter and place it over the hypodermic needle arm.

Step 13. Bend down the hypodermic needle arm and catheter and fasten them to the TAM device with UV glue (Figure 66).

Step 14. Insert the distal end of the small catheter into 2 cm of the large catheter. Use UV glue to hold them in place (Figure 67).

Step 15. Lastly, attach the osmotic pump to the distal end of the large catheter.

Step 16. Fill and prime the osmotic pump according to ALZET's guidelines: https://www.alzet.com/guide-to-use/filling-priming-alzet-pumps/

Step 17. The device is then ready to be inserted into the intestine, attached, and to deliver the drug according to the outline in "In vivo Experiment 1" of this document.

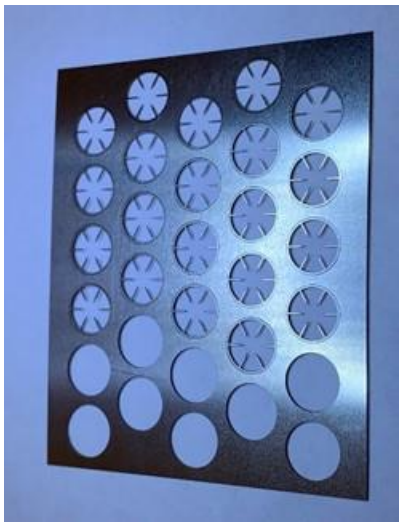

Figure 54. Laser-cut TAM needles.

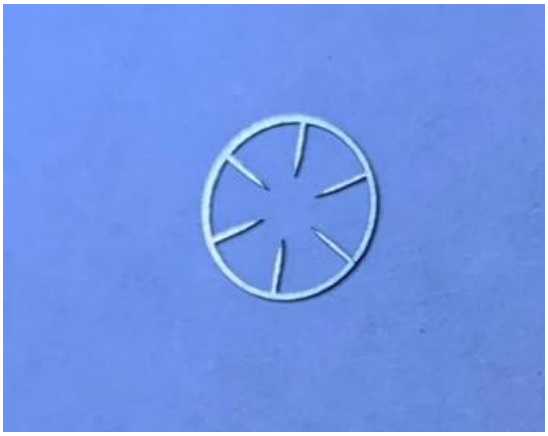

Figure 55. Non-bent TAM needle.

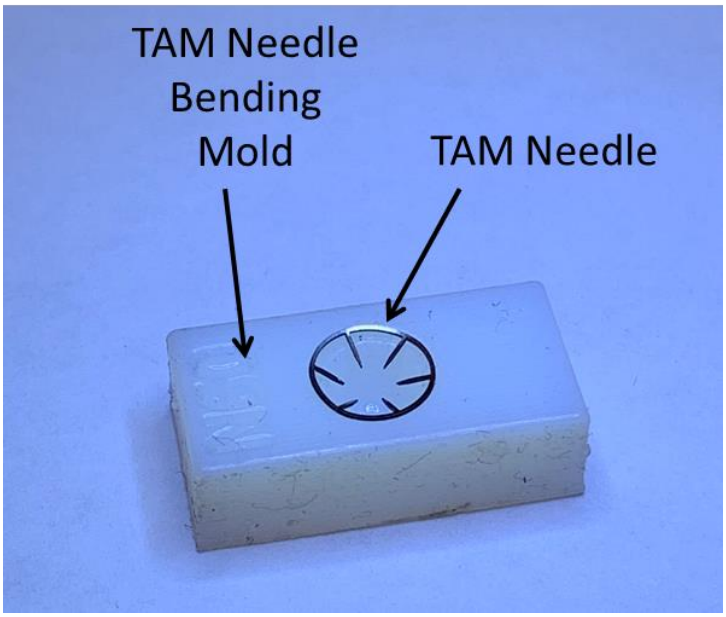

Figure 56. Non-bent TAM Needle in bottom 30-degree bending mold.

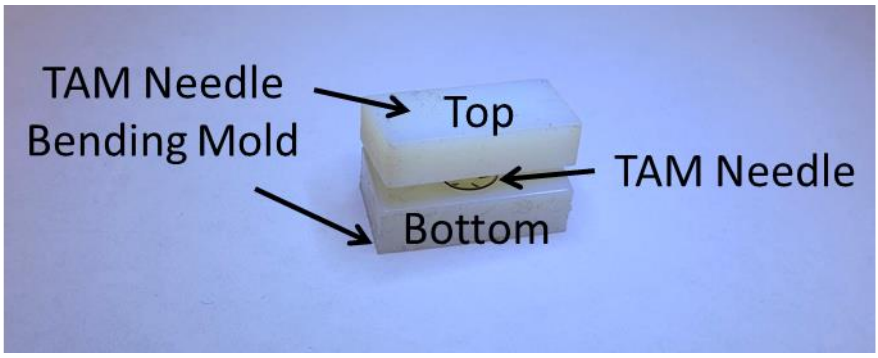

Figure 57. TAM Needle in 30-degree bending molds.

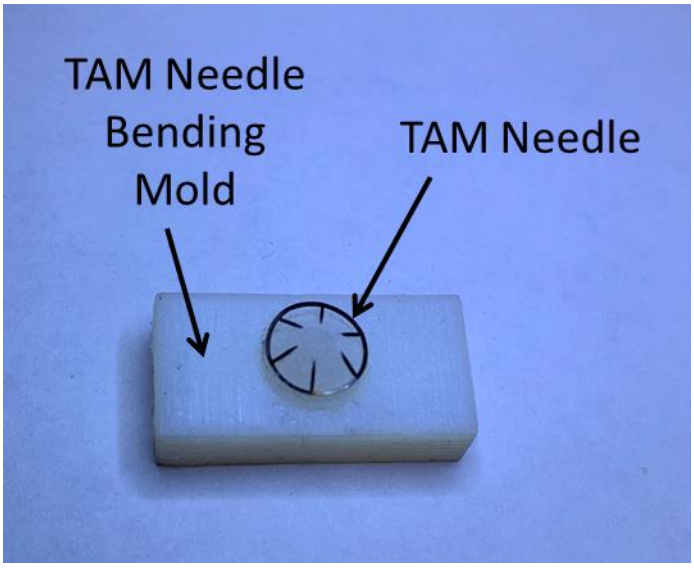

Figure 58. Bent TAM Needle in top 30-degree bending mold.

Figure 59. 30-degree TAM needle.

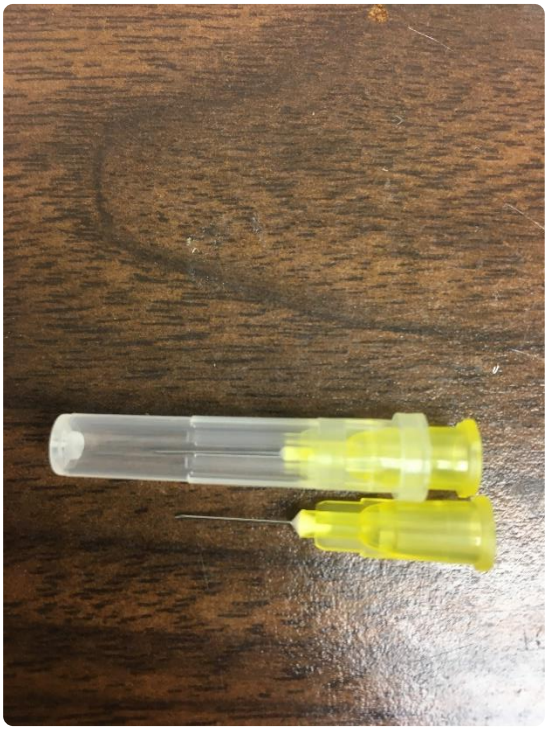

Figure 60. 1/2 inch 30-gauge hypodermic needle.

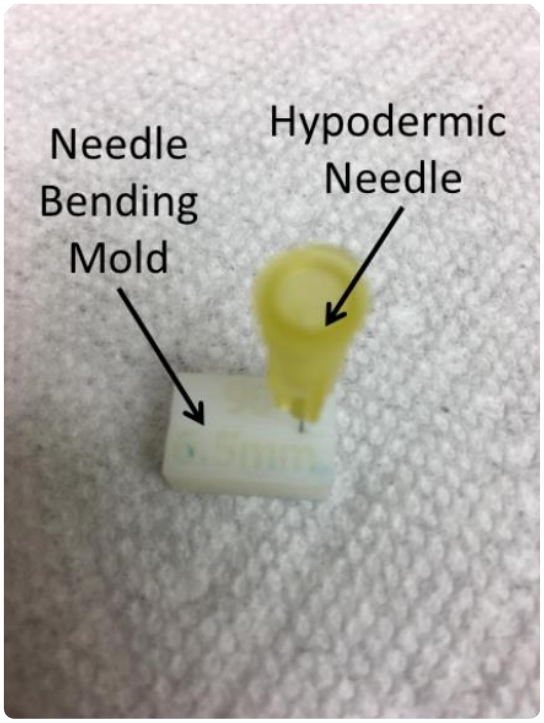

Figure 61. Hypodermic needle in bending mold.

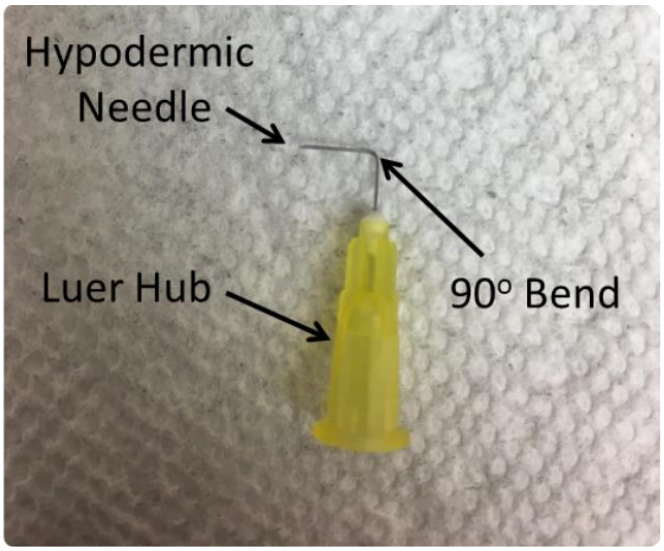

Figure 62. Hypodermic needle bent once.

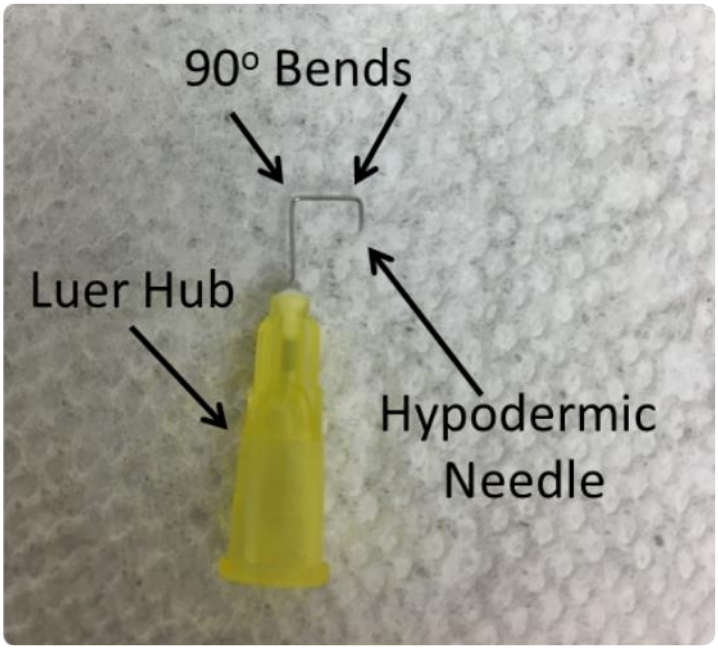

Figure 63. Hypodermic needle bent 90-degrees twice.

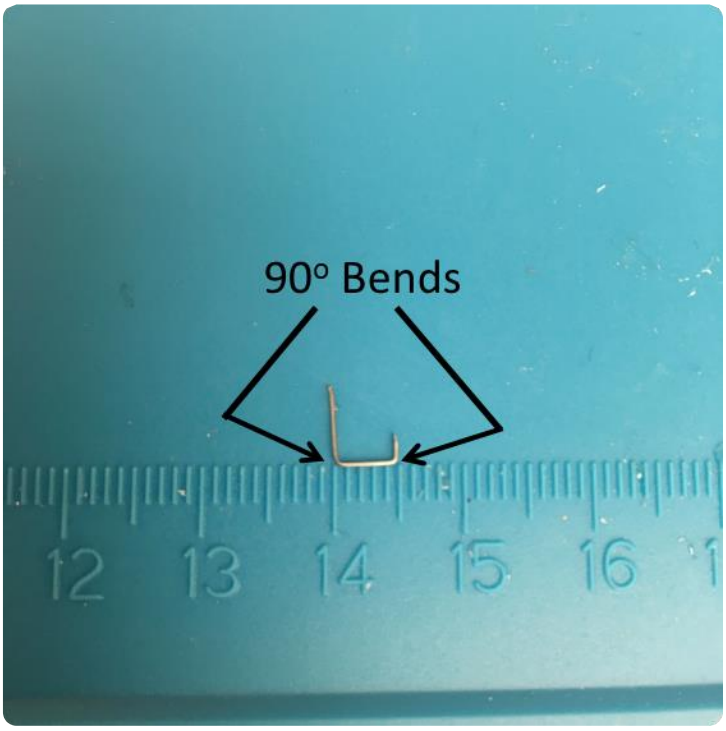

Figure 64. Hypodermic needle bent and snapped off from Luer lock.

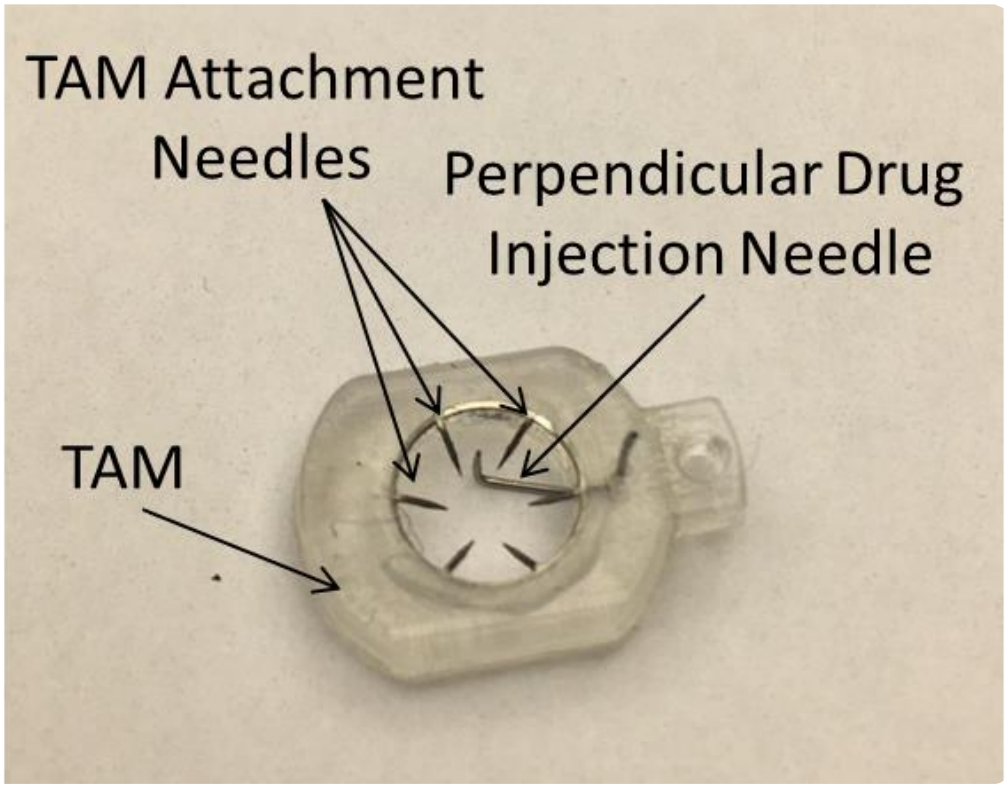

Figure 65. TAM with a drug injection needle (shorten arm used).

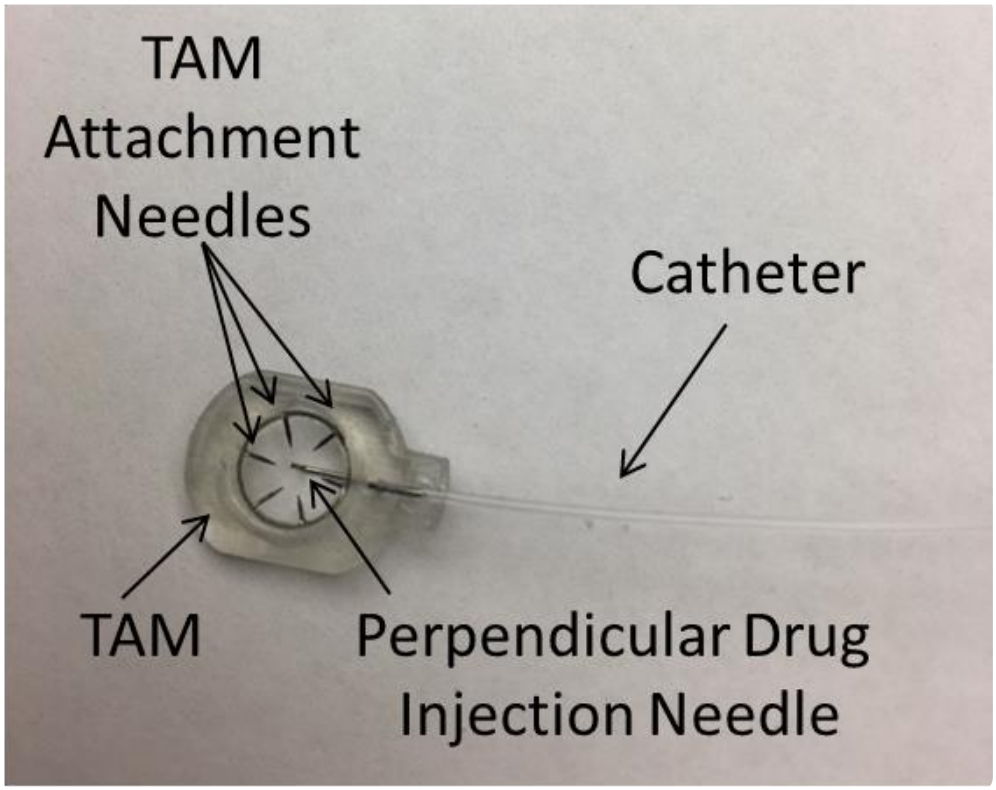

Figure 66. Needle arm bent down and glued to a small catheter.

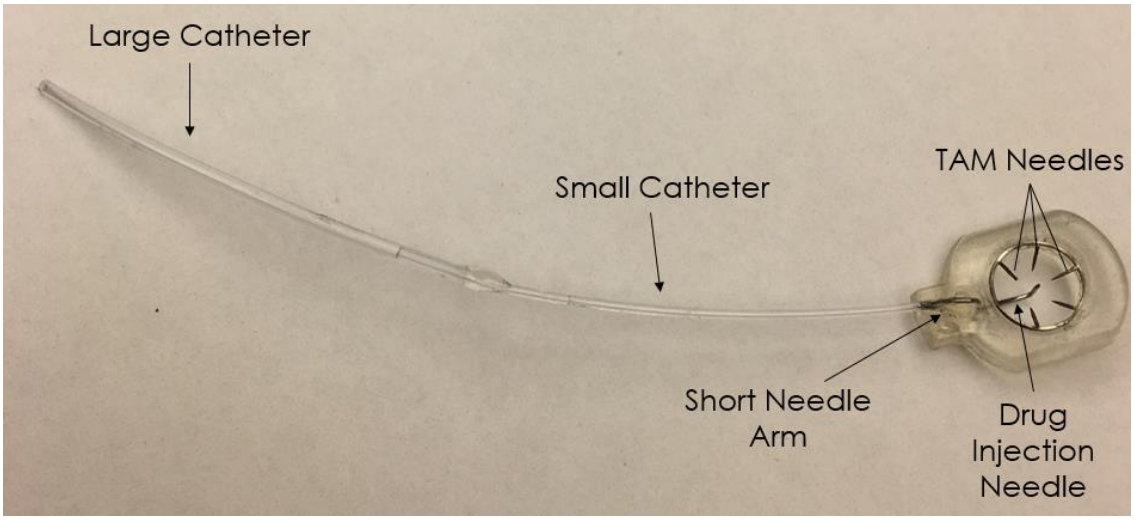

Figure 67. The final device without the osmotic pump.